

# **The apoptosis-regulator c-FLIP**

Functional role in urothelial carcinoma and autoimmunity

and

Identification of novel CD95 DISC-interacting proteins

## **Dissertation**

zur Erlangung des akademischen Grades

**doctor rerum naturalium**

**(Dr. rer. nat.)**

genehmigt durch die Fakultät für Naturwissenschaften

der Otto-von-Guericke-Universität Magdeburg

von Frida Kerstin Elisabeth Ewald, M. Sc.

geb. am 17. Juli 1982 in Sillerud, Schweden

Gutachter Prof. Dr. Ingo Schmitz

Prof. Dr. Ottmar Janßen

eingereicht am 25. Februar 2013

verteidigt am 28. Mai 2013



## Summary

Elimination of unwanted or damaged cells through apoptosis is critical during the embryonic development, in the immune system and to maintain tissue homeostasis in multicellular organisms. Apoptosis is strictly regulated by pro- and anti-apoptotic proteins. c-FLIP proteins inhibit death receptor-mediated apoptosis at the death-inducing signalling complex (DISC) by preventing caspase-8-processing. The aim of this thesis is to gain a better understanding of c-FLIP proteins' role in disease and to examine if there are unknown DISC-interacting proteins which could give a better insight into the complex signalling of the CD95 receptor.

Deregulation of apoptosis is common in cancer and is often caused by overexpression of anti-apoptotic proteins in tumour cells. The role of c-FLIP splice variants c-FLIP<sub>L</sub> and c-FLIP<sub>S</sub> in urothelial carcinoma was examined in this thesis. Unexpectedly, the c-FLIP<sub>L</sub> isoform was down-regulated in urothelial carcinoma tissues as well as in established carcinoma cell lines compared with normal urothelial tissues and cells, whereas c-FLIP<sub>S</sub> was unchanged. Nevertheless, both overexpression and knock-down through RNA interference of c-FLIP isoforms demonstrated that c-FLIP proteins, particularly c-FLIP<sub>L</sub>, are central resistance factors against CD95- and TRAIL-mediated apoptosis in urothelial tumours.

Non-apoptotic functions of CD95 DISC-interacting proteins have been described, including NF- $\kappa$ B activation, proliferation and T cell activation. However, the signalling mechanisms and how these proteins switch between apoptotic and survival signalling are not clear. The CD95 DISC was analysed by mass spectrometry to gain further insights into the DISC composition and the influence of c-FLIP<sub>L</sub>. Interestingly, TRAF2 and RIP1 were recruited to the DISC in a c-FLIP<sub>L</sub>-dependent manner. Moreover, the novel CD95 DISC-binding protein A20 was identified and its DISC interaction was verified by Western blotting.

c-FLIP<sub>R</sub> is the solely short c-FLIP isoform expressed in mice. Endogenous c-FLIP<sub>R</sub> was induced upon T cell stimulation with kinetics similar to c-FLIP<sub>S</sub> in humans. The mouse model vavFLIP<sub>R</sub> with constitutive expression of murine c-FLIP<sub>R</sub> was used to examine the functional role of c-FLIP<sub>R</sub> in the immune system. Lymphocytes from vavFLIP<sub>R</sub> mice were protected against CD95-mediated apoptosis, thus confirming functional c-FLIP<sub>R</sub> expression. Increased antigen-experienced and diminished naïve T cell populations were identified in one-year-old vavFLIP<sub>R</sub> mice in comparison to wild-type mice. Moreover, higher levels of kidney damage and elevated autoantibody titers were observed in vavFLIP<sub>R</sub> animals compared with wild-type littermates, suggesting a mild lupus-like phenotype of vavFLIP<sub>R</sub> mice.

---

## Table of contents

1. Introduction .....	1
1.1. Cell death mechanisms.....	1
1.2. Apoptosis .....	3
1.2.1. Caspases – mediators of apoptosis.....	4
1.2.2. The extrinsic pathway of apoptosis.....	6
1.2.3. The intrinsic pathway of apoptosis .....	7
1.2.4. Amplification of extrinsic apoptosis signals by the intrinsic pathway .....	10
1.3. FLICE-inhibitory proteins (FLIPs) .....	12
1.4. CD95-mediated apoptosis in the immune system.....	16
1.5. The role of death receptors and c-FLIP in cancer .....	19
1.6. Non-apoptotic functions of c-FLIP .....	20
1.7. Aim of the thesis .....	22
2. Materials.....	24
2.1. Chemicals.....	24
2.2. Materials and reagents for cloning.....	24
2.2.1. Restriction enzymes .....	24
2.3. DNA gel electrophoresis .....	25
2.4. Cell culture materials and devices.....	25
2.4.1. Cell culture reagents.....	26
2.4.2. Reagents and antibodies used for stimulation of cells .....	26
2.5. Cell lines .....	27
2.6. Mouse strain .....	27
2.7. Western blotting materials and reagents .....	27
2.7.1. Primary antibodies .....	28
2.7.2. Horseradish peroxidase conjugated secondary antibodies.....	28

---

2.8.	Materials and reagents for flow cytometry .....	29
2.8.1.	Flow cytometry devices .....	29
2.8.2.	Fluorescent dyes.....	29
2.8.3.	Human antibodies .....	29
2.8.4.	Murine antibodies .....	30
2.9.	Oligonucleotides .....	30
2.10.	Frequently used buffers.....	32
3.	Experimental procedures.....	34
3.1.	Molecular biology methods .....	34
3.1.1.	Polymerase chain reaction (PCR) .....	34
3.1.2.	DNA gel electrophoresis .....	34
3.1.3.	Cloning.....	35
3.1.4.	Transformation.....	35
3.1.5.	Quantitative real-time PCR of patient and tissue samples.....	36
3.2.	Cellular and protein biochemical methods.....	36
3.2.1.	Transfection and lentiviral infection of cells .....	36
3.2.2.	Lysis of cells .....	37
3.2.3.	Immunoprecipitation of the DISC complex.....	38
3.2.4.	SDS-polyacrylamide gel electrophoresis (SDS-PAGE) .....	38
3.2.5.	Western blotting.....	39
3.2.6.	Mass spectrometry .....	39
3.2.7.	Flow cytometry analysis .....	41
3.2.8.	Cell isolation by flow cytometry.....	41
3.3.	Mouse and primary murine cell methods.....	42
3.3.1.	Isolation of organs and cell preparation.....	42

---

3.3.2.	In vitro activation of T and B cells .....	42
3.3.3.	Apoptosis assays .....	42
3.3.4.	Activation induced cell death.....	43
3.3.5.	Experimental autoimmune encephalomyelitis (EAE).....	43
3.3.6.	Histology.....	44
3.3.7.	Analysis of anti-nuclear antibodies (ANA assay).....	44
3.4.	Statistical analysis .....	45
4.	Results.....	46
4.1.	The role of c-FLIP splice variants in urothelial tumours .....	46
4.1.1.	c-FLIP <sub>L</sub> expression is decreased in urothelial carcinoma.....	46
4.1.2.	Cycloheximide sensitises urothelial carcinoma cell lines towards CD95L- and TRAIL-induced apoptosis.....	47
4.1.3.	c-FLIP overexpression protects urothelial carcinoma cells against apoptosis....	49
4.1.4.	Knock-down of c-FLIP sensitises urothelial carcinoma cells for CD95L-induced apoptosis.....	51
4.1.5.	Urothelial carcinoma cells are sensitised for TRAIL-induced apoptosis by knock-down of c-FLIP .....	54
4.2.	Identification of novel CD95 DISC-interacting proteins.....	56
4.2.1.	Characterisation of Jurkat E6.1 clones overexpressing c-FLIP <sub>L</sub> .....	56
4.2.2.	Immunoprecipitation of the DISC complex in c-FLIP <sub>L</sub> overexpressing clones .	60
4.2.3.	Mass spectrometry analysis of proteins interacting at the DISC .....	62
4.3.	Constitutive expression of murine c-FLIP <sub>R</sub> causes autoimmunity in aged mice.....	66
4.3.1.	Endogenous expression of murine c-FLIP <sub>R</sub> .....	66
4.3.2.	The c-FLIP <sub>R</sub> transgenic mouse model - vavFLIP <sub>R</sub> .....	67
4.3.3.	vavFLIP <sub>R</sub> mice are protected against CD95-induced apoptosis and AICD.....	68
4.3.4.	Normal cell populations in young vavFLIP <sub>R</sub> mice .....	71
4.3.5.	Experimental autoimmune encephalomyelitis.....	75
4.3.6.	Altered cell populations in one year old vavFLIP <sub>R</sub> mice.....	76

---

4.3.7.	Damage of kidneys and increased ANA-titers in one year old vavFLIP <sub>R</sub> mice .	80
5.	Discussion .....	82
5.1.	The role of c-FLIP splice variants in urothelial carcinoma.....	82
5.2.	Identification of novel CD95 DISC-interacting proteins .....	85
5.3.	Constitutive expression of murine c-FLIP <sub>R</sub> causes autoimmunity in aged mice .....	88
5.4.	Concluding remarks .....	91
6.	Abbreviations .....	93
7.	References .....	98
8.	Acknowledgements .....	113
9.	Declaration of originality .....	114
10.	Curriculum Vitae.....	115

## 1. Introduction

### 1.1. Cell death mechanisms

Cell death plays a crucial role in the embryonic development and for regulation of tissue homeostasis in multicellular organisms by removal of unwanted or damaged cells. There are different modes of cell death depending on the stimulation and environment of the cell <sup>1</sup>. Cell death has long been postulated to either be regulated (apoptosis) or unregulated (necrosis). However, other non-apoptotic regulated cell death pathways such as necroptosis and autophagic cell death have also been described <sup>2</sup>.

Apoptosis and necrosis can be discriminated through distinct morphological and biochemical characteristics <sup>3</sup>. Before Kerr, Wyllie and Currie described apoptosis in 1972 <sup>4</sup>, all kinds of cell death was termed necrosis and apoptosis was first called ‘shrinkage necrosis’ due to the morphological features of dying cells <sup>3</sup>. Cells undergoing apoptosis are characterised by cell size reduction, chromatin condensation, nuclear fragmentation, membrane blebbing and formation of apoptotic bodies, which can be efficiently phagocytosed <sup>3, 5</sup> (Figure 1). In contrast, necrotic cell death is characterised by swelling of the cytoplasm and organelles, massive oxidative stress and rupture of the plasma membrane <sup>3</sup>. The lost cell integrity allows intracellular contents to leak to the extracellular space and attract immune cells <sup>3, 6</sup> (Figure 1).

Apoptosis is an evolutionarily conserved process driven by numerous apoptosis-regulating genes <sup>7</sup>. External stress such as withdrawal of growth factors, irradiation or cytotoxic drugs can induce apoptosis <sup>8</sup>. Further, death ligands of immune cells can trigger apoptosis signalling <sup>8</sup>. Apoptotic cells release ‘find me’ signals such as the chemoattractant lipid lysophosphatidylcholine to recruit phagocytic cells i.e. dendritic cells and macrophages <sup>9</sup>. As cells undergo apoptosis, the strict organisation of the phospholipids in the plasma membrane is disrupted. The phospholipid phosphatidylserine (PS) is located on the inside of the plasma membrane in healthy cells, but becomes exposed to the outside of the cell during apoptosis and is detected by phagocytes as an ‘eat me’ signal <sup>10, 11</sup>. Changes in carbohydrate composition of the plasma membrane and oxidised lipids are other engulfment signals. Phagocytic cells indirectly bind to the apoptotic cell through bridging molecules such as milk fat globule–EGF factor-8 protein (MFG-E8) and T cell immunoglobulin domain and mucin domain protein 4 (TIM4) <sup>12, 13</sup>. Phagocytes can also directly bind apoptotic cells by receptors recognising ‘eat me’ signals, for instance thrombospondin (TSP) and the scavenger receptors

CD36, SR-A and LOX1<sup>14-18</sup>. Macrophage lectins and integrins presumably also recognise apoptotic cells<sup>19-21</sup>. Other possible molecules/ligands acting as engulfment signals on dying cells are AnnexinI and the adhesion molecule intercellular adhesion molecule-3 (ICAM3)<sup>22, 23</sup>.

The absence of an inflammatory response is a further characteristic of apoptosis. The apoptotic cells are able to provide an anti-inflammatory environment by inducing macrophages to produce the anti-inflammatory cytokines transforming growth factor  $\beta$  (TGF- $\beta$ ) and interleukin 10 (IL-10), which ensures a 'silent' death without inflammation<sup>24</sup>.

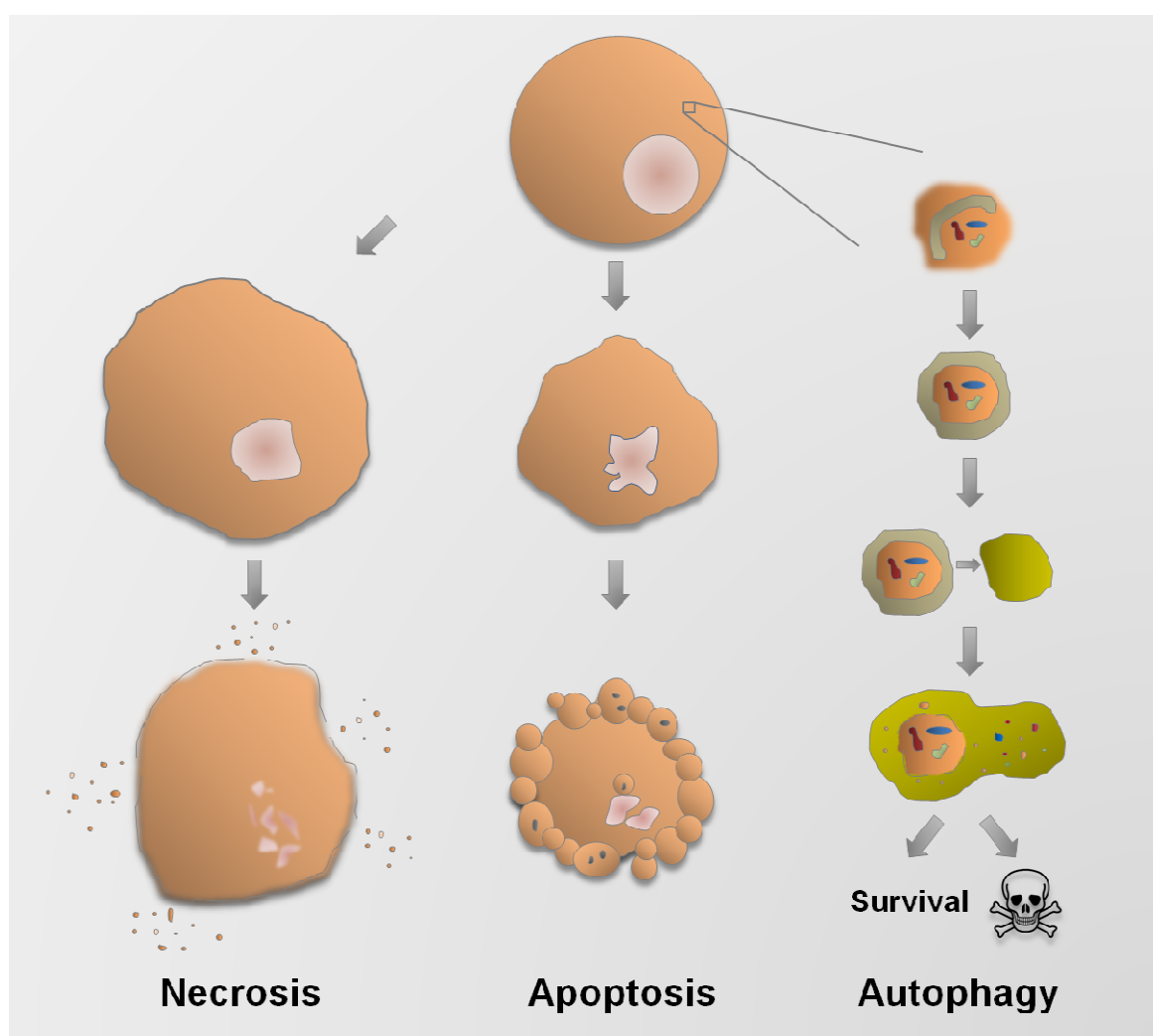


**Figure 1.** Cell death mechanisms. Necrosis is characterised by swelling of the cytoplasm and organelles. The membrane integrity is lost and intracellular contents leak to the extracellular space. In contrast, the apoptotic cell shrinks, DNA is fragmented and the membrane blebs. Further, apoptotic bodies are formed to facilitate phagocytosis. In autophagy, cellular contents are enclosed by a double-layer membrane forming the autophagosome. The autophagosome subsequently fuses with the lysosome and thereby degrades its contents.

Turning to necrosis, this cell death mode can be induced by direct cell trauma or harmful conditions such as hyperthermia, hypoxia, ischemia or toxic substances<sup>25</sup>. Moreover, stress can be sensed by the level of reactive oxygen species (ROS) production, increase in intracellular  $\text{Ca}^{2+}$  levels and depletion of intracellular ATP<sup>26</sup>. Several of these factors can also induce apoptosis. It presumably depends on the intensity level of the stimuli if apoptosis or necrosis is induced with low doses triggering apoptosis, whereas higher doses results in necrosis<sup>26</sup>. Necrosis is an immunogenic type of cell death. Inflammation is promoted by the passive release of high mobility group protein B1 (HMGB1), uric acid, heat shock proteins, genomic DNA and other molecules which attract innate immune cells such as dendritic cells, macrophages, natural killer cells (NK cells) and neutrophils<sup>5, 26, 27</sup>. Recently, a strictly regulated cell death mechanism with features of necrosis was identified and named necroptosis. If apoptosis is blocked, necroptosis can be induced by the same death ligands triggering apoptosis, which could be a back-up mechanism to ensure cell death<sup>28</sup>.

Autophagy is an intracellular process where parts of the cell can be digested to recycle nutrients or to remove damaged or unwanted organelles<sup>29</sup>. Moreover, intracellular pathogens can be eliminated by this pathway<sup>29</sup>. In autophagy, a double-layered membrane encloses the cytoplasmic contents to be removed<sup>29</sup>. The vesicle formed is called the autophagosome, which subsequently fuses with the lysosome to degrade its contents<sup>29</sup> (Figure 1). Autophagy is a survival mechanism which is induced due to starvation of the cell. However, increased autophagic flux can also be observed in dying cells. Autophagic cell death is morphologically characterised by massive cytoplasmic vacuolisation indicating an elevated autophagic flux<sup>30</sup>. Nevertheless, the existence of autophagic cell death has been lively debated. Presumably, in most cases autophagy is induced during cell death and is not actually executing the cell<sup>31</sup>.

## 1.2. Apoptosis

Apoptosis is essential in embryonic development and for maintaining tissue homeostasis<sup>32</sup>. Efficient elimination of cells by apoptosis is also crucial in the immune system, for instance in negative selection of T cells in the thymus and during the contraction phase of immune responses<sup>33, 34</sup>. Moreover, apoptosis can act as a defence against viral and bacterial pathogens by eliminating infected cells before pathogens spread to other cells<sup>5, 6, 33</sup>. There are two distinct pathways leading to apoptosis, the extrinsic and the intrinsic pathway<sup>35, 36</sup>. These signalling pathways involve numerous proteins; especially the caspase and Bcl-2 family

members are important mediators of apoptosis<sup>5, 32</sup>. The apoptosis pathways and involved proteins are described below.

### 1.2.1. Caspases – mediators of apoptosis

The cysteine proteases, called caspases, play a central role in the apoptotic machinery. Since the discovery of caspase-1 and its functional homologue CED-3 in *Caenorhabditis elegans* (*C. elegans*) in the early 1990's, a whole field of caspase research has developed<sup>37-39</sup>. So far 12 functional human caspases (caspase-1-10, 14 and 16) and 11 murine caspases (caspase-1, 2, 3, 6, 7, 8, 9, 11, 12, 14 and 16) have been identified<sup>40, 41</sup>. There are some differences between the human and murine caspases; caspase-10 is absent in the mouse genome and murine caspase-11 and -12 are the functional homologues of human caspase-4 and -5, respectively<sup>40, 41</sup>. Human caspase-8 has two functional splice variants; caspase-8/a and the 15 amino acid smaller caspase-8/b<sup>42</sup>. Moreover, most humans have a polymorphism in caspase-12 which results in a truncated protein mainly consisting of the caspase recruitment domain (CARD)-domain (caspase-12S). However, there are individuals of African origin who express the enzymatically inactive full-length caspase-12L<sup>43</sup>. Presumably, human caspase-12 function as a dominant-negative regulator of pro-inflammatory responses<sup>44</sup>.

Caspases consist of a prodomain followed by a large subunit (p20) and a small subunit (p10) with a cleavage site in-between the large and small subunits<sup>45</sup>. All caspases contain the catalytic residues His-237 and Cys-285, with numbering originating from human caspase-1<sup>46</sup>. The active site consists of a pentapeptide QACXG (where X denotes R, Q or G), including Cys-285<sup>45, 47</sup>. The caspases are categorised into groups according to their function in apoptosis or inflammation (Figure 2). The apoptotic caspases are subdivided into the initiator caspases 2, 8, 9 and 10, and the effector caspases 3, 6 and 7. The inflammatory caspases are caspases 1, 4, 5, 11 and 12<sup>45</sup>. Although caspase-14 and -16 are genetically closely related and caspase-14 is involved in terminal keratinocyte differentiation<sup>48, 49</sup>, caspase-16 was not expressed in epidermal keratinocytes<sup>40</sup>. Thus, the function of caspase-16 remains to be investigated. The apical caspases are present as inactive monomeric zymogens in the cell and are activated by proteolytical cleavage or dimerisation. Recruitment to signalling platforms via their death effector domain (DED) and CARD recruitment domains facilitates dimerisation and thereby activation<sup>50, 51</sup>. In contrast, the effector caspases exist as inactive dimers<sup>41, 45</sup>. Proteolytical cleavage of the intersubunit linker by an initiator caspase or another protease activates the effector caspases<sup>41, 45</sup>.

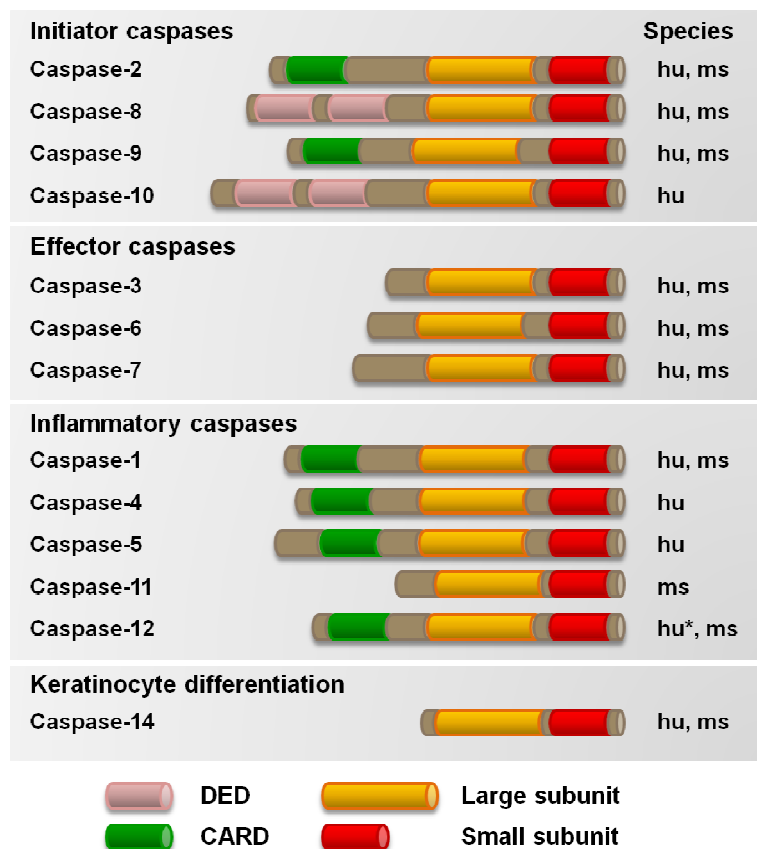


**Figure 2.** Structural overview of human (hu) and murine (ms) caspases. The caspases are divided into the apoptotic initiator and effector caspases as well as the inflammatory caspases. The initiator caspases 2, 8, 9 and 10 have a large C-terminal prodomain containing DED and CARD domains which are important for recruitment to signalling platforms. Caspases 3, 6 and 7 are effector caspases, whereas caspase-1, -4, -5, -11 and -12 are inflammatory caspases. Human caspase-12 contains a polymorphism, resulting in a truncated splice variant of caspase 12, which mainly consists of the CARD domain. Some individuals of African origin express catalytically inactive full-length caspase-12. Caspase-14 plays an important role in terminal keratinocyte differentiation. Adapted from Fuentes- Prior and Salvesen, 2004<sup>45</sup>.

Caspases cleave their substrates after a tetrapeptide sequence, P4-P3-P2-P1, with an aspartate in the P1 position<sup>52</sup>. The caspases have different tetrapeptide sequence specificities: the inflammatory caspases 1, 4 and 5 have a preference for the (W/L)EXD motif (X denotes any amino acid residue), caspase-3, -7 and -2 favour the sequence DEXD and the preferential tetrapeptide sequence of caspases 6, 8, 9 and 10 is (L/I/V)EXD<sup>41, 45, 52</sup>. The different cleavage preferences are also reflected in the substrate specificities of caspases. The pro-inflammatory caspases differ from the apoptotic caspases in that they regulate both cytokine processing and apoptosis. Recruitment of caspase-1 the inflammasome mediates activation of this caspase and active caspase-1 subsequently activates the cytokines IL-1 $\beta$  and IL-18 by processing of their proforms<sup>44</sup>. The initiator and effector apoptotic caspases differ in their substrate specificities in that initiator caspases cleave few specific substrates, whereas effector caspases process numerous substrates during the demolition phase of apoptosis<sup>41, 53</sup>. A substantial part of the morphological and biochemical changes of the cell during apoptosis are mediated by caspase cleavage<sup>5, 53</sup>. The rounding up and contraction of the cell seen in early stages of apoptosis is caused by caspase-mediated cleavage of cytoskeletal components<sup>5</sup>. Moreover,

caspase processing of the actin-stabilising protein Rho-associated coiled-coil-containing protein kinase I (ROCK I) is presumed to be involved in membrane blebbing of the apoptotic cell<sup>54, 55</sup>. Further, caspases cleave the inhibitor of caspase-activated DNase (ICAD), thereby releasing the active nuclease caspase-activated DNase (CAD) which translocates to the nucleus and starts DNA fragmentation<sup>56-58</sup>. Moreover, caspase-activity mediates exposure of PS and other engulfment signals to the cell surface as well as the fragmentation of the Golgi apparatus and the endoplasmic reticulum (ER)<sup>5, 53</sup>. Thus, caspase activity is crucial for apoptosis.

### 1.2.2. The extrinsic pathway of apoptosis

The extrinsic pathway of apoptosis is also called death receptor-mediated apoptosis. Death receptors belong to the tumour necrosis factor (TNF) receptor superfamily<sup>59</sup>. Six human death receptors have been identified, namely CD95 (Fas/ Apo-1), TNF-R1 (CD120a), TNF-related apoptosis-inducing ligand receptor 1 (TRAIL-R1; DR4/Apo-2), TRAIL-R2 (DR5/KILLER/TRICK-2), DR3 (Apo-3/WSL/TRAMP/LARD) and DR6 (Figure 3). Orthologues of all the human death receptors are found in mice, except TRAIL-R1 and TRAIL-R2 where a single orthologue for both receptors, TRAIL-R2, exists in mice<sup>60, 61</sup>. The death receptors consist of up to six extracellular cysteine-rich domains with high sequence similarity between the receptors<sup>62</sup>. Moreover, an intracellular 80-amino acid motif called the death domain (DD) is characteristic for the death receptors<sup>59, 63, 64</sup>. This domain is important for transducing signals upon activation by the respective death ligand<sup>59, 63, 64</sup>. Additionally, there are decoy receptors (DcRs) which lack the DD and therefore cannot transduce signals. These receptors compete with the death receptors for ligand binding. Decoy receptors for TRAIL are DcR1, DcR2 and Osteoprotegerin (OPG), whereas DcR3 is a decoy receptor for CD95L (Figure 3). The decoy receptors are presumably expressed to regulate the response to death ligands<sup>62</sup>.

The death receptors CD95 and TRAIL-R1/2 are activated upon binding of the death ligands CD95L and TRAIL, respectively, resulting in receptor oligomerisation and activation of the intracellular DDs<sup>65-67</sup>. The adaptor protein Fas-associated death domain (FADD) is recruited via its C-terminal DD and can in turn recruit procaspase-8 via its N-terminal DED domain<sup>68-70</sup>. The assembled signalling platform is called the death-inducing signalling complex (DISC)<sup>70</sup>. TNF-R1 require association with the adaptor protein TNFR-associated death domain (TRADD) in order to recruit FADD and caspase-8<sup>71</sup>. Humans express caspase-10 next to caspase-8<sup>72, 73</sup>. This protein is similar to caspase-8 and DISC-recruitment is facilitated

by its DED-domains<sup>72, 73</sup>. DISC-binding of procaspases 8 and 10 bring the proteins into close proximity which results in dimerisation, activation and autoproteolytical cleavage<sup>50, 51</sup>. Active caspase-8 and -10 process caspase-3, -6 and 7, thereby activating these effector caspases<sup>71</sup>. The active effector caspases cleave numerous substrates which results in apoptosis (Figure 5)<sup>41, 53</sup>.

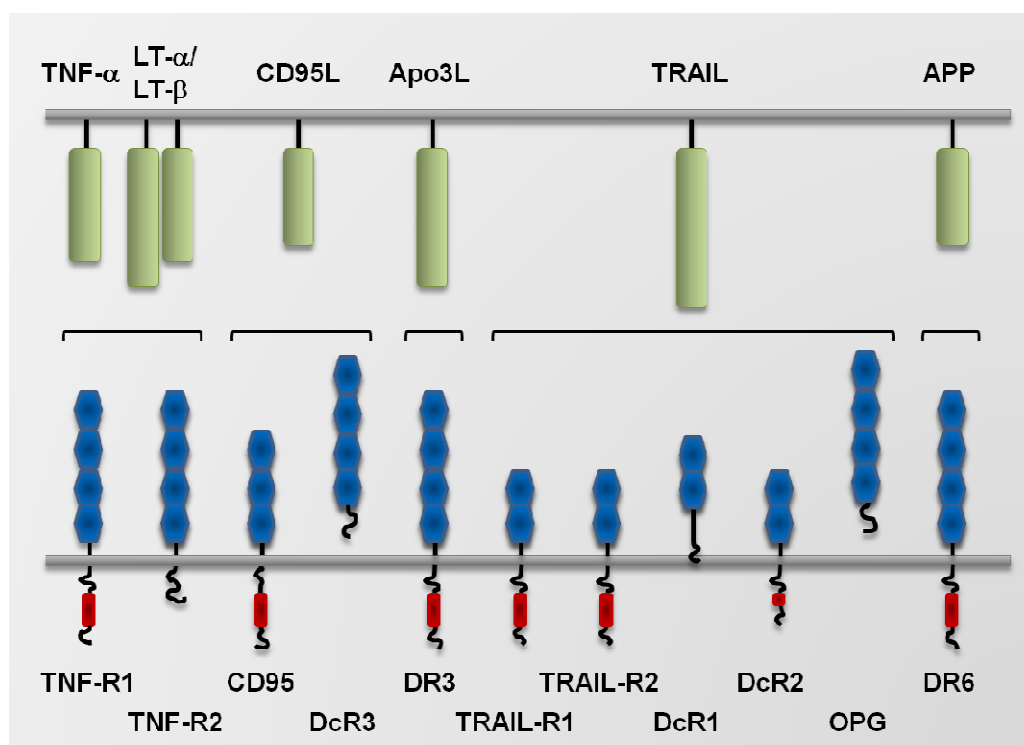


**Figure 3.** Death receptors and their ligands. The death and decoy receptors are illustrated at the bottom, with the extracellular cysteine-rich domains in blue and death domains (DDs) in red. The death ligands are shown at the top. TNF- $\alpha$  and LT- $\alpha$ /LT- $\beta$  bind to TNF-R1 and TNF-R2<sup>71</sup>. The ligand for the CD95 receptor and DcR3 is CD95L<sup>60</sup>. Apo3L only binds the receptor DR3, whereas TRAIL interacts with TRAIL-R1, TRAIL-R2, DcR1, DcR2 and OPG<sup>60</sup>.  $\beta$ -amyloid precursor protein (APP) binds to DR6<sup>74</sup>. Adapted from Igney and Kramer, 2002<sup>60</sup>.

### 1.2.3. The intrinsic pathway of apoptosis

The intrinsic pathway of apoptosis is induced by developmental cues or cellular stress, such as cytokine deprivation, DNA damage, UV radiation, elevated ROS production, low ATP levels or pH alterations<sup>75</sup>. This pathway is tightly regulated by the B cell lymphoma-2 (Bcl-2) protein family<sup>76</sup>. Bcl-2 was discovered as an oncogene in B cell follicular lymphomas<sup>77-79</sup>. In contrast to previously identified oncogenes, Bcl-2 promotes cell survival but not cell

proliferation<sup>80</sup>. Since these early findings, a whole family of anti- and pro-apoptotic Bcl-2 proteins have been identified and characterised.

The proteins in the Bcl-2 family share Bcl-2 homology (BH) domains<sup>81</sup>. They are divided into three groups according to their function and number of BH domains<sup>81</sup>. The first group contains the anti-apoptotic proteins Bcl-2, Bcl-2-like protein 2 (Bcl-w), Bcl-lymphoma-extra large (Bcl-x<sub>L</sub>), myeloid cell leukaemia 1 (Mcl-1) and Bcl-2-related protein A1 (A1). All of these proteins have four BH domains (BH1-4). The pro-apoptotic proteins Bcl-2-associated x protein (Bax), Bcl-2 antagonist killer 1 (Bak) and Bcl-2-related ovarian killer (Bok) contain BH domains 1-3 and belong to the second group. The last group consists of the BH3-only proteins which, as the name says, only contain the BH3 domain. The proteins included in this group are Bcl-2 antagonist of cell death (Bad), Bcl-2-interacting killer (Bik), Bcl-2 interacting domain death agonist (Bid), Harakiri (Hrk, also known as death protein 5; DP5), Bcl-2-interacting mediator of cell death (Bim), Bcl-2 modifying factor (Bmf), Noxa, p53-upregulated modulator of apoptosis (Puma) and Mcl-1 ubiquitin ligase E3 (Mule)<sup>76, 81</sup> (Figure 4A).

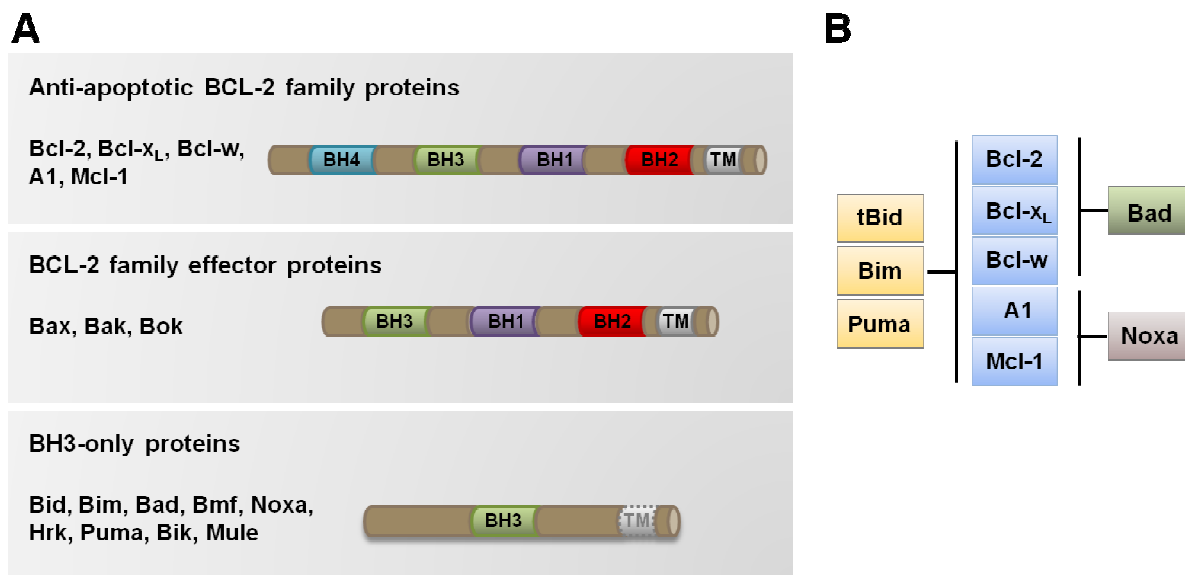


**Figure 4.** The Bcl-2 family proteins. **(A)** The proteins are divided into the anti-apoptotic Bcl-2 homologues, the effector proteins and the pro-apoptotic BH3-only proteins. **(B)** The BH3-only proteins have different binding specificities for the anti-apoptotic Bcl-2 proteins. tBid, Bim and Puma can bind all Bcl-2 homologues, whereas Bad selectively bind Bcl-2, Bcl-x<sub>L</sub> and Bcl-w, and Noxa only binds A1 and Mcl-1. The transmembrane domain (TM) is important for membrane integration. Adapted from Youle and Strasser, 2008<sup>76</sup>.

Proteins of the Bcl-2 family regulate the integrity of the outer mitochondrial membrane. Activation of the effector proteins Bax and Bak leads to insertion of the proteins into the outer mitochondrial membrane, homo-oligomerisation and mitochondrial outer membrane permeabilisation (MOMP)<sup>82</sup>. Stress-induced apoptosis requires one of the Bax or Bak proteins. Mice deficient for either Bax or Bak are healthy with minimal phenotypes, whereas most mice with both Bax and Bak deficiency die perinatally, with only a low percentage surviving to adult animals<sup>83, 84</sup>. There is not much known about the third protein of this group, Bok, but it does not seem to be as important as Bax and Bak for stress-induced apoptosis<sup>81</sup>. Mice with Bok deficiency appeared healthy and were fertile<sup>85</sup>.

The anti-apoptotic Bcl-2 family members can be integrated into the membranes of mitochondria, ER and nuclear envelope by their C-terminal transmembrane domain (TM)<sup>86</sup>. Bcl-2 is always membrane-localised, whereas Bcl-w and Bcl-x<sub>L</sub> are directed to membranes after a cytotoxic signal<sup>86</sup>. Bcl-2 and the other proteins of this group inhibit apoptosis by direct binding to Bax and Bak and thereby inhibiting their pro-apoptotic activities<sup>81, 87, 88</sup>. As the cell senses apoptotic signals, BH3-only proteins are transcriptionally induced or activated by post-translational modifications<sup>76</sup>. The BH3-only proteins act upstream of Bax and Bak, since apoptosis cannot be induced by BH3-only proteins without these effector proteins<sup>84</sup>. The pro-apoptotic activities of BH3-only proteins are primarily exerted by inhibiting the anti-apoptotic Bcl-2 family members<sup>89</sup>. BH3-only proteins can bind to the hydrophobic groove in the Bcl-2 homologues by their BH3 domain and thereby disrupting the inhibition of Bax and Bak, which leads to mitochondrial outer membrane permeabilisation and apoptosis<sup>89</sup>. Truncated Bid (tBid), Bim and Puma bind all the anti-apoptotic Bcl-2 proteins, whereas Bad only binds Bcl-2, Bcl-x<sub>L</sub> and Bcl-w, and Noxa selectively binds A1 and Mcl-1<sup>90</sup>. The ability to induce apoptosis is linked with the binding specificities of the BH3-only proteins; Bim and Puma alone can induce apoptosis, unlike Bad and Noxa where a combination of the proteins is required for efficient apoptosis induction<sup>90</sup> (Figure 4B). Consequently, mice deficient in Bad or Noxa are relatively healthy<sup>91-93</sup>. In contrast, Bim is important for leukocyte homeostasis. Consequently, Bim deficient mice develop lymphoproliferation and autoimmune disease<sup>94, 95</sup>. Puma transcription is induced by the tumour suppressor p53 in response to DNA damage<sup>96-98</sup>. Mice with Puma deficiency are viable and have normal development, but Puma was shown to be essential in  $\gamma$ -radiation-induced apoptosis in the thymus and central nervous system (CNS)<sup>93, 99</sup>.

Various stress stimuli such as DNA fragmentation, UV radiation or cytokine deprivation induce the intrinsic pathway of apoptosis, which results in permeabilisation of the outer mitochondrial membrane by the effector proteins Bax and Bak. Upon loss of mitochondrial membrane integrity, mitochondrial intermembrane space molecules are released to the cytosol including cytochrome c and second mitochondria-derived activator of caspase (Smac)/direct binding IAP protein with low pI (Diablo) as well as other apoptogenic factors<sup>82</sup>. Cytochrome c binds to apoptotic protease-activating factor-1 (Apaf-1) and thereby induce the formation of the apoptosome, a signalling platform consisting of seven Apaf-1 molecules ordered in a wheel-like structure<sup>100, 101</sup>. Apaf-1 is a monomer in the absence of apoptotic signals, but oligomerises as cytochrome c binds to its WD40 repeat domains<sup>100, 101</sup>. Moreover, Apaf-1 contains a CARD domain which facilitates caspase-9 association<sup>102</sup>. The monomeric form of caspase-9 is inactive, but it becomes activated as it dimerises at the apoptosome<sup>103, 104</sup>. Active caspase-9 can in turn activate the executioner caspases 3 and 7, which cleave further death substrates and thus, inevitably cause apoptosis<sup>105</sup> (Figure 5). However, apoptosis is further controlled by x-linked inhibitor of apoptosis protein (XIAP), which inhibits caspase activity by direct binding to active caspase-3, -7 and -9<sup>106</sup>. XIAP can in turn be inhibited by the mitochondrial proteins Smac/Diablo and Omi/HtrA2, thereby antagonising the inhibition of the caspases and facilitating apoptosis<sup>107-109</sup>. Further apoptogenic factors released upon MOMP are the flavoprotein apoptosis-inducing factor (AIF) and the endonuclease G (EndoG)<sup>110, 111</sup>. These proteins translocate to the nucleus and initiate large-scale DNA fragmentation (Susin 1999, Li 2001). The apoptosis-induction of AIF and EndoG is independent of caspases in mammalian cells, whereas upstream activation of the caspase homologue CED-3 is required in *C. elegans* for the worm AIF homologue (WAH-1)<sup>112, 113</sup>.

#### **1.2.4. Amplification of extrinsic apoptosis signals by the intrinsic pathway**

The extrinsic and intrinsic pathways can interplay to induce apoptosis. Type I cells have efficient DISC-formation, which facilitates massive activation of caspase-8 and the effector caspases<sup>114, 115</sup>. In contrast, type II cells have less DISC-assembly and consequently less activation of caspase-8. The small amount of active caspase-8 is not enough to directly process caspase-3, therefore an amplification of the death receptor signal via the mitochondrial pathway is necessary in type II cells<sup>114, 115</sup>. The extrinsic signal is amplified by caspase-8-processing of the BH3-only protein Bid. The active protein truncated Bid (tBid)

inhibits anti-apoptotic Bcl-2 family members and consequently permeabilisation of the outer mitochondrial membrane by Bax and Bak can occur<sup>116, 117</sup>. This leads to the release of apoptogenic molecules and ultimately apoptosis (Figure 5). The death-receptor-mediated apoptosis can be blocked in type II cells by overexpression of Bcl-2 or Bcl-x<sub>L</sub>, demonstrating the requirement of interplay between the extrinsic and intrinsic apoptosis pathways in these cells<sup>114, 118</sup>.

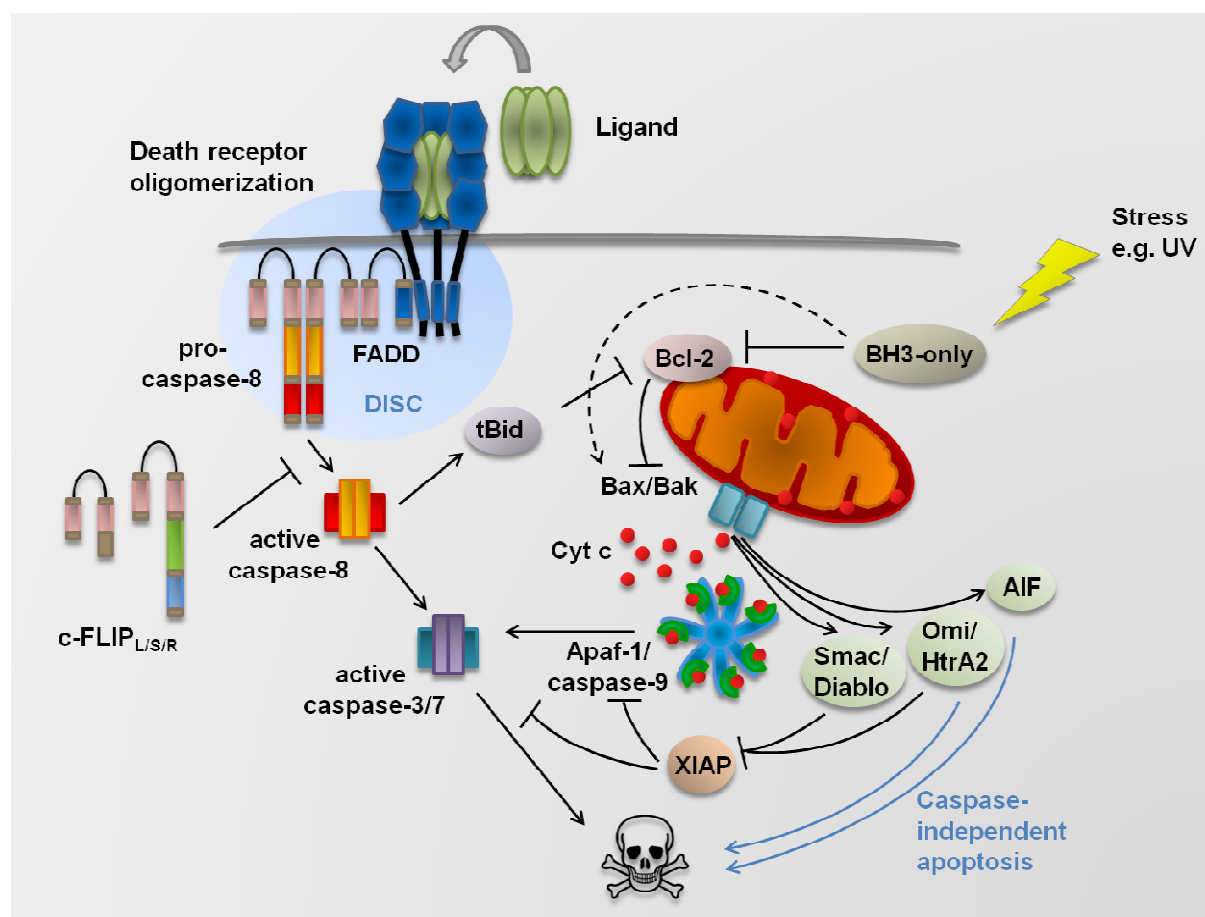


**Figure 5.** The extrinsic and intrinsic apoptosis pathways. The extrinsic pathway is triggered by ligand-binding to death receptors and assembly of the DISC complex where caspase-8 is activated. Active caspase-8 in turn activates caspase-3 and -7. The activated effector caspases cleave further substrates, which results in apoptosis. c-FLIP proteins inhibit the extrinsic pathway by interfering with caspase-8 processing. The intrinsic pathway is induced by cellular stress such as UV radiation or cytokine deprivation, leading to activation of the BH3-only proteins, which inhibit the anti-apoptotic Bcl-2 family members, thereby allowing Bax and Bak to permeabilise the outer mitochondrial membrane. Apoptogenic proteins from the mitochondrial intermembrane space are released to the cytosol due to the disrupted mitochondrial integrity. Cytochrome c (Cyt c) induces apoptosome formation and caspase-9 activation, which in turn activates caspase-3 and -7. Caspase-3, -7 and -9 are inhibited by XIAP, but XIAP can itself be inhibited by Smac/Diablo or Omi/HtrA2. Amplification of the extrinsic pathway via the intrinsic pathway is achieved by caspase-8-mediated cleavage of Bid to tBid, which subsequently inhibits anti-apoptotic Bcl-2 proteins. Caspase-independent apoptosis can be induced by Omi/HtrA2 and AIF. Adapted from Bouillet and O'Reilly, 2009<sup>8</sup>.

The apoptosis signalling in type I and type II cells differ in CD95 membrane localisation and internalisation. CD95 is directed to lipid rafts by post-translational palmitoylation<sup>119, 120</sup>. Notably, the lipid raft localisation of CD95 receptors is more pronounced in type I than type II cells<sup>121, 122</sup>. Moreover, lipid raft microdomains were reported to co-cluster with signalling protein oligomerisation transduction structures (SPOTS) formed at the plasma membrane upon CD95L-stimulation in type I cells<sup>123</sup>. Stimulation-dependent SPOTS formation was observed in type II cells as well, however without lipid raft co-clustering<sup>123</sup>. The large clusters formed upon triggering of the CD95 receptor are thought to be important for CD95 internalisation and thereby apoptosis signalling in type I cells. Type II cells do not internalise CD95, which suggests that type I and type II cells initiate CD95 signalling in different ways<sup>124, 125</sup>.

### 1.3. FLICE-inhibitory proteins (FLIPs)

Viral FLICE-inhibitory proteins (v-FLIPs) were identified through database screening for DED-containing proteins<sup>126</sup>. The v-FLIP proteins are expressed in  $\gamma$ -herpesviruses such as Kaposi's-sarcoma-associated human herpesvirus-8 (HHV8), herpesvirus saimiri and equine herpesvirus-2 as well as in molluscipoxviruses. Moreover, these proteins were shown to be inhibitors of death receptor-mediated apoptosis<sup>126-128</sup>.

A mammalian homologue was identified shortly thereafter, termed cellular FLIP (c-FLIP; also known as CASH, Casper, CLARP, FLAME-1, I-FLICE, MRIT and usurpin<sup>129-135</sup>). The human *CFLAR* gene is localised upstream of caspase-10 and caspase-8 on chromosome 2q33-34<sup>131, 132, 134-138</sup>, suggesting that these genes evolved by gene duplication<sup>135</sup>. Eleven c-FLIP splice variants have been reported<sup>139</sup>, but only three of these have been identified on the protein level, namely c-FLIP long isoform (c-FLIP<sub>L</sub>), c-FLIP short isoform (c-FLIP<sub>S</sub>) and c-FLIP Raji (c-FLIP<sub>R</sub>)<sup>118, 139-141</sup> (Figure 6).

c-FLIP<sub>L</sub> has the molecular weight 55 kDa and closely resembles caspase-8 (Figure 7). The protein has a caspase-like domain, but is catalytically inactive, since several amino acids in the active site have been substituted, including the catalytic residues His-237 and Cys-285<sup>45, 141</sup>. The two short isoforms, c-FLIP<sub>S</sub> and c-FLIP<sub>R</sub>, mainly consist of the two DED domains with molecular weights of 26 kDa and 24 kDa respectively. c-FLIP<sub>S</sub> has a unique C-terminal tail derived from exon 7, whereas c-FLIP<sub>R</sub> has a single nucleotide polymorphism (SNP) in the 3' splice site of intron 6 resulting in a premature stop-codon<sup>142</sup> (Figure 6, Figure 7). The SNP

in intron 6 is functional and influences whether exon 7 is spliced or not, consequently this SNP determines if c-FLIP<sub>S</sub> or c-FLIP<sub>R</sub> is produced<sup>142</sup>. The murine *Cflar* gene structure differs from the human *CFLAR* gene in that only c-FLIP<sub>L</sub> and c-FLIP<sub>R</sub> can be expressed<sup>143</sup> (Figure 6).

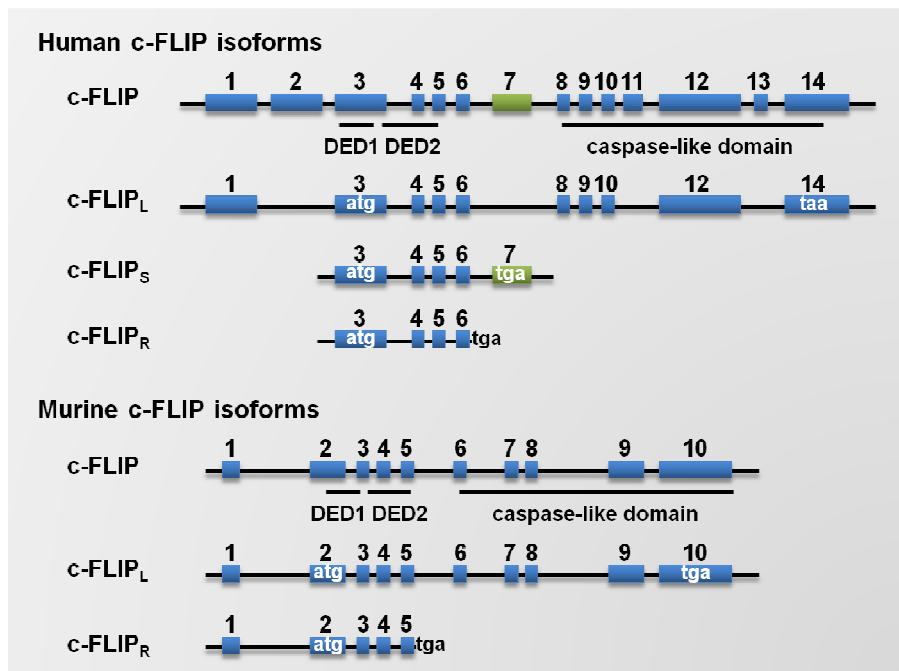


**Figure 6.** The intron-exon structure of the human and murine gene loci. Humans express c-FLIP<sub>L</sub>, c-FLIP<sub>S</sub> and c-FLIP<sub>R</sub> on the protein level. Exon 7, marked in green, is human-specific and gives c-FLIP<sub>S</sub> its unique C-terminal tail. The murine gene structure encodes for c-FLIP<sub>L</sub> and c-FLIP<sub>R</sub>. Adapted from Ueffing et al., 2008<sup>143</sup>.

c-FLIP is expressed abundantly in many tissues, for instance in neurons, cardiac myocytes, epithelial cells, macrophages, T and B cells<sup>144</sup>. The c-FLIP expression can be regulated by NF- $\kappa$ B, since various NF- $\kappa$ B stimuli such as TNF- $\alpha$  and IL-1, lipopolysaccharide (LPS) and CD40L for B cells as well as phorbol-12-myristate-13-acetate (PMA) and ionomycin or anti-CD3 and anti-CD28 for T cells induce upregulation of c-FLIP expression<sup>145, 146</sup>. Moreover, calcineurin-nuclear factor of activated T cells (NFAT) mediates induction of c-FLIP<sub>S</sub> in short-term activated T cells<sup>147</sup>. Cytokines such as IL-2, IL-4, IL-6, IL-10, IL-12 and interferon- $\gamma$  (IFN- $\gamma$ ) presumably also influence c-FLIP expression in T cells<sup>144</sup>.

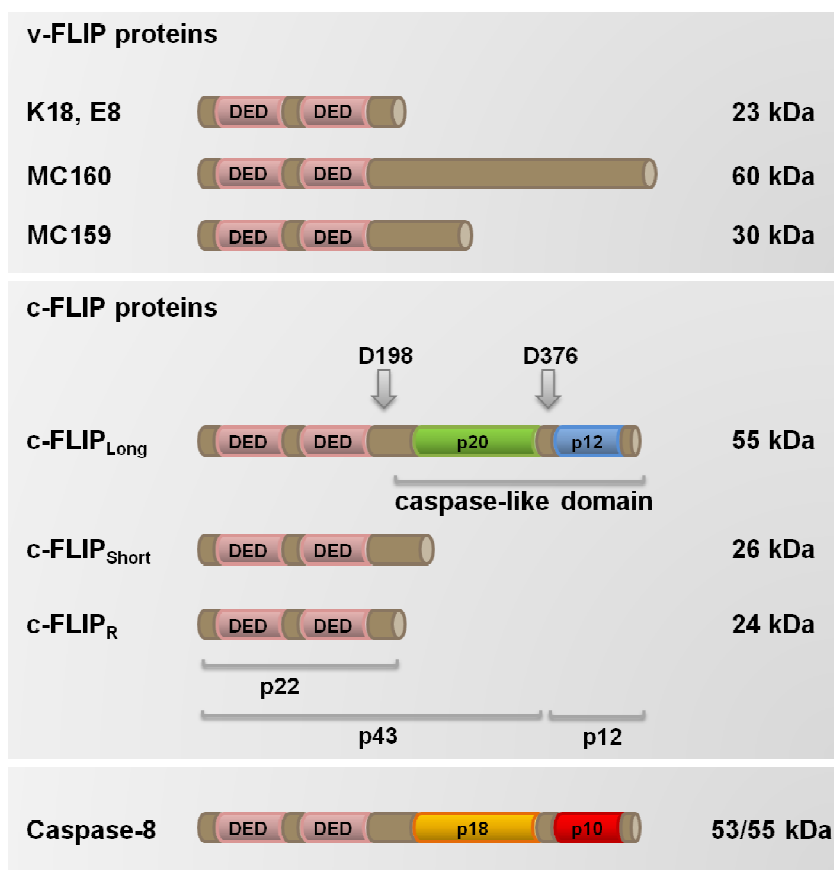


**Figure 7.** Structure of c-FLIP proteins. All viral and cellular FLIP proteins contain tandem DED domains. c-FLIP<sub>L</sub> has a similar structure as caspase-8, but lacks catalytic activity. The short splice variants of c-FLIP resemble the viral FLIP proteins. c-FLIP<sub>S</sub> has a unique C-terminal tail, whereas c-FLIP<sub>R</sub> is produced in individuals with a SNP in the 3' splice site of intron 6. All c-FLIP proteins can be cleaved at D198 which results in a p22 fragment, c-FLIP<sub>L</sub> can additionally be processed at D376<sup>130, 148</sup>. There are two functional splice variants of human caspase-8, termed caspase-8/a and caspase-8/b with the molecular weight 53 and 55 kDa respectively<sup>42</sup>. Adapted from Budd et al., 2006<sup>144</sup>.

c-FLIP proteins regulate death receptor-mediated apoptosis by interfering with caspase-8 activation<sup>118, 149</sup>. Stimulation of death receptors initiates DISC assembly, resulting in activation and processing of caspase-8. Full cleavage of caspase-8 releases the p10 and p18 products into the cytosol where the active enzyme is formed from two small p10 and two large p18 subunits<sup>150</sup>. The DED domains of the c-FLIP proteins allow recruitment to the DISC<sup>143</sup> and therefore these proteins compete with caspase-8 for DED binding sites at the DISC. c-FLIP proteins also inhibit cleavage of caspase-8<sup>149</sup>, hence the amount of active caspase-8 is reduced by c-FLIP and thereby the caspase cascade of apoptosis is prevented<sup>118, 140, 149</sup>.

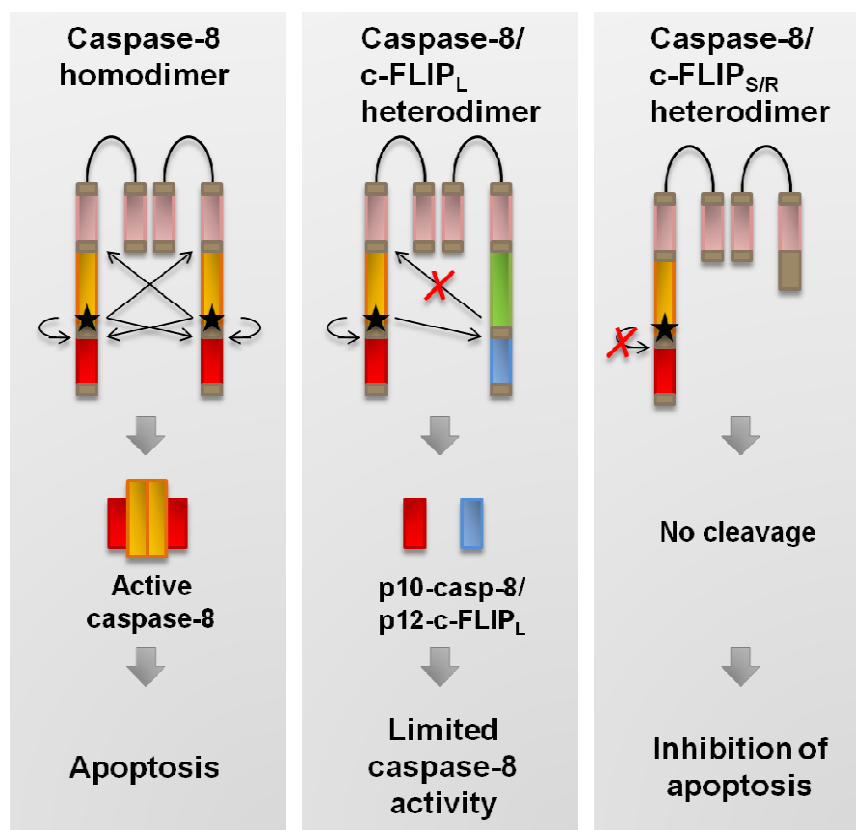


**Figure 8.** c-FLIP proteins regulate caspase-8 activity. Dimerised caspase-8 initiate activation and autoproteolytical cleavage of the caspase-8 molecules, which results in the active enzyme and ultimately apoptosis (left). Heterodimers of caspase-8 and c-FLIP<sub>L</sub> leads to activation of caspase-8, but only partial cleavage and therefore only limited caspase-8 activity (middle). Caspase-8 cannot be activated in heterodimers with c-FLIP<sub>S</sub> or c-FLIP<sub>R</sub>. Thus, cleavage does not occur and apoptosis is inhibited. Adapted from Krueger et al., 2001<sup>149</sup>.

c-FLIP<sub>L</sub> can activate caspase-8 via dimerisation at the DISC in contrast to c-FLIP<sub>S</sub>. This leads to initial processing of both caspase-8 and c-FLIP into the p41 (caspase-8/b) and p43 (caspase-8/a and c-FLIP<sub>L</sub>) fragments, although further cleavage to fully active caspase-8 is inhibited<sup>118, 149</sup> (Figure 8). The short c-FLIP splice variants only have anti-apoptotic functions<sup>140, 143, 149</sup>, in contrast to c-FLIP<sub>L</sub> where dual roles of the protein have been reported<sup>151, 152</sup>. Low levels of c-FLIP<sub>L</sub> facilitate caspase-8 processing and apoptosis, whereas high c-FLIP<sub>L</sub> levels inhibit apoptosis<sup>151, 152</sup>. Moreover, the strength of CD95 receptor stimulation also influences whether c-FLIP<sub>L</sub> acts pro- or anti-apoptotic<sup>153</sup>. Moderate expression of c-FLIP<sub>L</sub> was shown to promote apoptosis only upon strong receptor stimulation or in combination with overexpression of c-FLIP<sub>S</sub> or c-FLIP<sub>R</sub>. In contrast, high levels of c-FLIP<sub>L</sub> diminished the sensitivity for CD95-induced apoptosis and caspase-8 activation<sup>153</sup>.

#### 1.4. CD95-mediated apoptosis in the immune system

Functional CD95 receptor signalling ensures efficient removal of unwanted immune cells. *Lpr* and *gld* mice have defects in CD95-mediated apoptosis due to mutations in the CD95 receptor and ligand, respectively<sup>154, 155</sup>. These mice develop lymphoproliferation and systemic autoimmunity<sup>154, 155</sup>. Autoimmune lymphoproliferative syndrome (ALPS) was identified in humans as a disease resembling the murine *lpr/gld* phenotype<sup>156</sup>. Indeed, the majority of ALPS patients have mutations in genes encoding the CD95 receptor, ligand or proteins involved in CD95 signalling<sup>157</sup>. ALPS patients as well as *lpr/gld* mice accumulate an unusual population of CD3<sup>+</sup>CD4<sup>-</sup>CD8<sup>-</sup> (double negative; DN)  $\alpha\beta$  T cells in the periphery<sup>158-161</sup>. These DN T cells express B220, a marker generally associated with B cells<sup>162</sup>. Moreover, an elevated IL-10 production of the DN  $\alpha\beta$  T cells was observed in ALPS patients<sup>163</sup>. The cytokine profile with high levels of IL-10 in conjunction with increased levels of IL-4 and IL-5 as well as decreased IL-2 and IFN- $\gamma$  levels is characteristic for T helper type 2 (Th2) cells<sup>163</sup>. Since Th2 cells support humoral immune responses, the altered cytokine milieu might increase autoantibody production in ALPS patients.

The dynamics of T cell expansion and contraction is essential for the adaptive immune system. T cells become activated by interacting with antigen bound to major histocompatibility complex (MHC) together with co-stimulatory signals on antigen presenting cells (APCs). This induces differentiation and clonal expansion of T cells to efficiently clear the antigen. Most effector T cells need to be eliminated after successful antigen clearance to maintain the T cell homeostasis. Only few antigen-specific T cells persist as memory cells to ensure a rapid response upon re-encounter of the same antigen<sup>164, 165</sup>.

T cells can be eliminated by activation-induced cell death (AICD) or 'death by neglect' in the contraction phase of an immune response. Cytokine withdrawal induces 'death by neglect', which depends on the intrinsic pathway, whereas AICD is triggered by T cell receptor (TCR) restimulation of activated T cells<sup>33</sup>. TCR restimulation induces CD95L expression and thereby the CD95 signalling pathway<sup>166-169</sup>. The CD95L expression of T cells can induce autocrine apoptosis, but apoptosis can also be induced in neighbouring T cells, DCs and B cells (Figure 9)<sup>33, 170</sup>.

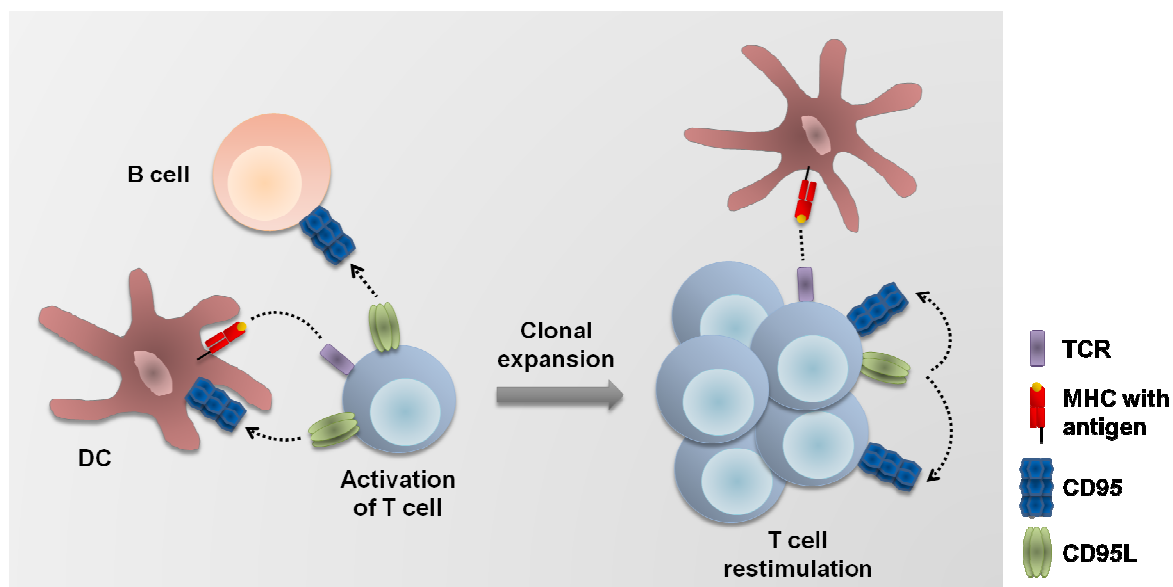


**Figure 9.** Activation-induced cell death of T cells. T cells are activated upon encounter of an antigen presented by APCs i.e. dendritic cells (DCs). Subsequently, T cells differentiate and clonally expand. CD95L expressed on T cells can induce apoptosis in B cells and DCs. Restimulation of activated T cells induces CD95L expression, which is an apoptosis-signal for the same or neighbouring cells. Adapted from Ramaswamy and Siegel, 2007<sup>170</sup>.

Resting T cells only express low levels of CD95 receptor and these cells are resistant to apoptosis<sup>171, 172</sup>. CD95 expression is induced upon T cell activation<sup>171, 172</sup>. Although both short- and long-term activated T cells have high CD95 expression, short-term activated T cells are apoptosis-resistant whereas long-term activated T cells are apoptosis-sensitive<sup>172, 173</sup> (Figure 10). Due to the comparable CD95 expression, AICD must be regulated down-stream of the death receptor. Indeed, short-term activated T cells have high c-FLIP<sub>s</sub> expression, which is downregulated in long-term activated T cells<sup>174, 175</sup>. Memory T cells are apoptosis-resistant and express CD95 at levels comparable with short-term activated T cells<sup>176</sup>.

The level of DISC formation distinguishes type I from type II cells. Short-term activated T cells have inefficient DISC assembly and behave like type II cells<sup>177</sup>. Additionally, these cells express high levels of Bcl-x<sub>L</sub>, which inhibits the mitochondrial pathway of apoptosis<sup>177</sup>. In contrast, long-term activated T cells have type I-characteristics with strong DISC formation and are sensitive for apoptosis<sup>177</sup>. Effector T cells secrete IL-2, which is a cytokine important for T cell proliferation and survival<sup>178</sup>. However, this cytokine also appears to regulate the elimination of T cells during the deletion phase of an immune response, since mice with IL-2 or IL-2 receptor deficiency accumulate activated T cells and develop autoimmunity<sup>179-181</sup>. Interestingly, long-term activated T cells cultured in the absence of IL-2 were considerably

less sensitive towards AICD<sup>177</sup>. This suggests that the switch from the apoptosis-resistant type II phenotype of short-term activated T cells to the apoptosis-sensitive type I characteristics of long-term activated T cells depends on IL-2.

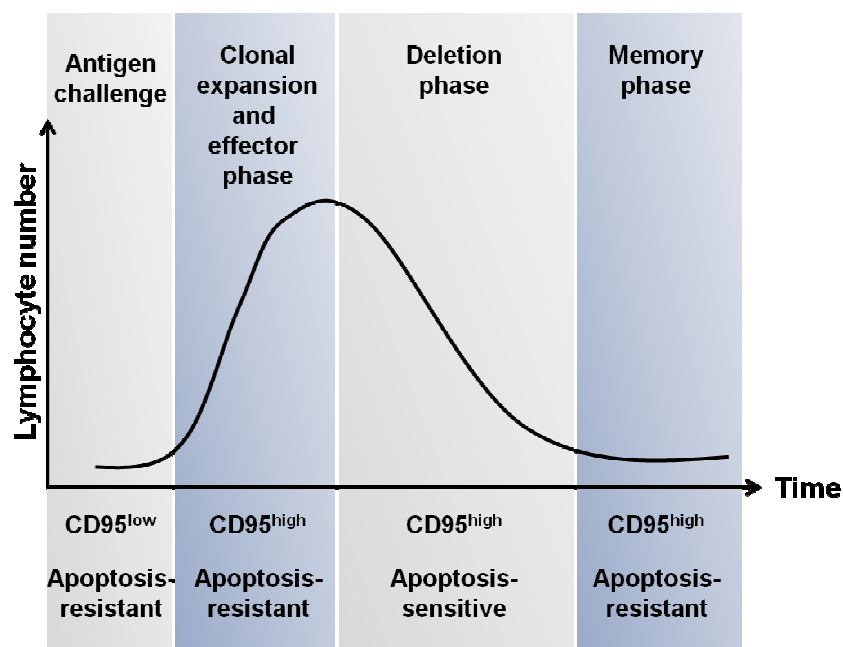


**Figure 10.** Naïve T cells express low levels of CD95 and are resistant to apoptosis. T cells become activated as they encounter an antigen, which leads to differentiation into effector T cells and clonal expansion. These T cells express high levels of CD95, but are resistant to apoptosis due to high c-FLIP<sub>s</sub> expression. The deletion phase begins when all antigen is removed. Down-regulation of c-FLIP sensitises T cells for AICD. Only few cells persist as memory cells to ensure a rapid immune response upon re-encounter of the same antigen. Memory T cells are apoptosis-resistant, although the expression level of CD95 is comparable to short-term activated T cells. Adapted from Krueger et al., 2003<sup>165</sup>.

The BH3-only protein Bim is also important for the shut-down of an immune response by sensing cytokine withdrawal and activating the intrinsic pathway<sup>94</sup>. Mice deficient in Bim and with mutated CD95 show drastic lymphoproliferation and rapidly develop severe autoimmunity, which suggests that Bim and CD95 cooperate to eliminate effector T cells in the deletion phase<sup>182-184</sup>. It is anticipated that Bim ensures deletion of T cells which received a strong antigen signal as for instance in an acute viral infection. In contrast, CD95 signalling is presumed to be more important in removal of the weakly stimulated T cells in chronic viral infections<sup>182-184</sup>.

CD95-mediated apoptosis is also critical in the elimination of antigen presenting cells. Naïve B cells only express very low levels of CD95, but the receptor is upregulated upon activation by e.g. CD40L<sup>185</sup>. Like T cells, B cells upregulate anti-apoptotic proteins upon activation to resist apoptosis, with c-FLIP playing an important role in the apoptosis-resistance<sup>186</sup>. Mice with CD95 deficiency in dendritic cells (DCs) or B cells develop systemic autoimmunity<sup>187</sup>. Clearly, the antigen-presenting cells need to be deleted to prevent accumulation of autoreactive B cells and chronically activated autoimmune T cells.

### 1.5. The role of death receptors and c-FLIP in cancer

Defects in the apoptosis machinery can lead to uncontrolled growth and tumour formation<sup>60</sup>. Notably, high levels of c-FLIP proteins have been identified in various cancer types<sup>188</sup>, prominently Hodgkin's lymphoma<sup>189, 190</sup> and melanoma<sup>141, 191</sup>. The upregulation of c-FLIP and other anti-apoptotic proteins is a mechanism for tumours to avoid apoptosis and evade immune surveillance<sup>188, 192, 193</sup>. Moreover, upregulation of c-FLIP has been suggested as a possible mechanism for resistance to therapeutic triggering of death receptors and the extrinsic apoptotic pathway, which is studied as a promising approach to cancer therapy. Current research apply genetic engineering to specifically direct the death ligands to tumour cells in order to circumvent the life-threatening side effects of systemic administration of TNF and CD95L<sup>194</sup>. In contrast to TNF and CD95L, TRAIL was reported to selectively induce apoptosis in various tumour cells *in vivo* without affecting cells in normal tissues<sup>195, 196</sup>. However, more recent studies described resistance against TRAIL-induced apoptosis in many primary tumour cells<sup>197</sup>. Upregulation of decoy receptors in tumour cells is a further proposed resistance-mechanism of cancer cells<sup>198</sup>. The decoy receptor DcR3 can bind CD95L, likewise is TRAIL interacting with DcR1 and DcR2<sup>71</sup>. However, it is still under debate whether decoy receptors can mediate tumour-resistance or not<sup>198</sup>. Interestingly, CD95 signalling also exerts non-apoptotic functions in tumour cells. Tumour growth is promoted by CD95 signalling<sup>199</sup>. Moreover, CD95 signalling induced invasiveness and motility, especially in apoptosis-resistant tumours<sup>200</sup>. These non-apoptotic functions of CD95 require activation of the NF-κB and mitogen-activated protein (MAP) kinase signalling pathways<sup>199, 200</sup>.

## 1.6. Non-apoptotic functions of c-FLIP

Proteins interacting at the death-inducing signalling complex (DISC) have additional functions apart from apoptosis-regulation. Complete knock-out of one of the proteins FADD, caspase-8 or c-FLIP results in embryonic lethality due to defects in vascularisation of the yolk sac and cardiac failure<sup>201-203</sup>, which clearly indicates that these proteins are crucial in embryonic development. FADD, c-FLIP<sub>L</sub> and caspase-8 have further non-apoptotic functions. Interestingly, these proteins have been reported to activate the NF- $\kappa$ B pathway<sup>204-207</sup>. However, it is not clear how c-FLIP<sub>L</sub> induces NF- $\kappa$ B activation. Kataoka and co-workers reported that overexpression of c-FLIP<sub>L</sub> in Jurkat cells lead to activation of NF- $\kappa$ B and the MAP kinase ERK as well as increased IL-2 production upon stimulation<sup>206</sup>. The activation of NF- $\kappa$ B was explained by recruitment of TNFR-associated factor 2 (TRAF2) and receptor-interacting protein 1 (RIP1) to the CD95 DISC by the p43 product of c-FLIP<sub>L</sub> (c-FLIP(p43)), which is a fragment arising from caspase-8 processing. Inhibition of caspase-8 blocked NF- $\kappa$ B activation induced by full-length c-FLIP<sub>L</sub> but not by c-FLIP(p43)<sup>206-208</sup>, suggesting that caspase-8 cleavage is necessary for the c-FLIP<sub>L</sub>-dependent NF- $\kappa$ B activation. Notably, Golks and colleagues reported cytoplasmic caspase-8 processing of c-FLIP proteins at D198, which results in a p22 fragment (p22-FLIP) consisting of the tandem DED domains<sup>148</sup>. p22-FLIP was observed to directly interact with the I $\kappa$ B kinase (IKK) complex and thereby induce NF- $\kappa$ B activation<sup>148</sup>. In contrast, effector T cells from mice overexpressing human c-FLIP<sub>S</sub> were reported to have reduced NF- $\kappa$ B activation<sup>209</sup>. Further investigation is necessary to clarify the role of c-FLIP proteins in NF- $\kappa$ B activation.

Caspase activity is required for T cell activation<sup>210, 211</sup> and mutations leading to inactive caspase-8 were shown to result in defects in lymphocyte activation both in mice<sup>212</sup> and men<sup>213</sup>. Caspase-8 deficiency is not lethal in humans in contrast to mice. This is probably due to the presence of caspase-10 in humans, which at least in part has the same function as caspase-8, whereas mice lack caspase-10<sup>214</sup>. Similar to caspase-8, c-FLIP<sub>L</sub> is important for T cell activation. Lens and colleagues reported increased proliferation in T cells from c-FLIP<sub>L</sub> transgenic mice upon stimulation with suboptimal doses of anti-CD3<sup>215</sup>. Likewise, Dohrman and co-workers showed increased proliferation and IL-2 responsiveness upon antigen stimulation of CD8<sup>+</sup> T cells from c-FLIP<sub>L</sub> transgenic mice, due to high CD25 expression<sup>208</sup>. Moreover, mice with T cell-specific c-FLIP deficiency had decreased IL-2 production and defective IL-2 responsiveness<sup>216, 217</sup>. Similar effects were observed in T cells both from mice

deficient in FADD or with dominant negative FADD expression<sup>203, 218, 219</sup> as well as mice with caspase-8 deficiency<sup>212</sup>. Additionally, T cell development was disturbed in mice with T cell-specific c-FLIP deficiency. Although mature lymphocytes developed in these mice, the numbers were severely reduced<sup>216, 217</sup>. Especially c-FLIP<sub>L</sub> was reported to play a central role in T cell proliferation. However, Zhang et al. showed that TCR stimulation induced normal activation of NF-κB and MAP kinase pathways in c-FLIP<sub>L</sub><sup>-/-</sup> mice<sup>220</sup>, which indicates that c-FLIP<sub>L</sub> mediates T cell proliferation independently of the NF-κB pathway.

Besides its function as an apoptosis-regulator, c-FLIP also regulates autophagy, a process where cytoplasmic components are recycled or removed. LC3 is a protein involved in autophagosome formation and becomes conjugated to the lipid phosphatidylethanolamine (PE) during this process<sup>29</sup>. The PE-binding of LC3 is catalysed by autophagy-related protein 3 (Atg3)<sup>29</sup> and c-FLIP proteins can inhibit autophagy by competing with LC3 for Atg3-binding<sup>221, 222</sup>.

Interestingly, the embryonic lethality of FADD-deficient mice was partially rescued by RIP1 deficiency<sup>223</sup> and the double knock-out of FADD and RIP3 completely rescued the embryonic development<sup>224</sup>. Likewise, the embryonic lethality of caspase-8-deficient mice was rescued by RIP3 deficiency<sup>225</sup>. The kinase activity of RIP1 and RIP3 is required for the cell death mode called necroptosis<sup>226</sup>. These kinases can be activated at complex IIb (also called the necrosome), which is formed upon TNF receptor stimulation or at the ripoptosome, which is assembled in response to double-stranded RNA or genotoxic stress<sup>28</sup>. Caspase-8 can inhibit necroptosis by processing of RIP1 and RIP3<sup>28</sup>. Notably, caspase-8 requires c-FLIP<sub>L</sub> heterodimerisation for catalytical activation and inhibition of RIP3-dependent necrosis<sup>227</sup>. These findings reveal a fine-tuned balance between apoptosis and necroptosis during the embryonic development, regulated by c-FLIP proteins.

Taken together, c-FLIP proteins are crucial regulators of life and death decisions in the cell. Further investigations are necessary to reveal the exact molecular mechanisms behind these decisions.

## 1.7. Aim of the thesis

c-FLIP proteins play a central role in the regulation of death receptor-mediated apoptosis. Caspase-8 activation is inhibited by c-FLIP proteins at the level of death receptors and thereby the apoptosis-signalling is disturbed<sup>118, 140, 149</sup>. There is a strict control of cell elimination and cell survival. Different diseases can develop if apoptosis is deregulated. Insufficient apoptosis may lead to tumour formation or autoimmunity, whereas immunodeficiency is a result of excessive apoptosis. The proteins interacting at the DISC complex are not only important regulators of apoptosis. c-FLIP<sub>L</sub>, caspase-8 and FADD have also been reported as activators of NF- $\kappa$ B signalling<sup>204, 206-208</sup>. Moreover, c-FLIP proteins were reported to regulate necroptosis and autophagy<sup>28, 221, 222</sup>. The aim of this thesis is to gain a better understanding of c-FLIP proteins' role in disease and to examine if there are unknown DISC-interacting proteins which could give a better insight into the complex signalling of the CD95 receptor. The three projects of this thesis are described below.

- c-FLIP proteins are often up-regulated in tumour cells as a mechanism to avoid apoptosis and to escape immune surveillance<sup>60</sup>. Moreover, high levels of c-FLIP can lead to resistance to therapeutics targeting death receptor-mediated apoptosis. Cancer of the urinary bladder is one of the most common cancers in the United States of America and Europe. The high morbidity and mortality of bladder cancers urge for improved treatment strategies and for understanding the mechanisms underlying resistance to immunotherapy and chemotherapy. For these reasons, the function of c-FLIP<sub>L</sub> and c-FLIP<sub>S</sub> isoforms in apoptosis-resistance of urothelial carcinoma was examined.
- DISC-interacting proteins not only have apoptotic functions, but have also been implicated in NF- $\kappa$ B signalling, proliferation and T cell activation. However, the exact signalling mechanisms are not fully understood. Moreover, the concept of the DISC model was questioned recently, since chain formation of DED-proteins at the DISC was revealed<sup>228, 229</sup>. The CD95 DISC and the influence of c-FLIP<sub>L</sub> on the complex was studied in this thesis to possibly identify novel interaction partners and gain further insight into the signalling pathways of death receptors.

- c-FLIP<sub>R</sub> is the only short isoform of c-FLIP expressed in mice. Nevertheless, it is so far unclear if c-FLIP<sub>R</sub> is expressed on the protein level and if so, the function of the protein remains to be investigated. c-FLIP proteins play an important role in immune cells and high expression levels are observed in activated T and B cells to protect these cells from apoptosis<sup>174, 186</sup>. The role of murine c-FLIP<sub>R</sub> in the immune system was investigated by using a mouse model with transgenic expression of murine c-FLIP<sub>R</sub> in all hematopoietic compartments.

## 2. Materials

### 2.1. Chemicals

Chemicals were purchased from Sigma Aldrich (Munich, Germany) or Roth (Karlsruhe, Germany) if not stated otherwise.

### 2.2. Materials and reagents for cloning

DNA for cloning was amplified by the proof-reading polymerase Phusion<sup>TM</sup> Flash (Finnzymes – Thermo Scientific, Vantaa, Finland) in peqSTAR 96 universal thermocyclers (PEQLAB Biotechnologie, Erlangen, Germany). Cleavage of vectors and inserts was performed with restriction enzymes from New England Biolabs (Ipswich, MA, USA), see 2.2.1. Cleaved vectors were ligated with the respective inserts by using T4 DNA ligase from New England Biolabs. Constructs were transformed into *Escherichia coli* (*E. coli*) strain Top10 (Life technologies, Grand Island, NY, USA) for amplification of plasmids. Bacteria were grown in LB-medium (1% w/v tryptone, 0.5% w/v yeast extract, 85.6 mM NaCl, 1 mM NaOH). Absorbance at 260 nm and 280 nm was measured by NANODROP 1000 spectrophotometer (PEQLAB) to determine the concentration of isolated DNA.

#### 2.2.1. Restriction enzymes

Restriction enzyme	Recognition site	Incubation temp.
<i>Bam</i> HI	5'...G   GATCC...3' 3'...CCTAG   G...5'	37 °C
<i>Nco</i> I	5'...C   CATGG...3' 3'...GGTAC   C...5'	37 °C
<i>Nhe</i> I	5'...G   CTAGC...3' 3'...CGATC   G...5'	37 °C
<i>Sma</i> I	5'...CCC   GGG...3' 3'...GGG   CCC...5'	25 °C
<i>Xba</i> I	5'...T   CTAGA...3' 3'...AGATC   T...5'	37 °C

### **2.3. DNA gel electrophoresis**

DNA was separated by gel electrophoresis in Perfect Blue™ Gel System (PEQLAB). Ethidium bromide containing gels were documented in a gel documentation system (INTAS science imaging, Goettingen, Germany).

### **2.4. Cell culture materials and devices**

Cells were cultured in cell culture flasks, 10 cm dishes, 6-well, 12-well, 24-well or 96-well plates from NUNC – Thermo Scientific (Waltham, MA, USA) in the incubator HERAcell 240 i (Thermo scientific) at 37°C, 5% CO<sub>2</sub> and 95% air humidity. Materials used for handling of cells were: 1.5 ml and 2 ml reaction tubes (Sarstedt, Nuembrecht, Germany), sterile 10 µl, 200 µl and 1000 µl pipette tips (Starlab, Ahrensburg, Germany), 5 ml, 10 ml and 25 ml pipettes (Sterilin - Thermo Scientific), 15 ml and 50 ml reaction tubes (Greiner-bio-one, Frickenhausen, Germany), 45 µm and 22 µm sterile syringe filters (Merck Millipore, Billerica, MA, USA). Centrifuges used were 5810R from Eppendorf (Hamburg, Germany) and Megafuge 1.0 from Heraeus SEPATECH (Osterode, Germany). Cells were handled in sterile hoods SterilGARD® III Advance° (The Baker Company, Sanford, ME, USA). Cell numbers were determined by Neubauer improved cell counting chambers (BRAND scientific, Wertheim, Germany) or Cellometer™ Auto T4 (Nexcelom Bioscience, Lawrence, MA, USA).

### 2.4.1. Cell culture reagents

Medium / supplement	Cat. No.	Company
DMEM (high glucose)	11965	Gibco <sup>®</sup> - Life technologies
IMDM	11875	Gibco <sup>®</sup> - Life technologies
RPMI 1640	12440	Gibco <sup>®</sup> - Life technologies
Fetal calf serum (FCS) (Lot. No. A 10108-2367)	A15-101	PAA (Pasing, Austria)
Sodium-pyruvate 100 mM	11360-070	Gibco <sup>®</sup> - Life technologies
Non-essential amino acids 100x	11140	Gibco <sup>®</sup> - Life technologies
Penicillin / streptomycin	15070	Gibco <sup>®</sup> - Life technologies
$\beta$ -mercaptoethanol 50 mM	21985-023	Gibco <sup>®</sup> - Life technologies
0.05% Trypsin/ EDTA	25300	Gibco <sup>®</sup> - Life technologies
Puromycin	P8833	Sigma Aldrich
G418	A 2912	Biochrom (Berlin, Germany)

### 2.4.2. Reagents and antibodies used for stimulation of cells

Reagent / antibody	Clone/ notation	Cat. No.	Reactivity	Company
anti-CD3	145-2C11	-	ms	self purified
anti-CD3	145-2C11	100331	ms	BioLegend (San Diego, CA, USA)
anti-CD28	E18	-	ms	self purified
anti-CD28	37.51	102112	ms	BioLegend
Concanavalin A	-	C2010	hu, ms	Sigma Aldrich
murine interleukin-2	-	402-ML	ms	R&D Systems (Minneapolis, MN, USA)
Phorbol 12-myristate 13-acetate (PMA)	-	P8139	hu, ms	Sigma Aldrich
Ionomycin (iono)	-	I-0634	hu, ms	Sigma Aldrich
CD95	2R2	-	hu	self purified
CD95	Jo2	554255	ms	BD Biosciences (Heidelberg, Germany)
CD95L	scErbB2	-	hu, ms	self purified
TRAIL	-	810904	hu	Novitec (Freiburg im Breisgau, Germany)
QVD - OPh	-	OPH109	hu, ms	MP Biomedicals (Aurora, OH, USA)
Protein A from <i>S. aureus</i>	-	6031	hu, ms	Sigma Aldrich
LPS from <i>E.coli</i>	-	L4516	hu, ms	Sigma Aldrich

The reactivity against mouse (ms) or human (hu) is shown.

## 2.5. Cell lines

HEK293T cells<sup>230-234</sup> were cultured in Dulbecco's modified Eagle's medium (DMEM) high glucose supplemented with 10% FCS and 50 µg/ml of penicillin and streptomycin. The parental urothelial cell lines VMcub1<sup>235</sup> and SD<sup>236</sup> were cultured in DMEM high glucose supplemented with FCS, penicillin and streptomycin as above. VMcub1 and SD cell lines stably transduced with shRNAs targeting a scramble sequence, c-FLIP<sub>L</sub>, c-FLIP<sub>S</sub> or both isoforms (c-FLIP<sub>L/S</sub>)<sup>237</sup> were cultured in DMEM high glucose with supplements as above. Jurkat E6.1 cells<sup>238, 239</sup> were cultured in Iscove's modified Dulbecco's medium (IMDM) supplemented with FCS, penicillin and streptomycin as above.

## 2.6. Mouse strain

The mouse strain vavFLIP<sub>R</sub> was generated by the transgenic core facility of the University of Duesseldorf, Germany from a transgenic construct with murine c-FLIP<sub>R</sub> cDNA in the vector HS21/45 vav-hCD4<sup>240</sup>. Mice carrying the transgenic construct were backcrossed for more than ten generations to C57BL/6 mice. WT littermates were used as control animals. Genotyping was performed by PCR on tail biopsies using KAPA Mouse Genotyping Hot Start Kit (PEQLAB) according to manufacturer's protocol. All of the animals were kept under specific pathogen free (SPF) conditions in the animal facilities of the Helmholtz Centre for Infection Research, Brunswick, Germany. All breeding and experiments were performed in accordance with the guidelines of national and local authorities.

## 2.7. Western blotting materials and reagents

Protein concentrations were determined by bicinchoninic acid (BCA) assay following manufacturer's instructions (Pierce Protein Research Products – Thermo Scientific, Rockford, IL, USA). The BCA assay was measured at 562 nm in the Infinite<sup>®</sup> M200 microplate-reader (TECAN, Maennedorf, Switzerland). Gel electrophoresis and protein transfer was performed in devices purchased from BioRad Laboratories (Hercules, USA). Western blots were developed with a chemiluminiscent reagent in the Fusion FX-7 camera (Vilber Lourmat, Eberhardzell, Germany).

### 2.7.1. Primary antibodies

Antibody	Clone/ notation	Reactivity	Isotype	Species	Company
A20	A-12	hu	IgG2a	mouse	Santa Cruz Biotechnology (Santa Cruz, CA, USA)
$\beta$ -actin	AC-74	ms, hu	IgG2a	mouse	Sigma Aldrich
Bcl-2	C-2	hu, ms, rt	IgG1	mouse	Santa Cruz Biotechnology
caspase-3	AF-605-NA	hu	IgG	goat	R&D Systems
cleaved caspase-3 (Asp175)	5A1E	hu, ms, rt, mk	IgG	rabbit	Cell Signaling Technology (Danvers, MA, USA)
caspase-8	1G12	ms	IgG	rat	Enzo Life Sciences (Loerrach, Germany)
caspase-8	12F5	hu	IgG2b	mouse	gift from Dr. K. Schulze-Osthoff (Tuebingen, Germany)
caspase-9	#9502	hu	IgG	rabbit	Cell Signaling Technology
CD95 / Fas	C-20	hu	IgG	rabbit	Santa Cruz Biotechnology
c-FLIP	Dave-2	hu, ms	IgG	rat	Enzo Life Sciences
c-FLIP	Dave-2	hu, ms	IgG	rat	Adipogen (San Diego, CA, USA)
c-FLIP	NF6	hu	IgG1	mouse	Enzo Life Sciences
FADD	1F7	hu, ms	IgG1	mouse	Merck Millipore
IKK $\alpha$	B-8	hu, ms, rt	IgG2b	mouse	Santa Cruz Biotechnology
IKK $\gamma$	FL-419	hu, ms, rt	IgG	rabbit	Santa Cruz Biotechnology
I $\kappa$ B $\alpha$	112B2	hu, ms, rt, mk	IgG2a	mouse	Cell Signaling Technology
p-I $\kappa$ B $\alpha$ (Ser32)	14D4	hu, ms, rt, mk	IgG	rabbit	Cell Signaling Technology
RIP	38	hu	IgG2a	mouse	BD Biosciences
TRAF-2	C90-481	hu	IgG2a	mouse	BD Biosciences
$\alpha$ -tubulin	DM-1A	hu, ms	IgG1	mouse	Sigma Aldrich
XIAP	48	hu, ms, rt	IgG1	mouse	BD Biosciences
FLAG <sup>®</sup> -tag	M2	-	IgG1	mouse	Sigma Aldrich
HA-tag	12CA5	-	IgG2b	mouse	Roche (Grenzach - Wyhlen, Germany)

The reactivity against human (hu), mouse (ms), rat (rt) or monkey (mk) is shown.

### 2.7.2. Horseradish peroxidase conjugated secondary antibodies

Reactivity	Species	Cat. No	Company
mouse IgG	goat	sc-2031	Santa Cruz Biotechnology
mouse IgG1	goat	1070-05	Southern Biotechnology (Birmingham, AL, USA)
mouse IgG2a	goat	1080-05	Southern Biotechnology
mouse IgG2b	goat	1090-05	Southern Biotechnology
goat IgG	rabbit	6165-05	Southern Biotechnology
rabbit IgG	goat	4030-05	Southern Biotechnology
rat IgG	goat	3050-05	Southern Biotechnology

## 2.8. Materials and reagents for flow cytometry

### 2.8.1. Flow cytometry devices

Fluorescently labelled cells were analysed in FACS Calibur, FACS Canto or LSRII (BD Biosciences). Sorting of cells was performed in an FACS Aria II (BD Biosciences) or MoFlo (Beckham Coulter, Indianapolis, IN, USA). Data was analysed by the FlowJo software (TreeStar, Ashland, OR, USA).

### 2.8.2. Fluorescent dyes

Reagent	Excitation	Emission	Company
LIVE/DEAD <sup>®</sup> Near IR fluorescent reactive dye	750 nm	775 nm	Life technologies
LIVE/DEAD <sup>®</sup> Blue fluorescent reactive dye	350 nm	450 nm	Life technologies
Tetramethylrhodamine ethyl ester (TMRE)	549 nm	574 nm	Enzo Life Sciences
7-amino-actinomycin D (7AAD)	543 nm	647 nm	BD Biosciences

### 2.8.3. Human antibodies

Reactivity	Fluorochrome	Clone/ notation	Isotype	Company
CD95	-	2R2	mouse IgG3	self-made
TRAIL-R1 (DR4)	-	HS101	mouse IgG1	Enzo Life Sciences
TRAIL-R2 (DR5)	PE	DJR2-4	mouse IgG1, $\kappa$	eBioscience
TNF-R1	-	H398	mouse IgG2a	gift of Dr. H. Wajant, Wuerzburg, Germany
CD3	Alexa Fluor <sup>®</sup> 647	HIT3a	rat IgG2a, $\kappa$	BioLegend
CD4	Pacific blue	RPA-T4	mouse IgG1, $\kappa$	BioLegend
CD8	PerCP Cy5.5	HIT8a	mouse IgG1, $\kappa$	BioLegend
CD25	PE	BC96	mouse IgG1, $\kappa$	BioLegend
CD69	APC Cy7	FN50	mouse IgG1, $\kappa$	BioLegend
Active caspase-3	Horizon V450	C92-605	rabbit IgG	BD Biosciences

TNF-R1, TRAIL-R1 and CD95 antibodies were labelled with PE-conjugated goat-anti-mouse secondary antibody (Jackson ImmunoResearch, Suffolk, UK).

#### 2.8.4. Murine antibodies

Reactivity	Fluorochrome	Clone/ notation	Isotype	Company
CD3	eF450	17A2	rat IgG2b, $\kappa$	eBioscience (San Diego, CA, USA)
CD3	FITC	145-2C11	hamster IgG1, $\kappa$	BD Biosciences
CD4	Pacific blue	RM4-5	rat IgG2a, $\kappa$	BioLegend
CD4	Horizon V500	RM4-5	rat IgG2a, $\kappa$	BD Biosciences
CD8	APC	53-6.7	rat IgG2a, $\kappa$	Biolegend
CD8	FITC	53-6.7	rat IgG2a, $\kappa$	BD Biosciences
CD11b	PE Cy7	M1/70	rat IgG2b, $\kappa$	eBioscience
CD11c	APC eFluor 780	N418	hamster IgG	eBioscience
CD19	PerCP Cy5.5	1D3	rat IgG2a, $\kappa$	eBioscience
CD19	FITC	1D3	rat IgG2a, $\kappa$	BD Biosciences
CD25	PE Cy7	PC61.5	rat IgG1, $\lambda$	BD Biosciences
CD44	PE	IM7	rat IgG2b, $\kappa$	eBioscience
CD45R (B220)	APC	RA3-6B2	rat IgG2a, $\kappa$	eBioscience
CD49b	APC	Dx5	rat IgM, $\kappa$	eBioscience
CD62L	PerCP Cy5.5	MEL-14	rat IgG2a, $\kappa$	eBioscience
CD95	PE	Jo-2	hamster IgG2, $\lambda$ 2	BD Biosciences
F4/80	PE	BM8	rat IgG2a, $\kappa$	eBioscience
Gr1	Pacific blue	RB6-8C5	rat IgG2b, $\kappa$	eBioscience
AnnexinV	APC	-	-	BD Biosciences

#### 2.9. Oligonucleotides

Salt free, HPSF or HPLC purified, lyophilised oligonucleotides were purchased from Eurofins MWG Operon (Ebersberg, Germany).

Cloning c-FLIP isoforms into the vector pIRES2-EGFP	
Sequence (5' → 3')	
5' c-FLIP fwd	GGC TAG CCA TGT CTG CTG AAG TCA TCC A
3' c-FLIP <sub>L</sub> rev	GCC CGG GCT TAT GTG TAG GAG AGG ATA A
3' c-FLIP <sub>R</sub> rev	GCC CGG GCT CAT GCT GGG ATT CCA TAT G
3' c-FLIP <sub>S</sub> rev	GCC CGG GCT CAC ATG GAA CAA TTT CCA A

<b>Attaching HA-tag to c-FLIP<sub>L</sub> and cloning into the vector pEF/myc/cyto</b>	
<b>Sequence (5' → 3')</b>	
HA-tag oligo fwd	GCA CCA TGG CCT ACC CAT ACG ACG TGC CTG ACT ACG CCT CTG CTG AAG TCA TCC ATC A
HA-tag oligo rev	TGA TGG ATG ACT TCA GCA GAG GCG TAG TCA GGC ACG TCG TAT GGG TAG GCC ATG GTG C
c-FLIP <sub>L</sub> HA-tag fwd	ACG ACG TGC CTG ACT ACG CCT CTG CTG AAG TCA TCC ATC AGG TTG
c-FLIP <sub>L</sub> HA-tag rev	CTA TCT AGA TTA TGT GTA GGA GAG GAT AAG TTT CT
HA-tag fwd	GCA CCA TGG CCT ACC CAT ACG AC
<b>Quantitative</b>	
<b>RT PCR</b>	
<b>Sequence (5' → 3')</b>	
c-FLIP <sub>L</sub> fwd	CCT AGG AAT CTG CCT GAT AAT CGA
c-FLIP <sub>L</sub> rev	TGG GAT ATA CCA TGC ATA CTG AGA TG
c-FLIP <sub>S</sub> fwd	GCA GCA ATC CAA AAG AGT CTC A
c-FLIP <sub>S</sub> rev	ATT TCC AAG AAT TTT CAG ATC AGG A
GAPDH fwd	ATC ACC ATC TTC CAG GAG CGA GAT C
GAPDH rev	GGC AGA GAT GAT GAC CCT TTT GGC
TBP fwd	CGA AAC GCC GAA TAT AAT CC
TBP rev	CGT GGC TCT CTT ATC CTC A
<b>Sequencing</b>	
<b>Sequence (5' → 3')</b>	
c-FLIP <sub>L</sub> fwd seq	TGG GAG AAG TAA AGA ACA AAG AC
c-FLIP <sub>L</sub> rev seq	AAG TGA AGG TGT CTC GAA GAA
CMV fwd	CGC AAA TGG GCG GTA GGC GTG
EF1alpha fwd	TCT CAA GCC TCA GAC AGT GGT TC
pCR3.1-BGH rev	TAG AAG GCA CAG TCG AGG
T7	TAA TAC GAC TCA CTA TAG GG
T3	AAT TAA CCC TCA CTA AAG GG
<b>Genotyping</b>	
<b>Sequence (5' → 3')</b>	
c-FLIP fwd	GCC TGA AGA ACA TCC ACA GAA TAG
SV40 poly A rev	CTC ATC AAT GTA TCT TAT CAT GTC
β-actin fwd	TGT TAC CAA CTG GGA CGA CA
β-actin rev	TCT CAG CTG TGG TGG TGA AG

## 2.10. Frequently used buffers

Group	Buffer	Contents
Flow cytometry buffers	PBS	155.17 mM NaCl
		2.97 mM Na <sub>2</sub> HPO <sub>4</sub>
		1.06 mM K <sub>2</sub> HPO <sub>4</sub>
		pH 7.4
	FACS buffer	2% w/v BSA in PBS
		0.01% v/v NaN <sub>3</sub>
	10x annexinV binding buffer	0.1 mM HEPES / NaOH
		1.4M NaCl
		25 mM CaCl <sub>2</sub>
		pH 7.4
Lysis buffers and additives	TPNE lysis buffer	PBS
		ad 300 mM NaCl
		2mM EDTA
		1% v/v Triton X-100
	DISC lysis buffer	30 mM Tris/HCl
		150 mM NaCl
		10% v/v glycerol
		1% v/v Triton X-100
	100x protease inhibitors	2 mM EDTA
		10mM NaF
pH 7.4		
100 µg/ml aprotinin		
	100 µg/ml leupeptin	
	100 µg/ml pepstatin A	
	100 µg/ml chymostatin	

Group	Buffer	Contents
Western blot buffers	5x reducing sample buffer	50 mM Tris, pH 6.8
		50% v/v glycerol
		10% w/v SDS
		25% v/v $\beta$ -mercaptoethanol
	Running buffer	0.25 mg/ml bromphenol blue
		25 mM Tris, pH 8.0
		192 mM glycerol
	Transfer buffer	1% v/v SDS
		25mM Tris, pH 8.0
		192 mM glycerol
	TBS	20% v/v methanol
		137 mM NaCl
2.68 mM KCl		
24.76 mM Tris		
Blocking buffer	pH 7.8	
	5% w/v non-fat dry milk	
Wash buffer	0.05% v/v Tween-20 in TBS	
	0.05% Tween-20 in TBS	

### 3. Experimental procedures

#### 3.1. Molecular biology methods

##### 3.1.1. Polymerase chain reaction (PCR)

PCR amplifications for cloning were performed with the proof-reading polymerase Phusion™ Flash (Finnzymes – Thermo Scientific). Each reaction contained 1-10 ng of template DNA, 0.5 µM of both forward and reverse primer, 2× Phusion™ Flash PCR Master Mix (Finnzymes – Thermo Scientific) and dH<sub>2</sub>O to a final volume of 20 µl. The PCR was performed in peqSTAR 96 universal thermocyclers (PEQLAB) with the standard programme:

Cycle step	Temp.	Time	Cycles
Initial denaturation	98 °C	10s	1
Denaturation	98 °C	1s	30
Annealing	x °C	5s	
Elongation	72 °C	15s/kb	
Final extension	72 °C	1min	1
	8 °C	hold	

The annealing temperature was set 2-3 °C below the melting temperature ( $T_M$ ) of the primers.

##### 3.1.2. DNA gel electrophoresis

Loading dye (Thermo Scientific) was added to samples before separation by gel electrophoresis in 1-2%-agarose gels containing 0.5µg/ml ethidium bromide (EtBr) in 1×TAE buffer (40 mM Tris Base, 20 mM acetic acid, 1mM EDTA, pH 8.5). The samples were separated in an electric field at 10V/cm for 45-60 minutes. The DNA fragments with intercalated EtBr were visualised under ultraviolet light ( $\lambda=254$  nm). GeneRuler™ 1 kb DNA ladder (Thermo Scientific) was used to determine the size of DNA fragments.

For DNA to be used for cloning; bands of interest were cut out of the gel and purified with Zymoclean™ Gel DNA Recovery kit (Zymo Research, Irvine, CA, USA), according to the manufacturer's manual.

### 3.1.3. Cloning

Vectors and inserts were cleaved with restriction enzymes from New England Biolabs (NEB; see 2.2.1.). The reactions contained 2-3 µg plasmid or PCR product from an 25-50 µl amplification, 5 U restriction enzyme/enzymes (New England Biolabs), the appropriate NEB buffers and dH<sub>2</sub>O to a final volume of 50 µl. The samples were incubated at 37 °C for up to 3 h. The incubation time was shortened for time-saver enzymes or enzymes with star activity.

20-80 ng of linearised vector and insert were ligated in reactions containing 1µl T4 DNA ligase (New England Biolabs), 10× ligase buffer and dH<sub>2</sub>O added to 20 µl. Samples were incubated for 1 h at room temperature or at 15 °C over night.

c-FLIP<sub>L</sub> was cloned into pBluescript (Stratagene – Agilent Technologies, Santa Clara, CA, USA) with the enzymes *Bam*HI and *Xba*I. The c-FLIP isoforms c-FLIP<sub>L</sub>, c-FLIP<sub>S</sub> and c-FLIP<sub>R</sub> were inserted into the pIRES2-EGFP vector (Clontech, Mountain View, CA, USA) by *Nhe*I and *Sma*I cleavage. HA-c-FLIP<sub>L</sub> was cleaved with the enzymes *Nco*I and *Xba*I followed by insertion into the vector pEF/myc/cyto (Life technologies).

### 3.1.4. Transformation

Plasmids were transformed into competent *E.coli* Top10 bacteria (Life technologies). *E.coli* Top10 were thawed on ice, thereafter 100-200 ng plasmid DNA was added to the bacteria and the bacterial suspension was incubated on ice for 20 min. Bacteria were heat shocked in a water bath at 42 °C for 30 sec followed by incubation on ice for 2 min. 500 µl LB-medium (see 2.2.) was added to the tubes followed by incubation at 37 °C, 800 rpm in a Thermomixer comfort (Eppendorf) for 45 min. Bacteria was plated on LB-agar plates containing the appropriate antibiotics (100 µg/ml ampicillin or 50 µg/ml kanamycin) and the plates were incubated at 37 °C over night. The next day, colonies were picked into 5 ml LB medium for mini cultures followed by incubation at 37 °C, 280 rpm, over night. Plasmid DNA was isolated by Zyppy<sup>TM</sup> Plasmid Miniprep kit (Zymo research) according to supplier's protocol. For maxi cultures, 500 µl from a mini culture was inoculated into 200 ml LB-medium. Flasks containing the bacterial suspension were incubated at 37 °C, 180 rpm, over night. The next day, plasmid DNA was isolated by QIAfilter<sup>TM</sup> Plasmid Maxi kit (Qiagen, Hilden, Germany) by following the manufacturer's manual. DNA concentrations were determined by measuring

the absorbance at 260 nm and 280 nm in a NANODROP 1000 spectrophotometer (PEQLAB). 1 µg plasmid was analytically cleaved with 1 U restriction enzyme/enzymes (New England Biolabs), the appropriate NEB buffer and dH<sub>2</sub>O to a final volume of 30 µl. The samples were incubated at 37 °C for up to 1.5 h.

### **3.1.5. Quantitative real-time PCR of patient and tissue samples**

Tissue samples were obtained from patients undergoing cystectomy for urothelial carcinoma at the Department of Urology of the Heinrich-Heine-University Duesseldorf between 1995 and 2004. Twenty-four patients were male and seven were female; average age at surgery was 69.9 years (range 54–94 years). The samples were selected to comprise all stages and included three tumours each staged as pTa or pT1, 5 staged as pT2, 11 staged as pT3 and 7 staged as pT4. Lymph node metastases were present in seven patients. The lymph node status was not determined further for two additional patients with >pT2 cancers. Eleven cancers were graded as G2 and 20 as G3. Morphologically normal tissue from 10 patients was used for comparison. The use of patient tissues was approved by the Ethics Committee of the Medical Faculty of the Heinrich-Heine-University Duesseldorf. Total RNA was isolated from 5-10×10<sup>6</sup> cells with the RNeasy kit (Qiagen). Real-time PCR was carried out on an Applied Biosystems 7300 Real-Time PCR system using the QuantiTect SYBR Green RT-PCR Kit (Qiagen) according to the manufacturer's instructions. Measurements were run in triplicates and normalised to glyceraldehyde 3-phosphate dehydrogenase (GAPDH) or TATA-binding protein (TBP) values. These assays were performed in cooperation with Dr. Nana Ueffing, Prof. Wolfgang Schulz and Christiane Hader, Heinrich-Heine-University, Duesseldorf.

## **3.2. Cellular and protein biochemical methods**

### **3.2.1. Transfection and lentiviral infection of cells**

Transient transfections of HEK293T, VMCub1 and SD cells were performed with JetPEI (Polyplus transfection, Illkirch, France) according to the manufacturer's manual.

VMCub1 and SD cells were stably transduced by lentiviral infections of shRNA targeting c-FLIP<sub>L</sub>, c-FLIP<sub>S</sub> or both isoforms (c-FLIP<sub>L/S</sub>). Generation of c-FLIP<sub>S</sub> shRNA was previously

described<sup>147</sup>. The c-FLIP MISSION TRC shRNA Target Set was purchased from Sigma-Aldrich. shRNAs were cloned into the lentiviral vector pLKO.1. Lentiviral vectors were co-transfected with the envelope vector pMD2.G (Addgene no. 12259) and the gag-pol expression plasmid pCMV\_dR8.2dvpr (Addgene no. 8455) into HEK293T cells as described above. Lentiviruses (LVs) were collected 24 and 48 h after transfection. Crude virus was filtered through 0.45 µm PVDF filters (Merck Millipore), concentrated by ultracentrifugation at 19 500 × g for 2 h at 12°C and stored at -80°C until further use. SD and VMCub1 cells were infected by adding LVs and 5 µg/ml polybrene (Sigma Aldrich) to 2×10<sup>6</sup> cells. Cells were centrifuged at 860 g for 1.5 h at 30°C followed by incubation at 37°C over night. Stably transfected clones were selected by limited dilution in medium containing 4 µg/ml puromycin (Sigma Aldrich). Specific knockdown of the various c-FLIP isoforms was verified by Western blotting.

Foreign DNA was introduced to Jurkat E6.1 cells by electroporation. For this purpose, 20×10<sup>6</sup> cells were washed with PBS containing Ca<sup>2+</sup> and Mg<sup>2+</sup> (Biochrom). Thereafter cells were resuspended in 350µl PBS containing Ca<sup>2+</sup> and Mg<sup>2+</sup> and transferred to a cuvette (Electroporation Cuvette Plus<sup>TM</sup>, gap size 4 mm, BTX<sup>®</sup> Harvard Apparatus, Holliston, MA, USA). 30 µg DNA was added to the cuvette, cells and DNA were mixed directly followed by pulsing in a BioRad Gene Pulser<sup>®</sup> II with 230 V/ 950 µF, high capacitance. Debris formed were removed and cells were transferred back to cell culture flasks with medium. Cells were allowed to rest for one day, thereafter two weeks selection with 2 µg/ml puromycin or 2 mg/ml G418 started. Clones were generated by seeding single cells in 96-well plates.

### 3.2.2. Lysis of cells

5-10×10<sup>5</sup> cells were lysed in 30-50 µl TPNE lysis buffer for Western blot analyses (see 2.10.) with addition of 1 mM PMSF and 1 µg/ml of each leupeptin, aprotinin, chymostatin and pepstatin A). 10-50×10<sup>6</sup> cells to be used for immunoprecipitation were lysed in 0.75-1.5 ml DISC lysis buffer (see 2.10. with addition of PMSF, leupeptin, aprotinin, chymostatin and pepstatin A as above). Samples were incubated on ice for 15-30 min followed by centrifugation at 14,000 rpm, 4 °C for 15 min in an Eppendorf table centrifuge 5417R. Supernatants were transferred to 1.5 ml reaction tubes to be used for further experiments.

### 3.2.3. Immunoprecipitation of the DISC complex

10-50×10<sup>6</sup> cells per sample (2×10<sup>6</sup> cells/ml) were either left untreated or stimulated with CD95L (scErbB2; sc – single chain, ErbB2 – part of the EGF receptor which enhances multimerisation) or 2 µg/ml anti-CD95 (2R2) crosslinked with 10 ng/ml protein A for 30 min. The stimulation was stopped by adding 5 volumes of ice-cold PBS, followed by centrifugation at 4°C, 1500 rpm, for 5 min. The cells were washed one further time with PBS and were thereafter lysed as described above (3.2.2.). 15-20 µl of the whole cell lysates were saved for the Western blot as input control. The remaining supernatants were transferred to reaction tubes containing the appropriate pre-washed beads for the immunoprecipitation (protein A sepharose – Sigma Aldrich, protein G Dynabeads<sup>®</sup> - Life technologies, Oslo, Norway, Flag<sup>®</sup>M2-agarose – Sigma Aldrich, monoclonal anti-HA-agarose – Sigma Aldrich, anti-mouse IgG (whole antibody)-agarose for preclears – Sigma Aldrich). Beads for unstimulated samples were pre-incubated with 500 µl CD95L or 2 µg anti-CD95 (2R2) in 500 µl TBS for 2 h with rotation at 4 °C. Thereafter beads were washed three times with 500 µl TBS before whole cell lysates were incubated on beads with rotation at 4 °C for 1.5-3 h. After incubation, unbound proteins were removed by washing the beads three times with 500 µl DISC lysis buffer. Dry beads were resuspended in 25 µl 1×RSB buffer (see 2.10.) and boiled at 95 °C for 5 min. Interacting proteins were identified by SDS-PAGE (see 3.2.4.) followed by Western blot analysis (see 3.2.5.) or mass spectrometry analysis (see 3.2.6.).

### 3.2.4. SDS-polyacrylamide gel electrophoresis (SDS-PAGE)

Total protein concentration in samples was determined by BCA assay (Pierce Protein Research Products – Thermo Scientific) according to manufacturer's instructions. 5×RSB buffer (see 2.10.) was added to 20-40 µg of each sample and boiled at 95 °C for 5 min. Proteins were separated in 12% polyacrylamide gels in 1×running buffer (see 2.10.) with the standard PageRuler<sup>™</sup> prestained protein ladder (Thermo Scientific) at 80-120 V in a BioRad "Tetra Cell". Proteins were either blotted onto PVDF membranes (see 3.2.5.) or the gels were stained with coomassie. For coomassie staining, gels were washed three times 5 min in dH<sub>2</sub>O, thereafter fixed two times 1 h in gel fixation buffer (30% ethanol, 10% acetic acid in dH<sub>2</sub>O) and stained with coomassie (PageBlue<sup>™</sup> Protein Staining Solution, Thermo Scientific, Rockford, IL, USA) for 1-2 h and washed again three times 5 min in dH<sub>2</sub>O.

### 3.2.5. Western blotting

A BioRad “Criterion blotter” was used to transfer proteins separated by SDS-PAGE to a PVDF membrane (GE Healthcare, Buckinghamshire, UK) in 1× transfer buffer (see 2.10.) at 75 V for 1.5 h. After transfer, membranes were incubated in 5% non-fat dry milk in TBS/Tween (blocking buffer; see 2.10.) for 1 h. Membranes were thereafter incubated in primary antibodies over night at 4 °C. The next day, unbound antibodies were removed by washing membranes three times 10 min in TBS/Tween (see 2.10.) followed by incubation in horse-radish peroxidase-coupled secondary antibodies (1:3,000 – 1:20,000) for 1 h at room temperature. Subsequently, membranes were washed again as above and developed with one of the chemiluminiscent reagents SuperSignal<sup>®</sup> West Dura Extended Duration Substrate, SuperSignal<sup>®</sup> West Femto Maximum Sensitivity (Pierce Protein Research Products – Thermo Scientific) or ECL Select<sup>™</sup> Western Blotting Detection Reagent (GE Healthcare) in the Fusion FX-7 camera (Vilber Lourmat). Antibodies were removed from membranes by using ReBlot plus mild antibody stripping solution (Merck Millipore) according to manufacturer’s protocol.

### 3.2.6. Mass spectrometry

#### 3.2.6.1. *Preparation of gel pieces*

Slices from the coomassie gel were cut in small pieces, washed with 30% acetonitrile (ACN) in 50 mM ammonium hydrogencarbonate (BIC), reduced with 50 mM dithiothreitol in 50 mM BIC for 1 h at 56°C, followed by alkylation with 50 mM iodoacetamide in 50 mM BIC for 1 h and incubation in 100% ACN. Finally, gel slices were dried in a SpeedVac centrifuge.

#### 3.2.6.2. *Tryptic digest*

Dried gel pieces were rehydrated in 50 mM BIC containing trypsin at a final ratio of 50:1 (protein:protease) followed by incubation at 37°C over night. Peptides were washed out three times with at least 10 gel volumes of water, 1% trifluoroacetic acid (TFA) and finally with 0.2% TFA in 30% ACN.

### **3.2.6.3. RP18 CleanUp**

After evaporation of all fluid in the SpeedVac, the peptides were desalted onto ZipTip's. Peptides were resolubilised in 3% ACN containing 0.2% TFA and adsorbed to the RP18 material. After washing with binding solution, the peptides were eluted with 60% ACN containing 0.2% TFA. The peptides were dried in a SpeedVac to remove the organic phase, resolubilised in 12 µl 3% ACN containing 0.2% TFA and centrifuged in an ultracentrifuge. Peptides were used for LC-MSMS.

### **3.2.6.4. LC-MS/MS and data analyses**

LC-MS/MS analyses were performed on a Dionex UltiMate 3000 n-RSLC system connected to an LTQ Orbitrap Velos mass spectrometer (Thermo Scientific). Peptides were loaded onto a C18 pre-column (3 µm, Acclaim, 75 µm x 20 mm, Dionex), washed for 3 min at a flow rate of 6 µl/min. Subsequently, peptides were separated on a C<sub>18</sub> analytical column (3 µm, Acclaim PepMap RSLC, 75 µm x 25 cm, Dionex) at 350 µl/min via a linear 30-min gradient from 100% buffer A (0.1% formic acid in water) to 25% B (99.9% acetonitrile with 0.1% formic acid) followed by a 15 min gradient from 25% buffer to 80% UPLC buffer B. The LC system was operated with Chromeleon Software (version 6.8, Dionex), which was embedded in the Xcalibur software (version 2.1, Thermo Scientific). The effluent from the column was electrosprayed (Pico Tip Emitter Needles, New Objectives, Woburn, MA, USA) into the mass spectrometer. The mass spectrometer was controlled by Xcalibur software and operated in the data-dependent mode allowing the automatic selection of a maximum of 5 doubly and triply charged peptides and their subsequent fragmentation. A dynamic exclusion allowed up to 3 repeats. Peptide fragmentation was carried out using LTQ settings (Min signal 2000, Isolation width 4, Normalised collision energy 35, Default Charge State 4 and Activation time 10 ms). MS/MS raw data files were processed via Mascot Daemon-aided (version 2.8, Matrix Science) searches against UniProtKB/Swiss-Prot protein database (release 2011\_03, with 525,997 entries on a Mascot server (V. 2.3.02, Matrix Science, Boston, MA, USA) or using the Proteome Discoverer program Version 1.3 (Thermo Scientific). The following search parameters were used: enzyme - trypsin; maximum missed cleavages - 1; fixed modification - Carbamidomethylation (C); variable modifications - oxidation (M), phosphorylation of S, T and Y, respectively; peptide tolerance, 5 ppm; MS/MS tolerance, 0.4 Da. The mass spectrometry analyses were performed by Dr. Josef Wissing (Cellular Proteome Research group, Helmholtz Centre for Infection Research, Brunswick, Germany)

### 3.2.7. Flow cytometry analyses

For flow cytometry analysis,  $1 \times 10^6$  cells were washed in 1 ml PBS at 4 °C, 1500 rpm, 5 min. Cells were resuspended in 100 µl PBS and stained with LIVE/DEAD<sup>®</sup> (see 2.7.1.; Life technologies) for 30 min, 4 °C in the dark, if required. Thereafter cells were washed in 1 ml PBS as above.

Surface markers were stained in 100 µl FACS buffer (see 2.10.). Cells were incubated with appropriate dilutions of fluorochrome-conjugated or unconjugated antibodies (see 2.7.2. and 2.7.3.) at 4 °C for 20 min in the dark. Unbound antibodies were washed away with 1 ml FACS buffer. In the case of unconjugated antibodies, cells were incubated with a secondary PE-conjugated antibody (0.75 µg per test) for 20 min as above followed by another wash step.

For intracellular staining of active caspase-3, cells were fixed and permeabilised in 100 µl BD Cytotfix/Cytoperm<sup>™</sup> fixation and permeabilisation solution for 20 min at 4 °C. Thereafter cells were washed two times with 1 ml 1× BD Perm/Wash<sup>™</sup> buffer. Staining of active caspase-3 was done in 50 µl BD Wash/Perm<sup>™</sup> buffer with incubation at 4 °C for 30 min followed by a further washing step with 1× BD Perm/Wash<sup>™</sup> buffer as above.

Apoptosis was assayed by AnnexinV and 7-amino-actinomycin D (7AAD) staining. For this staining, surface marker staining was first performed as above. Thereafter cells were resuspended in 100 µl 1× annexin binding buffer (see 2.10.) containing 3 µl AnnexinV and 0.2 µg 7AAD. Samples were incubated at room temperature for 15 min and finally, 150 µl 1× annexin binding buffer was added.

Another method used to assay apoptosis was quantification of the sub-G1 DNA content. For this assay, PBS washed cells were incubated in 250 µl Nicoletti buffer (see 2.10.) for at least 1 h at 4 °C in the dark, before flow cytometry analysis.

### 3.2.8. Cell isolation by flow cytometry

Primary cells were stained with surface markers as in 2.2.7. and were sorted in the FACS Aria II (BD Biosciences) or MoFlo (Beckman and Coulter). Isolated cells were collected in tubes containing 1 ml primary cell medium (see 3.3.1.). Sorting was performed in cooperation with Dr. Lothar Groebe at the flow cytometry facility, Helmholtz Centre for Infection Research, Brunswick, Germany.

### 3.3. Mouse and primary murine cell methods

#### 3.3.1. Isolation of organs and cell preparation

Lymphoid organs (peripheral lymph nodes (pLN), mesenteric lymph nodes (mLN), spleen and thymus) were isolated from mice sacrificed by CO<sub>2</sub>. Organs were homogenised through a 70 µm nylon mesh and washed with PBS. Erythrocytes were removed by 2 min incubation in ACK lysis buffer (0.15 M NH<sub>4</sub>Cl, 1 mM KHCO<sub>3</sub>, 0.1 mM EDTA, pH adjusted to 7.3 with NaOH) at room temperature followed by a further washing step.

Primary murine cells were cultured in RPMI 1640 supplemented with 10% FCS, 50 µg/ml of penicillin and streptomycin, 1% non-essential amino acids, 2 mM L-glutamine and 1 mM sodium pyruvate.

#### 3.3.2. In vitro activation of T and B cells

T cells were activated by seeding  $1 \times 10^6$  splenocytes or lymph node cells in 24-well plates followed by stimulation with 2 µg/ml concanvalin A (Con A; Sigma Aldrich) or 2 µg/ml anti-CD3 (145-2C11, BioLegend) and 2 µg/ml anti-CD28 (37.51, BioLegend), both plate-bound, for up four days.

CD19<sup>+</sup> cells were sorted from spleen, peripheral and mesenteric lymph nodes of 8-12 weeks old mice. After sorting, cells were activated by stimulating  $2 \times 10^6$  cells per well in 24-well plates with 10 µg/ml LPS for 48 h.

#### 3.3.3. Apoptosis assays

For assaying thymocyte apoptosis,  $1 \times 10^6$  thymocytes isolated from 6-8 weeks old mice were seeded in 24-well plates and either left untreated or stimulated for up to 16 h with 50 ng/ml CD95L (scErbB2), 1 µg/ml anti-CD95 (Jo-2; BD Biosciences) crosslinked with 10 ng/ml protein A (Sigma Aldrich) or 1 µM dexamethasone (Sigma-Aldrich). Viable cells were quantified by flow cytometry by staining with AnnexinV and 7AAD as described in 3.2.7.

CD4<sup>+</sup> and CD8<sup>+</sup> cells were sorted from spleen, pLN and mLN of 8-12 weeks old mice.  $5 \times 10^5$  cells were seeded per well in 96-well plates and stimulated with 50 ng/ml CD95L or 1 µM

dexamethasone for 16 h. Apoptosis was assayed by staining with AnnexinV and 7AAD as above.

Sorted and activated B cells (see 3.3.2.) were seeded with  $4 \times 10^5$  cells per well in 96-well plates and stimulated for 16 h with 100 ng/ml CD95L or 1  $\mu$ M dexamethasone. Thereafter, cells were stained for AnnexinV and 7AAD as described above. The specific apoptosis was calculated as  $((\text{experimental apoptosis (\%)} - \text{spontaneous apoptosis (\%)}) / (100\% - \text{spontaneous apoptosis})) \times 100$ .

#### **3.3.4. Activation induced cell death**

Peripheral lymph node cells were isolated from 6-8 weeks old mice.  $1 \times 10^6$  cells were seeded per well in 24-well plates coated with 10  $\mu$ g/ml anti-CD3 (145-2C11) and 2  $\mu$ g/ml anti-CD28 (E18). 20 ng/ml IL-2 was added to the media. The cells were taken off the anti-CD3, anti-CD28 stimuli on day 2 and expanded for 3 further days in the presence of IL-2. On day 5, T cell blasts were tested for activation induced cell death (AICD) by 6 h restimulation with 10  $\mu$ g/ml plate-bound anti-CD3. The cells were thereafter stained for AnnexinV and 7AAD as described in 3.2.7. The specific apoptosis was calculated as described in 3.3.3.

#### **3.3.5. Experimental autoimmune encephalomyelitis (EAE)**

EAE was induced in 10-12 weeks old WT and *vav*FLIP<sub>R</sub> mice by injecting 200  $\mu$ g MOG(35-55)-peptide (MEVGWYRSPFSRVVHLYRNGK) together with 4 mg/ml mycobacteria in CFA subcutaneously at four sites. 200 ng pertussis toxin was injected intraperitoneally to open the blood-brain-barrier. The pertussis toxin injection was repeated two days later. Mice were monitored daily for clinical signs of EAE from day 3 to day 40 according to table 1. Mice with a score higher than 3 were sacrificed. The EAE was performed in cooperation with Michaela Annemann (Systems-oriented Immunology and Inflammation Research, Helmholtz Centre for Infection Research, Brunswick, Germany/ Institute of Molecular and Clinical Immunology, Otto-von-Guericke University, Magdeburg).

**Table 1.** EAE scoring system

Score	Symptoms
0	None
0.5	Partial limp tail
1	Limp tail
2	Delayed rotation from dorsal position
2.5	Hindleg weakness
3	Complete hindleg paralysis
3.5	Starting foreleg weakness
4	Paralysis of one foreleg
5	Moribund, death

### 3.3.6. Histology

Kidneys and livers were isolated from one year old WT and *vavFLIP<sub>R</sub>* mice. Organs were fixed in 4% paraformaldehyde and embedded in paraffin for histological analysis. 1.5-2  $\mu$ m sections from liver and kidney were stained with hematoxylin and eosin (H&E). Moreover, kidney sections were stained with periodic acid schiff (PAS) staining. Kidney sections were analysed for thickening of the Bowman's capsule and protein casts in glomeruli and distal tubuli. The liver sections were analysed for the amount of microgranuloma and liver associated lymphoid tissue. Scoring was performed in a blinded manner by Dr. Marina Pils (Histology facility at Helmholtz Centre for Infection Research, Brunswick, Germany) as follows: 0 – no alteration, 1 – low grade (slightly visible), 2 – moderate (clearly visible), 3 – severe. Scores were added to a total score for each organ.

### 3.3.7. Analysis of anti-nuclear antibodies (ANA assay)

Anti-nuclear antibodies in sera from 1 year old WT and *vavFLIP<sub>R</sub>* mice were analysed semi-quantitatively by incubating HEp-2 cells seeded on microscope slides with sera diluted 1:80 – 1:1280 for 30 min at room temperature. Slides were washed two times 5 min in PBS followed by incubation with FITC-conjugated donkey anti-mouse IgG (Dianova, Hamburg, Germany) for 30 min in the dark. Thereafter slides were washed two times 5 min PBS, transferred to cover slips and sealed. Slides were analysed by fluorescence microscopy where a

homogenous pattern was considered as positive for ANAs. The ANA assays were performed in cooperation with Prof. Dr. Dirk Reinhold (Institute of Molecular and Clinical Immunology, Otto-von-Guericke University, Magdeburg), who prepared and analysed the slides.

### **3.4. Statistical analysis**

The software Graph Pad Prism from Graph-Pad-Software Inc (La Jolla, CA, USA) was used for all statistical analyses. One- or two-tailed non-parametric Mann Whitney *U* tests were performed to calculate statistical significances. Error bars were presented as standard deviation (s.d.) or standard error of the mean (s.e.m.).

## 4. Results

### 4.1. The role of c-FLIP splice variants in urothelial tumours

#### 4.1.1. c-FLIP<sub>L</sub> expression is decreased in urothelial carcinoma

c-FLIP expression has been reported to be upregulated in several types of cancer, i.e. Hodgkin's lymphoma<sup>189, 190</sup> and melanoma<sup>141, 191</sup>. Cancer of the urinary bladder is one of the most common cancer types in men in Europe and the United States. For this reason, expression of c-FLIP<sub>L</sub> and c-FLIP<sub>S</sub> mRNA in urothelial carcinoma samples were analysed. Surprisingly, c-FLIP<sub>L</sub> mRNA levels were moderately but significantly decreased in tumour samples compared to normal urothelial tissue (Figure 11A). Similarly, the expression of c-FLIP<sub>L</sub> as quantified by real-time PCR was lower in urothelial carcinoma cell lines than in cultured normal urothelial cells (NUC; Figure 11B). c-FLIP<sub>S</sub> was not differentially expressed between either tissues or cell lines (Figure 11A, B).

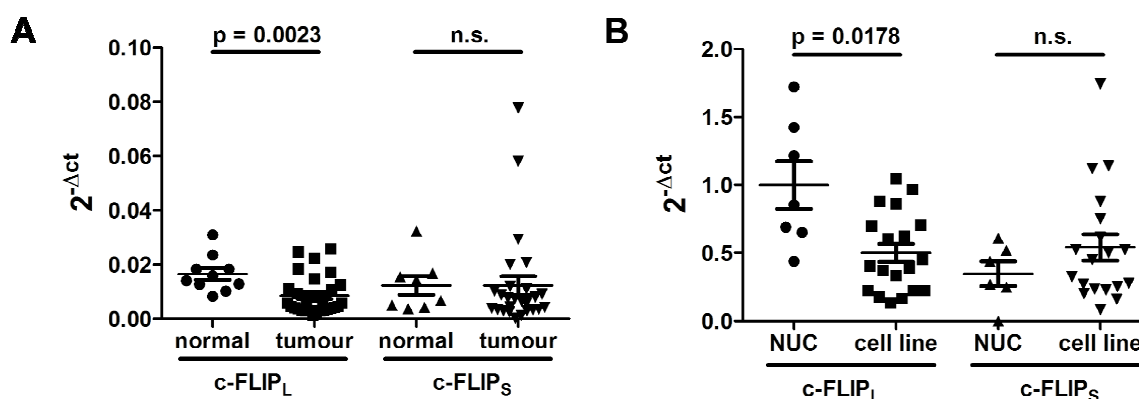


**Figure 11.** (A) Quantification of c-FLIP<sub>L</sub> and c-FLIP<sub>S</sub> mRNA levels in normal urothelial tissues (normal; n=10) and urothelial carcinoma samples (tumour; n=28) by quantitative RT-PCR. Values were normalised to GAPDH expression. Horizontal lines represent the mean; error bars display the standard deviation (s.d.). (B) Quantification of c-FLIP<sub>L</sub> and c-FLIP<sub>S</sub> mRNA levels in normal urothelial cells (NUCs; n=7) and urothelial cell lines (cell line; n=19) by quantitative RT-PCR. Values were normalised to TBP expression levels. Horizontal lines display the mean  $\pm$  s.d. Statistical analyses were performed by non-parametric two-tailed Mann Whitney *U* tests.

The urothelial carcinoma cell lines VMCub1 and SD were chosen as cell models to determine whether even lower levels of c-FLIP can mediate resistance towards death receptor-mediated

apoptosis and to investigate the role of c-FLIP splice variants in urothelial carcinoma. The cell lines were selected based on their death receptor and c-FLIP expression profile.

#### 4.1.2. Cycloheximide sensitises urothelial carcinoma cell lines towards CD95L- and TRAIL-induced apoptosis

To investigate whether the extrinsic pathway can be triggered in VMcub1 and SD, the death receptor expression of these cell lines was analysed by surface staining and flow cytometry analysis of the death receptors CD95, TRAIL-R1, TRAIL-R2 and TNF-R1. VMcub1 cells had a moderate to high expression of CD95, TRAIL-R2 and TNF-R1, whereas SD cells had a moderate to high expression of all four death receptors (Figure 12).

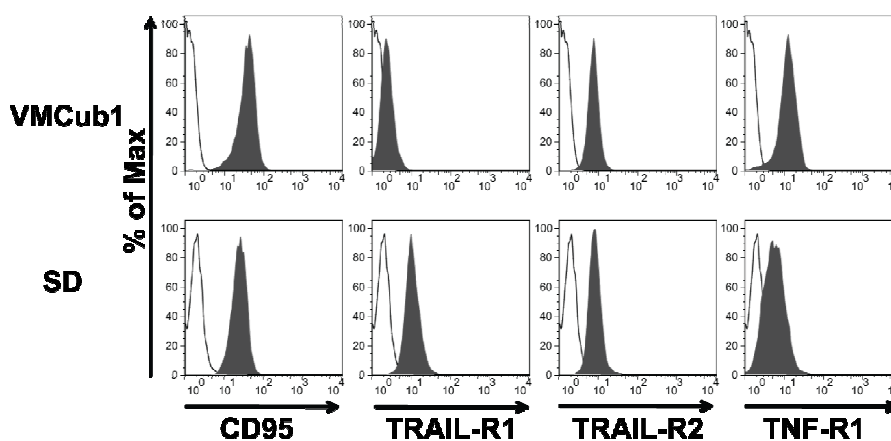


**Figure 12.** Death receptor expression of urothelial carcinoma cell lines. VMcub1 and SD cell surface expression of the death receptors CD95, TRAIL-R1, TRAIL-R2 and TNF-R1 analysed by flow cytometry (grey). Unstained cells are shown in white.

To assess CD95L- and TRAIL-induced apoptosis of VMcub1 and SD, cells were stimulated with the ligands for 16 h and 24 h, respectively, before measurement of DNA fragmentation. Both urothelial carcinoma cell lines showed low sensitivity towards CD95L-induced (Figure 13A) as well as TRAIL-induced (Figure 13B) apoptosis. However, VMcub1 and SD cells were strongly sensitised towards apoptosis by addition of the protein translation inhibitor cycloheximide (CHX; Figure 13A, B).

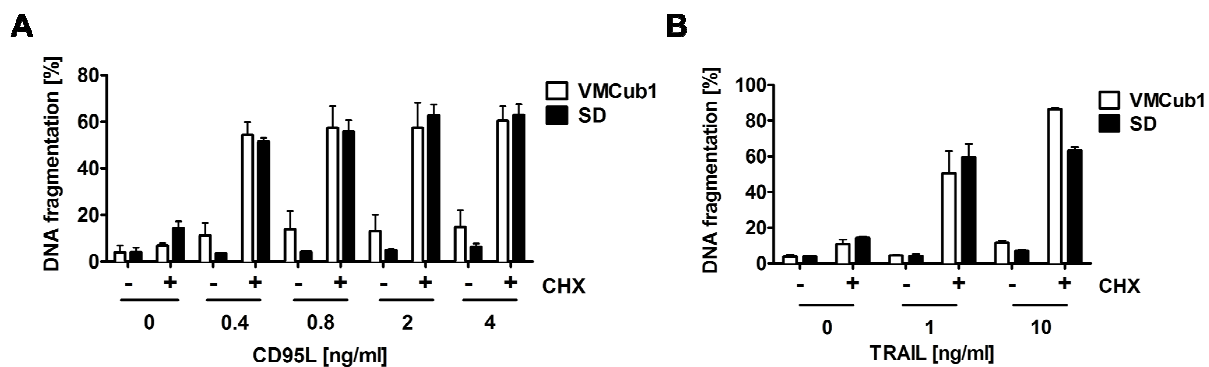


**Figure 13.** Urothelial carcinoma cell lines VMCub1 and SD are sensitised to apoptosis by cycloheximide (CHX). For analysis of apoptosis sensitivity, urothelial carcinoma cells were left untreated or stimulated for 16 h or 24 h, respectively, with the indicated concentrations of CD95L (**A**) or TRAIL (**B**) in the presence or absence of 10  $\mu$ g/ml CHX. The amount of apoptotic cells was determined by quantification of sub-G1 DNA content by flow cytometry. Data are displayed as the mean of at least three measurements ( $\pm$  s.d.).

An additional method to measure apoptosis is analysis of caspase processing, as the initiator caspase-8 and the effector caspase-3 are activated by proteolytic cleavage upon death receptor stimulation. For this purpose, VMCub1 and SD cells were stimulated either with CD95L for up to 8 h (Figure 14A) or with TRAIL for up to 24 h (Figure 14B) in the absence or presence of cycloheximide, followed by Western blotting to examine caspase cleavage as an early event during apoptosis. There was only minimal cleavage of caspase-8 and caspase-3 after stimulation with CD95L or TRAIL alone, whereas the presence of cycloheximide caused substantial processing of both caspases. Taken together, the results indicate that short-lived proteins play an important role in protecting the urothelial carcinoma cells against apoptosis. In particular, at least one short-lived protein protects against apoptosis at a step prior to caspase-8 activation, for which c-FLIP is the most likely candidate<sup>175, 241</sup>. It was previously shown in the working group that both c-FLIP<sub>L</sub> and c-FLIP<sub>S</sub> have a short half-life in VMCub1 and SD cells<sup>237</sup>, giving further evidence that c-FLIP proteins are likely candidates for causing the reduced susceptibility to apoptosis in the urothelial carcinoma cell lines.

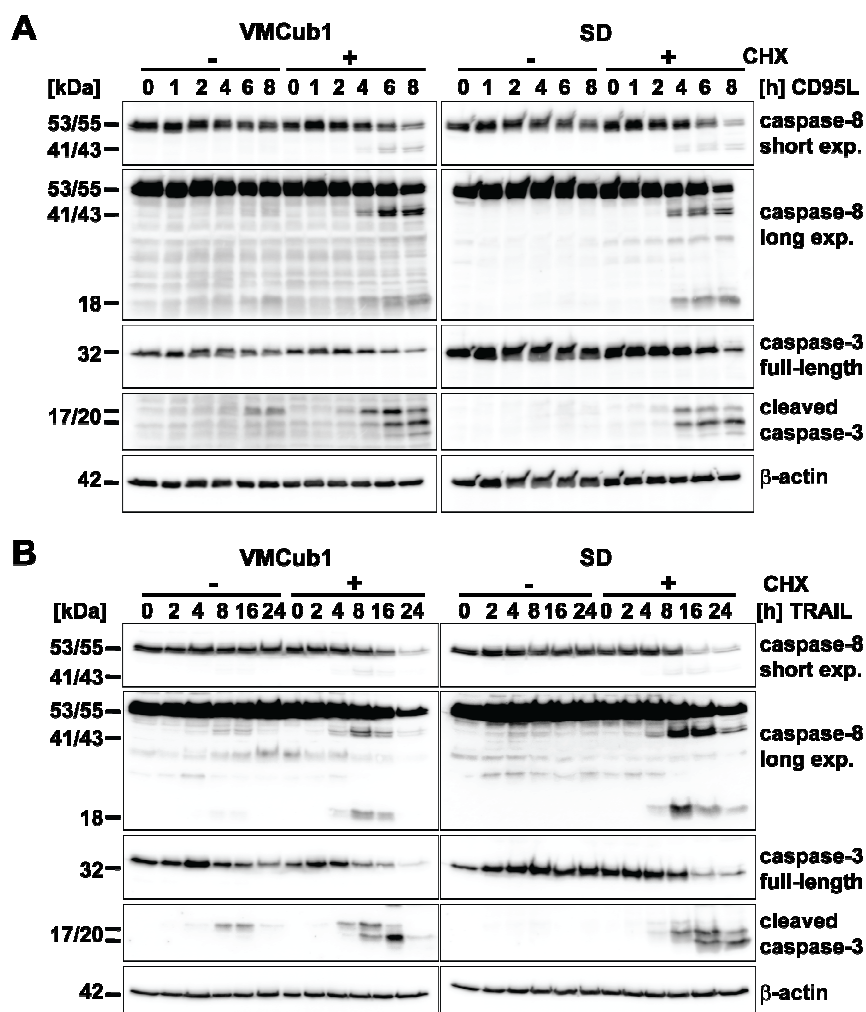


**Figure 14.** Analysis of CD95L- and TRAIL-induced apoptosis in urothelial carcinoma cells. VMCub1 and SD cells were left untreated or stimulated for the indicated times with 0.4 ng/ml CD95L (**A**) or 25 ng/ml TRAIL (**B**) in the presence or absence of 10  $\mu$ g/ml CHX. Cleavage of caspase-8 and caspase-3 was analysed by Western blotting with  $\beta$ -actin as the loading control.

#### 4.1.3. c-FLIP overexpression protects urothelial carcinoma cells against apoptosis

It is known that all three human c-FLIP splice variants can inhibit death receptor-mediated apoptosis<sup>118, 140, 149</sup>. For this reason, it was investigated whether overexpression of any c-FLIP isoform could protect VMCub1 and SD cells against apoptosis. The three c-FLIP splice variants c-FLIP<sub>L</sub>, c-FLIP<sub>S</sub> and c-FLIP<sub>R</sub> were cloned into a vector, which allows tracking of transfected cells by internal ribosomal entry site (IRES)-driven GFP expression. The generated constructs were first transiently transfected into HEK293T cells to verify that the respective c-FLIP variants were expressed at the protein level together with GFP (Figure 15A). Thereafter, VMCub1 and SD cells were transiently transfected with either the empty

vector or one of the c-FLIP constructs. The cells were stimulated with CD95L and the intracellular levels of active caspase-3 were examined by flow cytometry. Indeed, both VMcub1 (Figure 15B, C) and SD cells (Figure 15D, E) were protected by overexpression of any c-FLIP variant against CD95L-mediated apoptosis. The protective effect of c-FLIP overexpression was also confirmed by staining of transfected and stimulated cells using tetramethylrhodamine ethyl ester (TMRE, Figure 16).

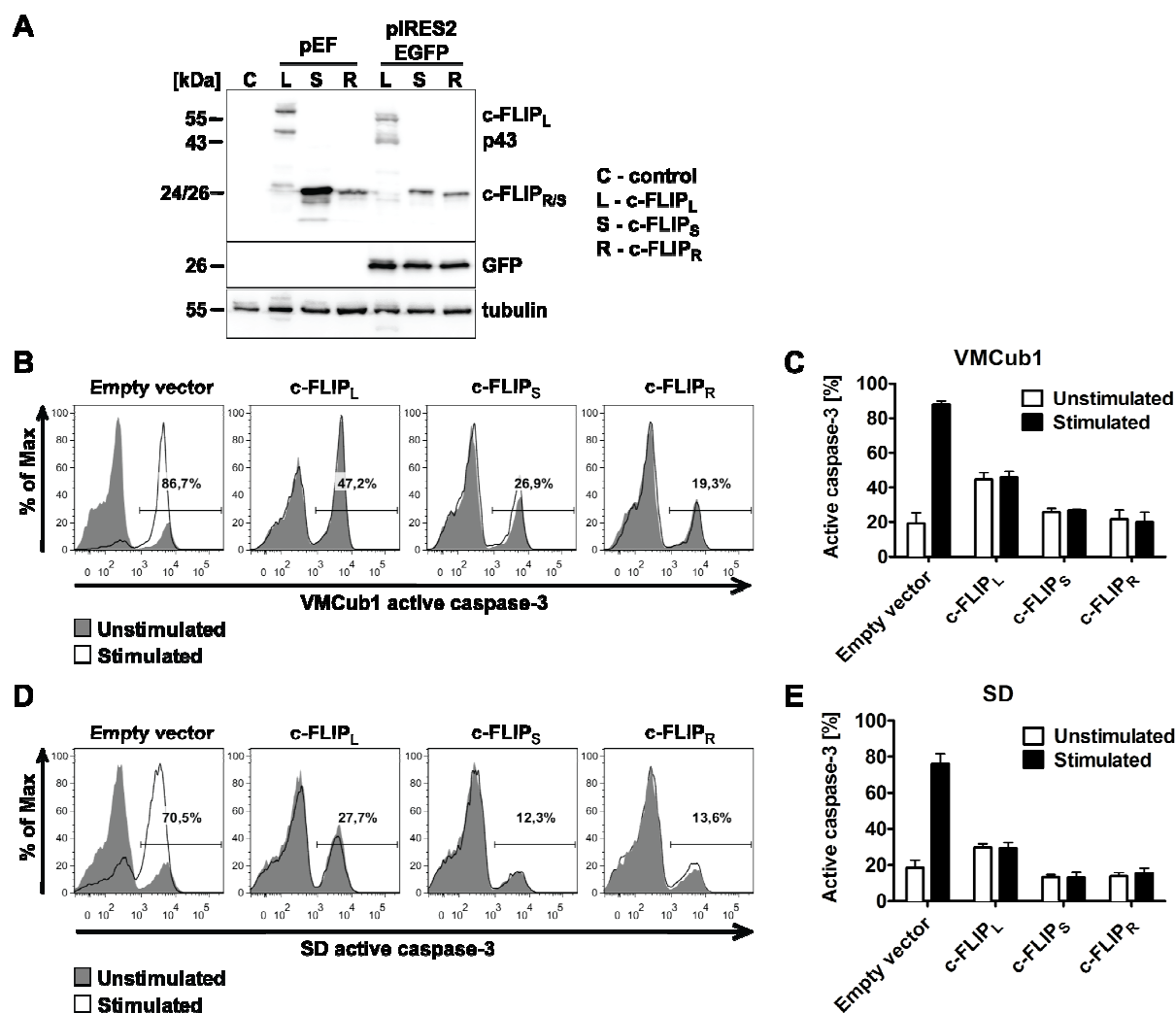


**Figure 15.** Overexpression of c-FLIP proteins protect urothelial carcinoma cells against CD95-mediated apoptosis. (A) Original pEF-vectors and the generated pIRES2EGFP-c-FLIP constructs were transiently transfected into HEK293T cells. The c-FLIP and GFP protein expression was analysed by Western blotting with tubulin as the loading control. pIRES2EGFP-c-FLIP constructs were transiently overexpressed in VMcub1 cells (B, C) and SD cells (D, E). The urothelial carcinoma cells were left untreated or stimulated with 1 ng/ml CD95L for 4 h. Sensitivity to apoptosis in transfected cells was analysed by flow cytometry. Intracellular staining of active caspase-3 was used as a marker for apoptotic cells and the transfected cells were identified by GFP expression. (B, D) Histograms are representative for three independent experiments with percentages shown for stimulated samples. (C, E) Data are shown as the percentages within the GFP-positive population with the mean of three independent experiments ( $\pm$  s.d.).

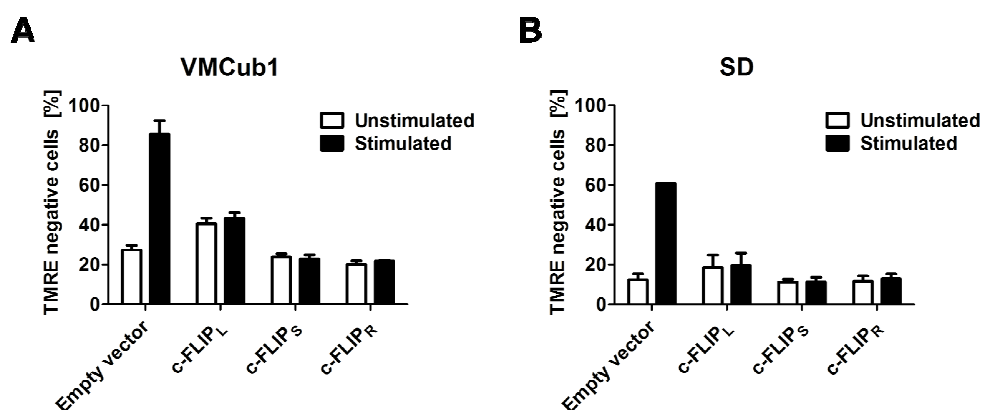


**Figure 16.** CD95-mediated apoptosis is inhibited by overexpression of c-FLIP proteins. VMCub1 (A) and SD cells (B) were transiently transfected with pIRES2EGFP-c-FLIP constructs followed by CD95L-stimulation as described in figure 5. Cells were stained with TMRE and analysed by flow cytometry. Apoptotic cells within the GFP-positive population were identified as TMRE negative. Data are represented as the mean of two independent experiments ( $\pm$  s.d.) except stimulated empty vector control of SD cells where one measurement is shown.

#### 4.1.4. Knock-down of c-FLIP sensitises urothelial carcinoma cells for CD95L-induced apoptosis

As high expression of all c-FLIP isoforms is reported to block death receptor-mediated apoptosis<sup>118, 140, 242</sup>, a loss-of-function approach was followed to determine specific functions of the different c-FLIP splice variants. For this, previously generated VMCub1 and SD cells stably transduced with lentiviral shRNA constructs targeting c-FLIP<sub>L</sub>, c-FLIP<sub>S</sub> or both c-FLIP<sub>L/S</sub> isoforms were used (Figure 17). The knock-down of c-FLIP<sub>L</sub> was less efficient than the c-FLIP<sub>S</sub> and c-FLIP<sub>L/S</sub> knock-downs.

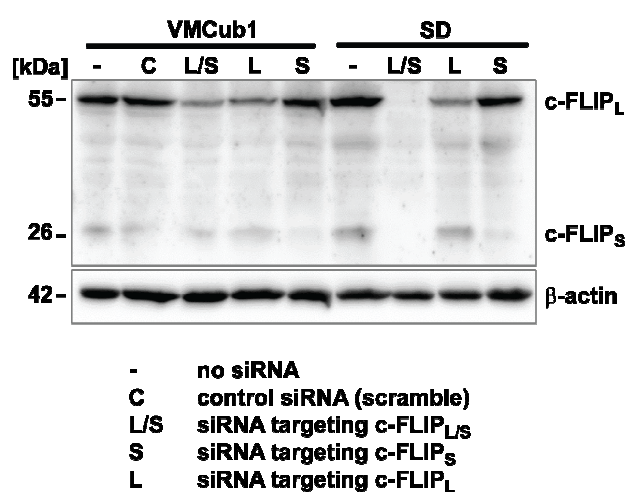


**Figure 17.** Stably transduced VMCub1 or SD cells lentivirally infected with a control shRNA (C) or shRNAs targeting c-FLIP<sub>L</sub> (L), c-FLIP<sub>S</sub> (S) or both c-FLIP<sub>L</sub> and c-FLIP<sub>S</sub> (L/S). Knock-down of the c-FLIP isoforms was confirmed by Western blotting.  $\beta$ -actin served as the loading control.

As assessed by measurement of DNA fragmentation, stimulation of VMCub1 and SD knock-down cells with increasing concentrations of CD95L led to elevated levels of apoptosis in the c-FLIP<sub>L/S</sub> double knock-down cells (Figure 18A, B). The effect was most prominent for the SD cells expressing shRNAs targeting both c-FLIP<sub>L</sub> and c-FLIP<sub>S</sub>, where the extent of apoptosis was comparable to those of wild type SD cells treated with cycloheximide (Figure 13A). This finding strongly supports the argument that c-FLIP is a prominent short-lived anti-apoptotic protein in these cells. Moreover, SD cells with knock-down of c-FLIP<sub>L</sub> alone were highly susceptible towards CD95L-induced apoptosis, whereas SD cells with knock-down of c-FLIP<sub>S</sub> alone remained resistant (Figure 18B). VMCub1 cells with single knock-down of c-FLIP<sub>L</sub> or c-FLIP<sub>S</sub> showed a mild, but statistically significant increase in CD95L-mediated apoptosis (Figure 18A).

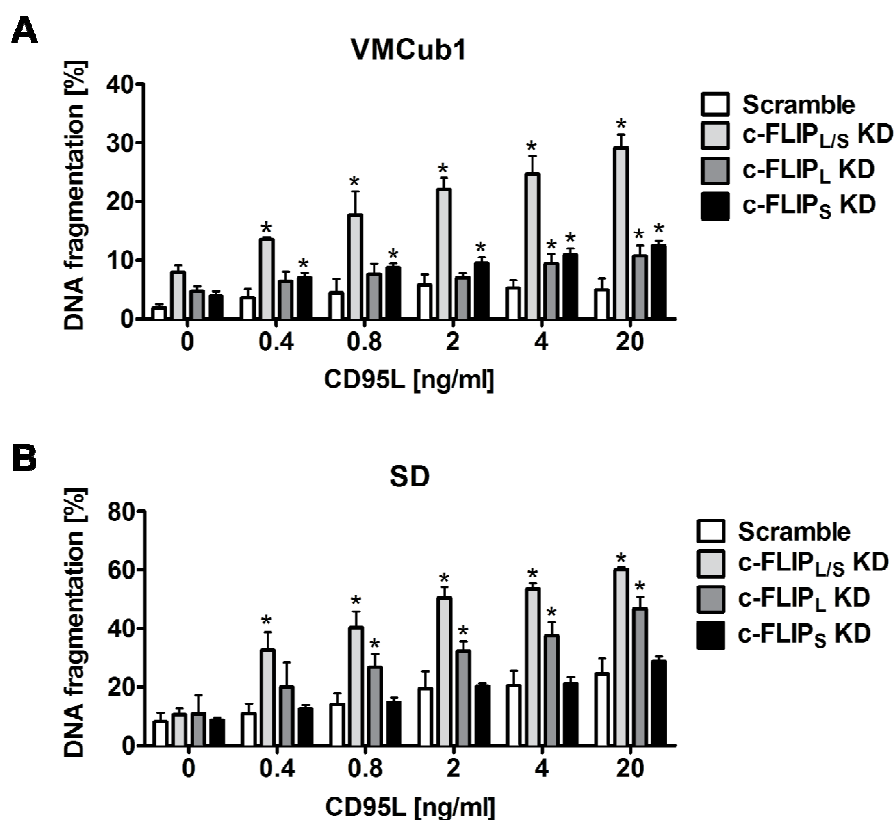


**Figure 18.** Knock-down of c-FLIP<sub>L/S</sub> sensitises VMCub1 and SD cells towards CD95L-induced apoptosis. For analysis of apoptosis sensitivity, VMCub1(A) and SD cells (B) stably transduced with the indicated shRNAs against c-FLIP<sub>L</sub>, c-FLIP<sub>S</sub> or both isoforms (c-FLIP<sub>L/S</sub>) were left untreated or stimulated for 16 h with the indicated concentrations of CD95L. The amount of apoptotic cells was quantified by DNA fragmentation analysed by flow cytometry. Data are shown as the mean of four measurements ( $\pm$  s.d.). Statistical analyses was performed by two-tailed Mann Whitney *U* tests, asterisks (\*) indicate  $p < 0.05$  with respect to scramble controls.

The effects of c-FLIP<sub>L</sub> or c-FLIP<sub>S</sub> knock-down on DNA fragmentation were paralleled by effects on caspase processing. The most extensive cleavage of caspase-8 and caspase-3 was observed in VMCub1 and SD c-FLIP<sub>L/S</sub> double knock-down cells as well as SD c-FLIP<sub>L</sub> single knock-down cells, where the proform of caspase-8 was extensively processed to the cleavage products p41/43 and p18 of caspase-8 as well as p17/20 of caspase-3 (Figure 19A, B). In contrast, both caspase-8 and caspase-3 remained uncleaved in VMCub1 and SD cells transduced with scramble shRNA. Thus, c-FLIP proteins protect the urothelial carcinoma cells against CD95L-induced apoptosis. Furthermore, the long c-FLIP isoform appears to be more important.

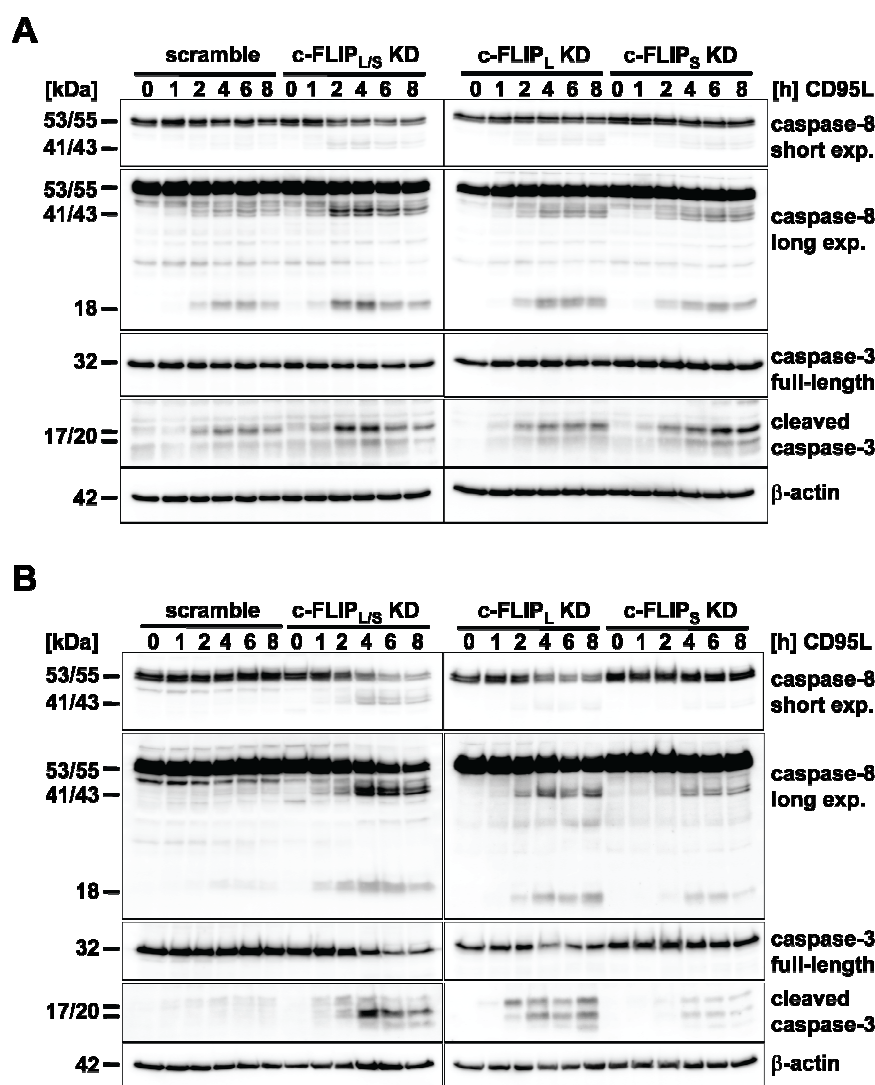


**Figure 19.** Analysis of caspase-8 and caspase-3 processing upon CD95L-stimulation. VMCub1 (A) and SD cells (B) with knock-down of c-FLIP<sub>L/S</sub>, c-FLIP<sub>L</sub> or c-FLIP<sub>S</sub> were left untreated or stimulated with 0.4 ng/ml and 0.8 ng/ml CD95L, respectively, for the times indicated. Cleavage of caspase-8 and -3 was analysed by Western blotting. Expression of β-actin is presented as the loading control.

#### 4.1.5. Urothelial carcinoma cells are sensitised for TRAIL-induced apoptosis by knock-down of c-FLIP

Next, the effect of isoform-specific c-FLIP knock-down on TRAIL-mediated apoptosis in VMcub1 and SD cells was investigated. Susceptibility to TRAIL-induced apoptosis was assayed by measurement of DNA fragmentation. Comparable to the CD95L-induced apoptosis assays, the VMcub1 and SD c-FLIP<sub>L/S</sub> double knock-down cells as well as the SD c-FLIP<sub>L</sub> single knock-down cells showed elevated levels of apoptosis upon TRAIL stimulation (Figure 20A, B).

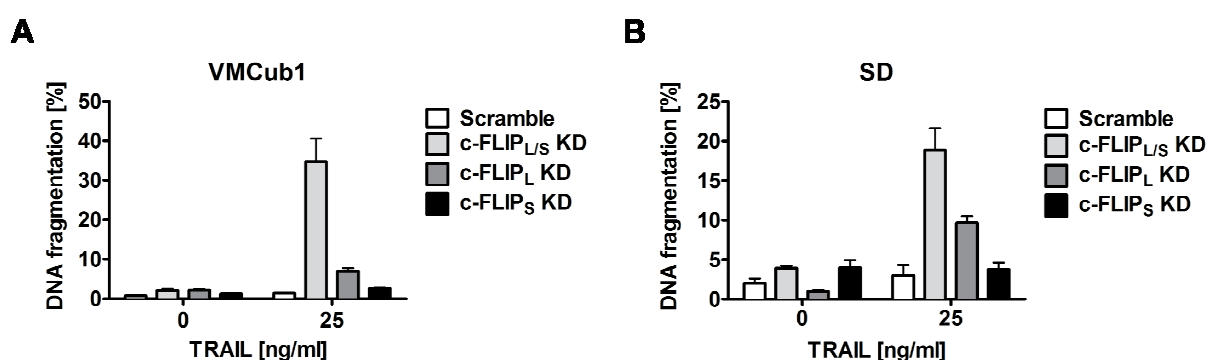


**Figure 20.** Effect of c-FLIP isoform knockdown on the susceptibility of urothelial carcinoma cells to TRAIL-induced apoptosis. VMcub1 (A) and SD cells (B) with knockdown of c-FLIP<sub>L</sub>, c-FLIP<sub>S</sub> or both isoforms (c-FLIP<sub>L/S</sub>) were left untreated or stimulated with 25 ng/ml TRAIL for 24 h. The amount of apoptotic cells was quantified by measuring the sub-G1 DNA content by flow cytometry. Data are shown as the mean of at least three measurements ( $\pm$  s.d.).

To assess activation of caspase-8 and caspase-3, cells were stimulated with TRAIL for up to 24 h. The cleavage products of caspase-8 and caspase-3 were readily detected in the VMcub1 c-FLIP<sub>L/S</sub> double knock-down cells upon TRAIL-stimulation, indicating activation of both caspases (Figure 21A). Small amounts of both processed caspases could also be detected in VMcub1 cells expressing shRNAs targeting c-FLIP<sub>L</sub> or c-FLIP<sub>S</sub> alone, suggesting that the c-FLIP isoforms are not complementary. In SD cells, the cleavage products p18/41/43 of caspase-8 and p17/20 of caspase-3 were clearly detected in c-FLIP<sub>L/S</sub> double knock-down cells as well as in c-FLIP<sub>L</sub> single knock-down cells. Moreover, the proform of both caspase-8 and caspase-3 was extensively degraded in SD cells expressing shRNAs targeting both c-FLIP<sub>L</sub> and c-FLIP<sub>S</sub> at later time points (Figure 21B). In contrast, both caspases remained

uncleaved in VMCub1 and SD cells stably transduced with scramble shRNAs suggesting that c-FLIP proteins confer broad resistance to death receptor activation in urothelial carcinoma.

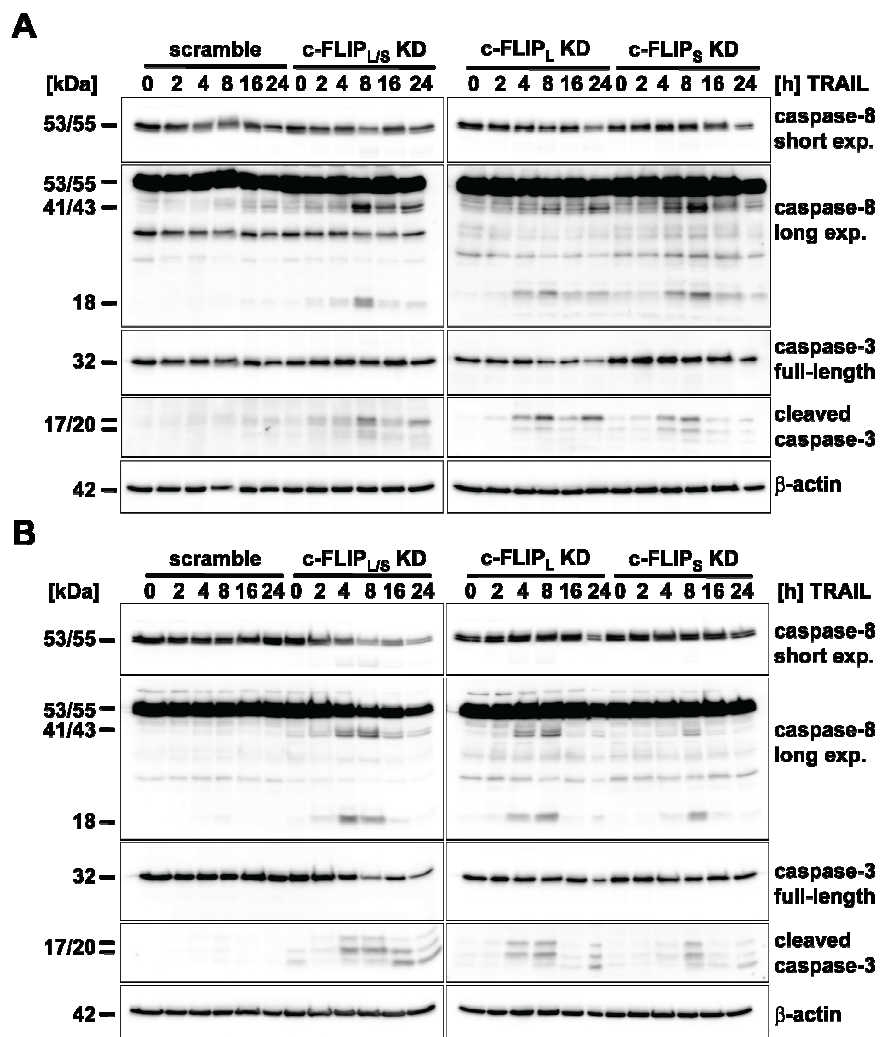


**Figure 21.** Analysis of caspase-8 and caspase-3 processing upon TRAIL-stimulation. For analysis of caspase-8 and caspase-3 cleavage, VMCub1 (**A**) and SD cells (**B**) stably transduced with the indicated shRNAs directed against c-FLIP<sub>L</sub>, c-FLIP<sub>S</sub> or both (c-FLIP<sub>L/S</sub>) were left untreated or stimulated with 25 ng/ml TRAIL for times as indicated. Lysates were analysed by Western blotting with β-actin as the loading control.

## 4.2. Identification of novel CD95 DISC-interacting proteins

### 4.2.1. Characterisation of Jurkat E6.1 clones overexpressing c-FLIP<sub>L</sub>

The Jurkat E6.1 cell line was chosen for mass spectrometry (MS) analysis, since the MS analyses require a high amount of protein. Moreover, Jurkat cells are well characterised and different knock-out cell lines are available<sup>243-245</sup>.

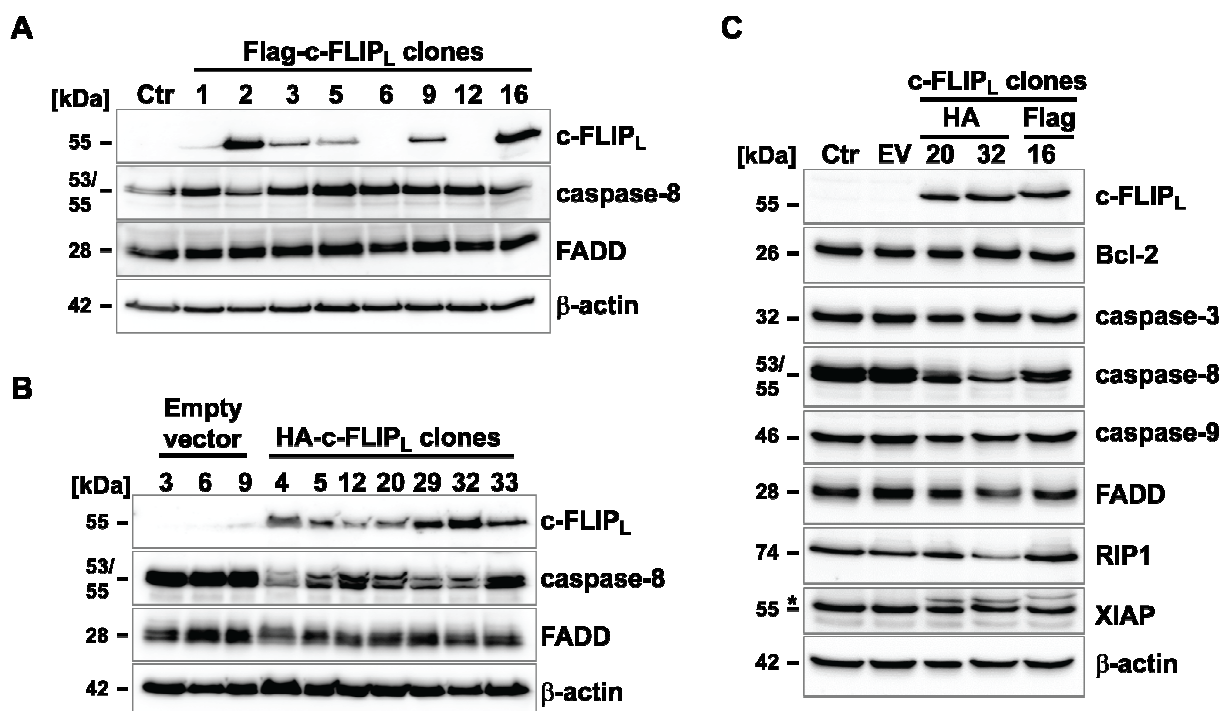


**Figure 22.** Protein expression in Jurkat E6.1 c-FLIP<sub>L</sub> overexpressing clones. The expression of c-FLIP<sub>L</sub>, caspase-8 and FADD in Jurkat E6.1 clones overexpressing Flag-c-FLIP<sub>L</sub> (A) or HA-c-FLIP<sub>L</sub> (B) was analysed via Western blotting. Expression of β-actin ensured equal loading. Parental Jurkat E6.1 cells were used as control (Ctr) in (A). (C) Lysates of parental Jurkat E6.1 cells (Ctr), empty vector control (EV) and HA-c-FLIP<sub>L</sub> cl. 20 and cl. 32 as well as Flag-c-FLIP<sub>L</sub> cl. 16 were immunoblotted to analyse the expression of c-FLIP<sub>L</sub>, Bcl-2, caspase-3, -8, -9, FADD, RIP1 and XIAP. β-actin served as the loading control. Left-over of c-FLIP<sub>L</sub> is marked by an asterisk (\*).

HA- or Flag-tagged c-FLIP<sub>L</sub> was stably overexpressed in Jurkat E6.1 cells and single clones were generated by limited dilution. The protein expression of c-FLIP<sub>L</sub>, caspase-8 and FADD was analysed by Western blotting to identify clones with high expression of c-FLIP<sub>L</sub> (Figure 22A, B). HA-tagged c-FLIP<sub>L</sub> clones 20 and 32 as well as Flag-tagged c-FLIP<sub>L</sub> clone 16 were chosen for further experiments. Moreover, a clone stably transfected with the empty vector

was chosen as control. In these clones, the expression of further apoptosis proteins (Bcl-2, caspase-3, -8, -9, FADD, RIP1 and XIAP) was analysed. The expression levels remained constant; the only exception was caspase-8 where slightly less protein could be detected in c-FLIP<sub>L</sub> overexpressing clones (Figure 22C). Furthermore, overexpression of c-FLIP<sub>L</sub> did not affect the death receptor expression. High expression of CD95 was observed in parental Jurkat cells and all clones. The expression of TRAIL-R2 and TNF-R1 was low to moderate in all cell lines (Figure 23).

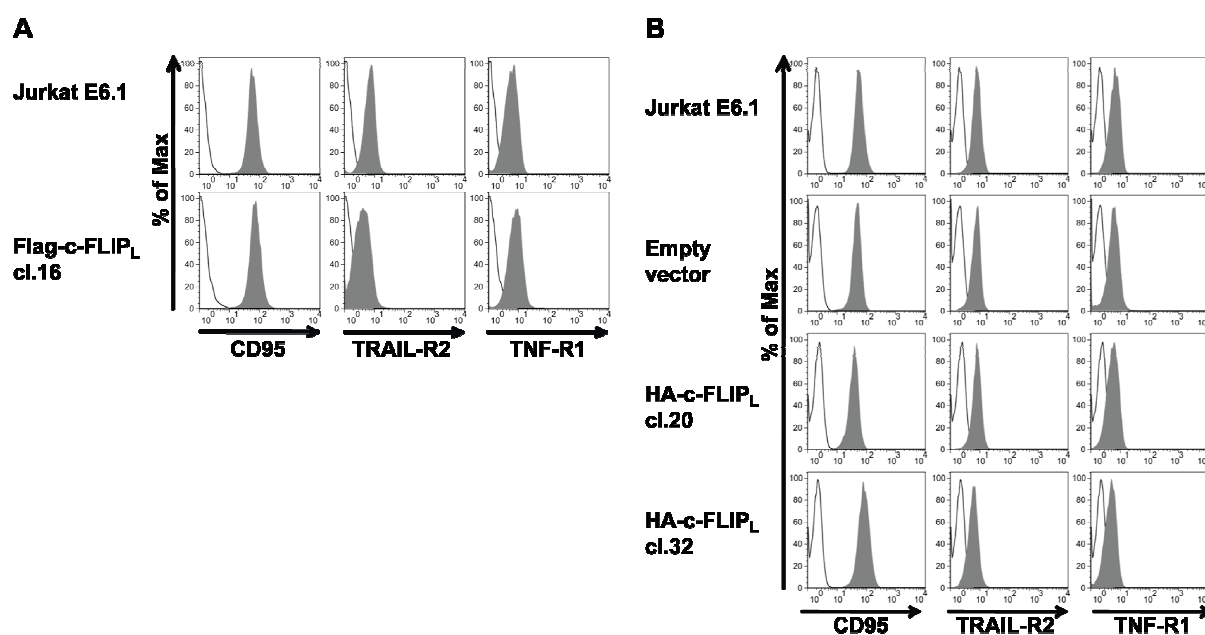


**Figure 23.** Death receptor expression of Jurkat E6.1 c-FLIP<sub>L</sub> overexpressing clones. Expression of the death receptors CD95, TRAIL-R2 and TNF-R1 was analysed by flow cytometry. Parental Jurkat cells and Jurkat Flag-c-FLIP<sub>L</sub> cl. 16 are shown in (A) with cells stained for death receptors in grey and unstained cells in white. The death receptor expression of parental Jurkat cells, empty vector control and HA-c-FLIP<sub>L</sub> clones 20 and 32 are shown in (B). Cells stained for death receptors are shown in grey; white histograms represent Jurkat cells stained with secondary antibody alone.

c-FLIP proteins are well-known inhibitors of apoptosis<sup>118, 140, 141, 149</sup>. Therefore, the sensitivity towards CD95-induced apoptosis was analysed in Jurkat clones overexpressing c-FLIP<sub>L</sub> by measurement of sub-G1 DNA content (Figure 24A, C). The clones were stimulated with anti-CD95 for up to eight hours, followed by flow cytometry analysis. A large fraction of empty vector control cells and parental Jurkat E6.1 cells were dying already after four hours stimulation, whereas Jurkat cells overexpressing c-FLIP<sub>L</sub> were protected against CD95-

induced apoptosis. Additionally, HA-c-FLIP<sub>L</sub> clones 20 and 32 were stimulated with the indicated concentrations of anti-CD95 over night (Figure 24B). 0.1 µg/ml anti-CD95 was enough to induce apoptosis in empty vector control cells, whereas only background apoptosis could be identified in c-FLIP<sub>L</sub> overexpressing clones. Moreover, lower levels of DNA fragmentation were observed upon stimulation with 1 µg/ml anti-CD95 in c-FLIP<sub>L</sub> overexpressing clones in comparison to the empty vector control. Finally, the apoptosis sensitivity was compared between the Flag-c-FLIP<sub>L</sub> cl. 16 and HA-c-FLIP<sub>L</sub> cl. 32. The c-FLIP<sub>L</sub> overexpressing clones were similarly protected against CD95L-induced apoptosis (Figure 24D).

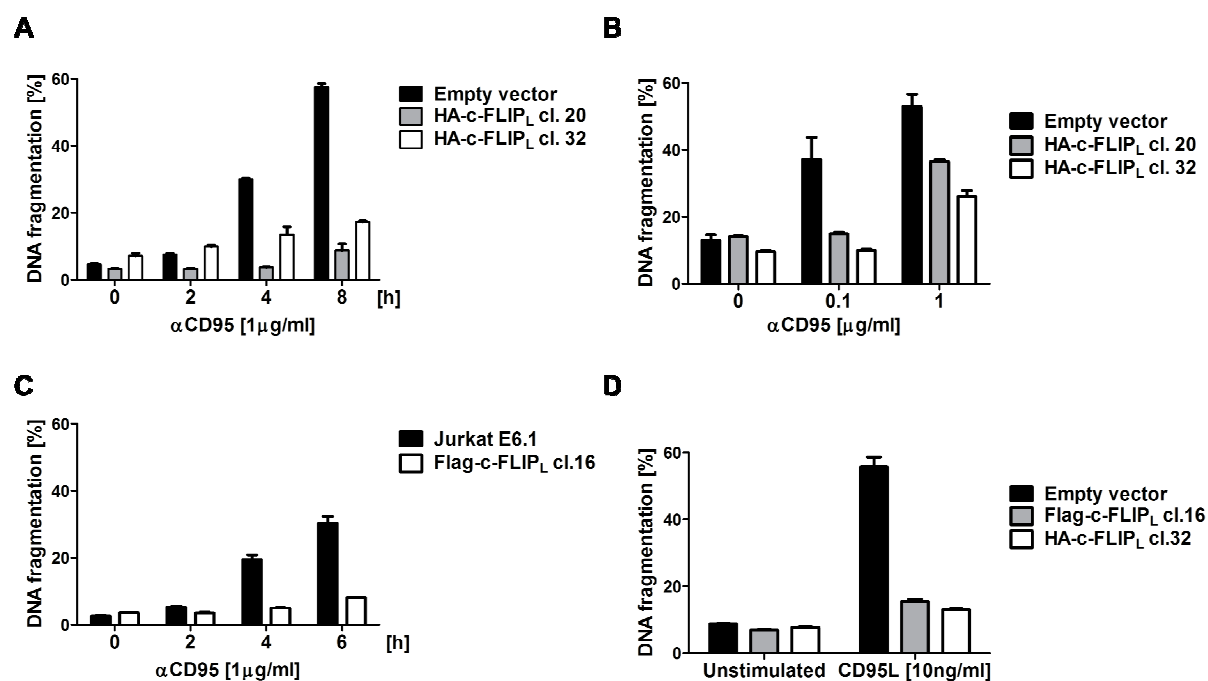


**Figure 24.** CD95-induced apoptosis of Jurkat clones overexpressing c-FLIP<sub>L</sub>. (A, C) For assaying apoptosis, Jurkat empty vector control, HA-c-FLIP<sub>L</sub> clones 20 and 32 (A) as well as Flag-c-FLIP<sub>L</sub> cl. 16 (C) were stimulated with 1µg/ml anti-CD95 (2R2) for the indicated times. (B, D) The Jurkat clones HA-c-FLIP<sub>L</sub> 20, 32 and Flag-c-FLIP<sub>L</sub> cl. 16 were stimulated with the indicated concentrations of anti-CD95 (B) or CD95L (D) for 16 h. The amount of apoptotic cells was quantified as DNA fragmentation analysed by flow cytometry. Data are shown as the mean (± s.e.m.) of triplicates.

Further, the apoptosis sensitivity was assayed by analysing the early apoptosis events of caspase-8 and caspase-3 processing upon CD95L-stimulation. For this, Jurkat empty vector control cells as well as HA-c-FLIP<sub>L</sub> overexpressing clones 20 and 32 were stimulated with CD95L for up to eight hours. The cleavage of caspase-8 into the p41/43 and p18 fragments as



#### 4.2.2. Immunoprecipitation of the DISC complex in c-FLIP<sub>L</sub> overexpressing clones

The death-inducing signalling complex (DISC) was immunoprecipitated upon CD95L-stimulation in empty vector control cells as well as HA-c-FLIP<sub>L</sub> clones 20 and 32. The complex consisted of the CD95 receptor, the adaptor protein FADD as well as the DED-containing proteins c-FLIP and caspase-8 in all cell lines. Caspase-8 becomes enzymatically activated at the DISC, which was identified by caspase-8- and c-FLIP<sub>L</sub>-cleavage in immunoprecipitated samples. Caspase-8 was fully processed into the p41/43 products in all cell lines as well as p18 for empty vector control cells, whereas some full-length c-FLIP<sub>L</sub> still could be detected in c-FLIP<sub>L</sub> overexpressing cells. c-FLIP proteins or heterodimers of c-FLIP and caspase-8 have higher affinity for the DISC complex<sup>118</sup>. Therefore, it was not unexpected that less caspase-8 was identified in the DISCs of c-FLIP<sub>L</sub> overexpressing cells compared to empty vector control cells.

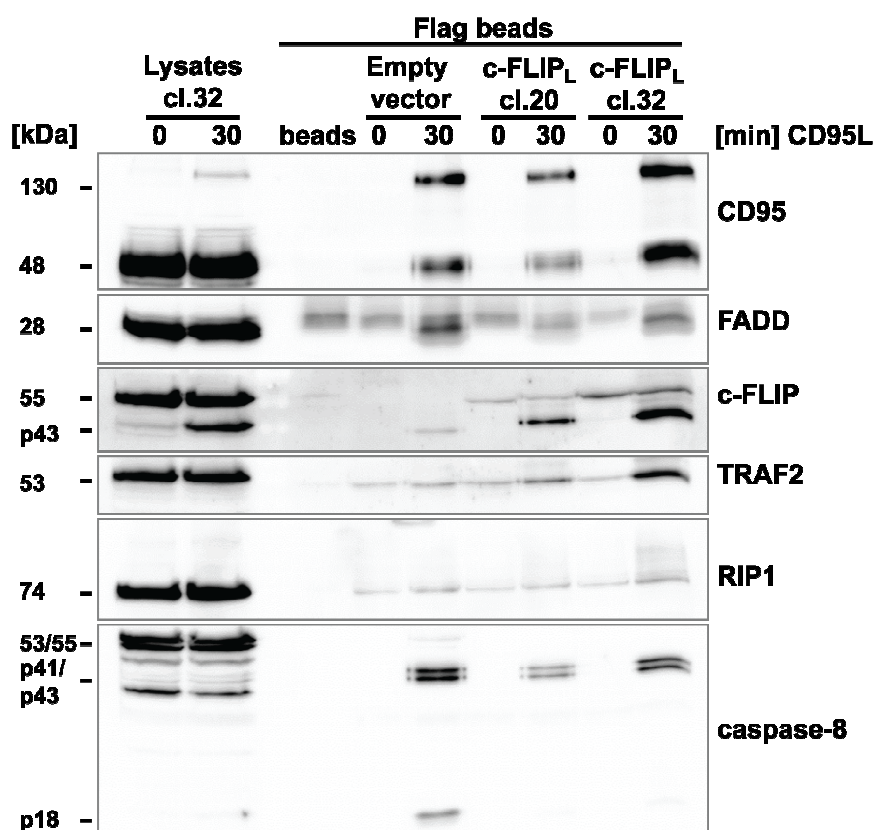


**Figure 26.** Immunoprecipitation of the DISC complex in Jurkat clones overexpressing HA-c-FLIP<sub>L</sub>. Jurkat clones overexpressing HA-c-FLIP<sub>L</sub> cl. 20 and 32 as well as empty vector control cells ( $10 \times 10^6$  cells per sample) were stimulated with Flag-tagged CD95L for 30 min or left untreated, followed by lysis of the cells and immunoprecipitation of the DISC-complex on Flag-beads. Western blotting was performed to analyse the DISC complex, with antibodies directed against CD95, FADD, c-FLIP, TRAF2, RIP1 and caspase-8 proteins.

A small amount of RIP1 was identified in all DISCs with slightly more RIP1 in the DISC of cl. 32, which has the highest c-FLIP<sub>L</sub> expression. TRAF2 was recruited to the DISC in a c-FLIP<sub>L</sub>-dependent manner (Figure 26).

Next, c-FLIP<sub>L</sub> was immunoprecipitated with interacting proteins. The Jurkat cells were either left untreated or stimulated with CD95L or anti-CD95, followed by immunoprecipitation on anti-HA or anti-Flag beads. The DISC-components caspase-8, FADD and the CD95 receptor was immunoprecipitated upon stimulation in both HA-c-FLIP<sub>L</sub> and Flag-c-FLIP<sub>L</sub> clones (Figure 27A, B). Additionally, TRAF2 was recruited to Flag-c-FLIP<sub>L</sub> upon stimulation. c-FLIP<sub>L</sub>-interaction and cleavage of RIP1 could also be observed upon stimulation in Flag-c-FLIP<sub>L</sub> overexpressing cells (Figure 27B).

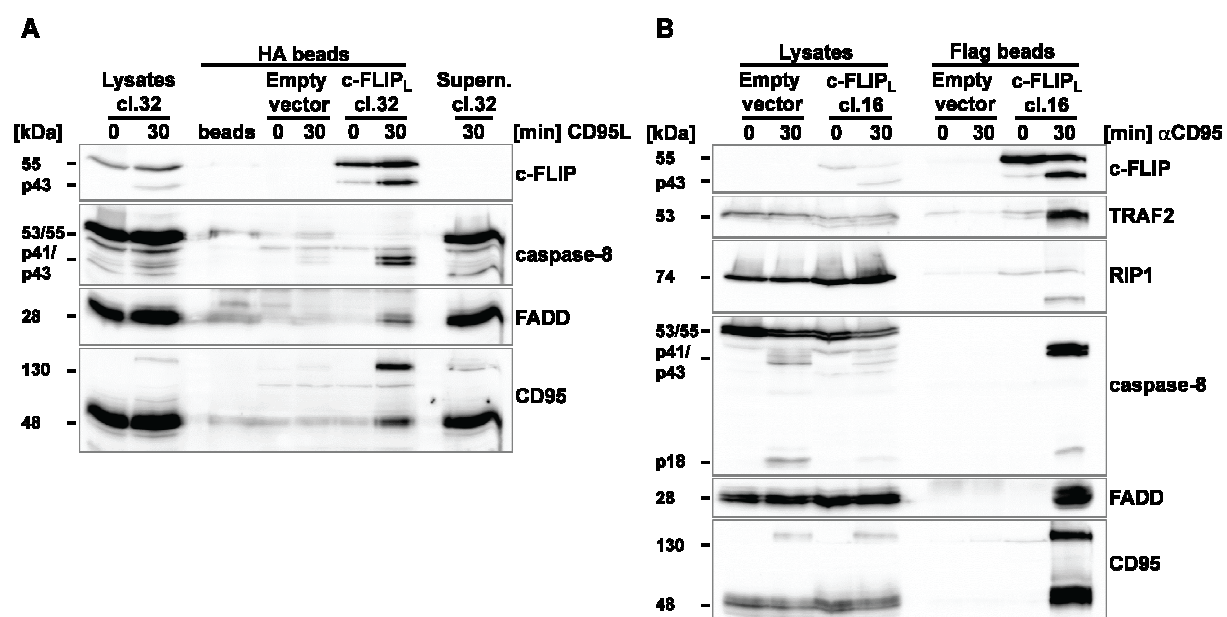


**Figure 27.** Immunoprecipitation of c-FLIP<sub>L</sub> upon CD95L- or anti-CD95-stimulation. Jurkat clones overexpressing HA-tagged (A) and Flag-tagged (B) c-FLIP<sub>L</sub> as well as empty vector controls were either left untreated or stimulated with (A) CD95L ( $10 \times 10^6$  cells per sample) or (B)  $2 \mu\text{g/ml}$  anti-CD95 (2R2) crosslinked with  $10 \text{ ng/ml}$  Protein A ( $30 \times 10^6$  cells per sample), followed by immunoprecipitation of c-FLIP<sub>L</sub> on HA- or Flag-agarose beads. Western blot analyses of c-FLIP, caspase-8, FADD, CD95, TRAF2 and RIP1 were performed to identify interacting proteins.

### 4.2.3. Mass spectrometry analysis of proteins interacting at the DISC

Mass spectrometry can identify large numbers of proteins from one single immunoprecipitation and abundant proteins can cause difficulties in identifying low-expressed proteins. Therefore, it is of importance that the beads used give rise to as little unspecific binding as possible to increase the chance of identifying specific interactions. For this reason HA-c-FLIP<sub>L</sub> cl. 32 cells were left untreated or stimulated with CD95L, subsequently lysed and divided up onto HA- and Flag-beads. The coomassie-staining of the immunoprecipitations clearly showed that the Flag-beads give rise to less unspecific binding (Figure 28). Consequently, these beads were used for the immunoprecipitations for the mass spectrometry analyses.

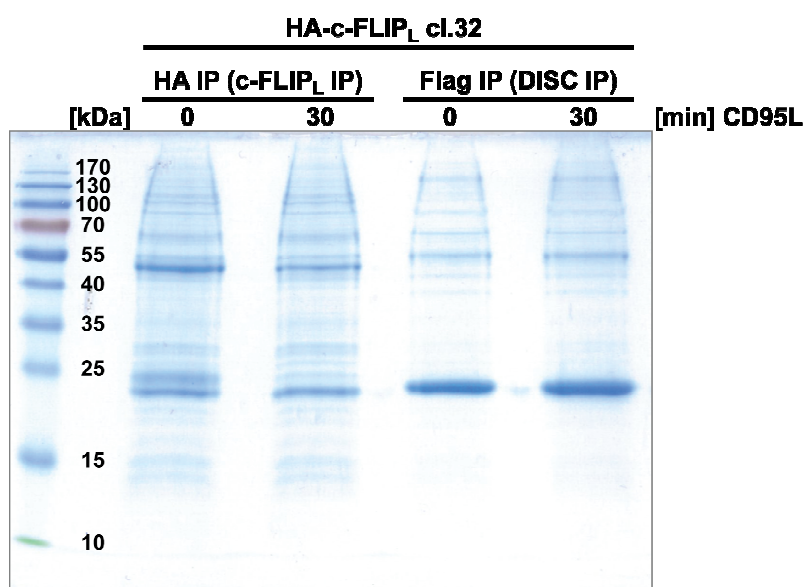


**Figure 28.** Comparison between HA IP (c-FLIP<sub>L</sub> IP) and Flag IP (DISC IP).  $100 \times 10^6$  Jurkat HA-c-FLIP<sub>L</sub> cl.32 cells were either left untreated or stimulated with Flag-tagged CD95L for 30 min. Cells were thereafter lysed and divided onto HA- and Flag-agarose beads for immunoprecipitation. Immunoprecipitated samples were run on an SDS-gel followed by coomassie-staining.

Immunoprecipitations for mass spectrometry analyses were performed with  $1.5 \times 10^8$  cells for each sample. Samples were incubated two times on control IgG beads before the actual Flag-immunoprecipitation to reduce unspecific binding. The Flag-immunoprecipitation was controlled by Western blotting (Figure 29A) before samples were run on an SDS-gel followed by coomassie-staining. The lanes on the coomassie-gels were cut in 17 slices and these slices were analysed by mass spectrometry (Figure 29B).

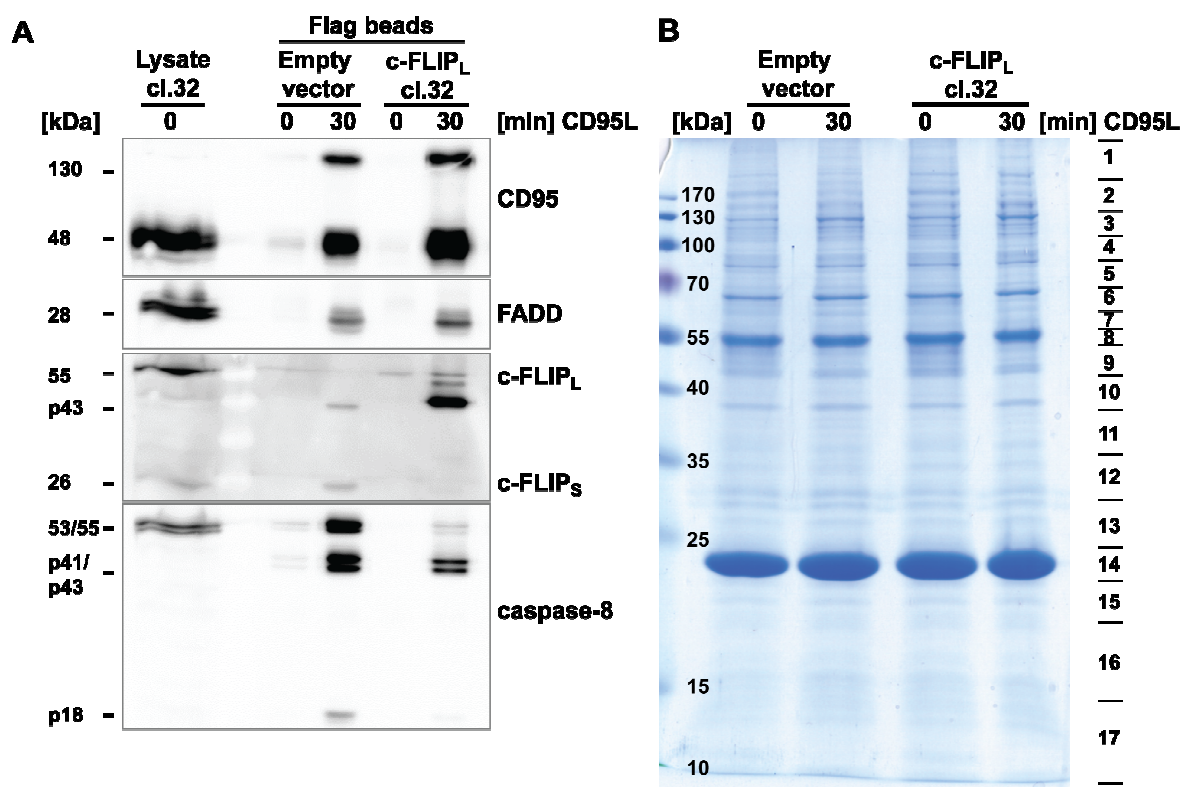


**Figure 29.** DISC immunoprecipitation for mass spectrometry analysis. DISC formation was induced by stimulating  $1.5 \times 10^8$  Jurkat HA-c-FLIP<sub>L</sub> cl. 32 and empty vector control cells with CD95L for 30 min compared with unstimulated samples. Immunoprecipitation was performed on Flag-agarose-beads. **(A)** 10% of samples were loaded onto an SDS-gel followed by Western blotting with analysis of the proteins CD95, FADD, c-FLIP and caspase-8 as control for efficient DISC formation. **(B)** The rest of the samples were run on an SDS-gel followed by gel fixation and coomassie-staining. Each lane was cut in 17 gel slices as indicated and analysed by mass spectrometry. The immunoprecipitation shown is representative for two independent experiments.

The core components of the DISC complex identified by mass spectrometry in the empty vector control cells were the CD95 receptor, caspase-8 and caspase-10. For the c-FLIP<sub>L</sub> overexpressing cells, the core components identified were the CD95 receptor, FADD, c-FLIP, caspase-8 and TRAF2 (Table 2). Surprisingly, FADD could not be detected in the empty vector control cells by mass spectrometry. However, FADD was identified in the control Western blot and DED-containing proteins such as caspase-8 and caspase-10 should not be able to bind to the DISC without an adaptor protein<sup>246, 247</sup>. Caspase-10 was not identified in the DISC of c-FLIP<sub>L</sub> overexpressing cells. This is not unexpected since DED-containing proteins are competing for the binding sites at the DISC. It is therefore likely that the overexpression of c-FLIP<sub>L</sub> is outcompeting caspase-10-binding.

Furthermore, comparison of the DISCs revealed four potentially new DISC interacting proteins with c-FLIP<sub>L</sub>-dependent binding (Table 2). These proteins were the zinc finger protein A20 (Tumour necrosis factor alpha-induced protein 3), multiple myeloma tumour-associated protein 2 (hMMTAG2), SAP domain-containing ribonucleoprotein (Hcc-1) and suppressor of SWI4 homologue (Ssf-1).

**Table 2.** Core components of the DISC complexes in Jurkat empty vector and HA-c-FLIP<sub>L</sub> cl.32 cells according to MS data.

Jurkat E6.1 empty vector	Jurkat E6.1 HA-c-FLIP <sub>L</sub> cl.32
CD95	CD95
caspase-8	FADD
caspase-10	c-FLIP
	caspase-8
	TRAF2
	<b>Potential candidates:</b>
	A20
	Multiple myeloma tumour-associated protein 2
	SAP domain-containing ribonucleoprotein
	Suppressor of AWI4 homolog

The zinc finger protein A20 (hereafter called A20) is known to interact with the TNF-R1 complex and thereby regulate NF- $\kappa$ B activation<sup>248, 249</sup>. Reagents for this protein were available and therefore it was chosen for further validation. A20-association to the DISC was validated by immunoprecipitation of the DISC complex in both empty vector control cells and c-FLIP<sub>L</sub> overexpressing cells. The DISC complex assembled in both cell lines upon CD95L-stimulation since the recruitment of CD95, FADD, caspase-8 and c-FLIP could be detected. TRAF2 only associated to the complex in c-FLIP<sub>L</sub> overexpressing cells consistent with the experiments described above. Indeed, A20 was recruited to the DISC upon CD95L-stimulation, but a c-FLIP<sub>L</sub>-dependent DISC-recruitment of A20 could not be confirmed since A20-interaction was detected both in empty vector control cells and c-FLIP<sub>L</sub> overexpressing cells (Figure 30A). The DISC complex was identified in c-FLIP<sub>L</sub>-immunoprecipitates upon anti-CD95 stimulation and A20 was detected in this immunoprecipitation as well (Figure

30B). Ubiquitinated RIP1 is described to activate NF- $\kappa$ B by interacting with the I $\kappa$ B kinase (IKK) complex<sup>248, 250</sup> and A20 regulates the NF- $\kappa$ B activation by de-ubiquitination of RIP1<sup>249</sup>. Nevertheless, an association of the IKK complex subunits IKK $\alpha$  and IKK $\gamma$ /NEMO with the DISC complex was not identified (Figure 30A, B).

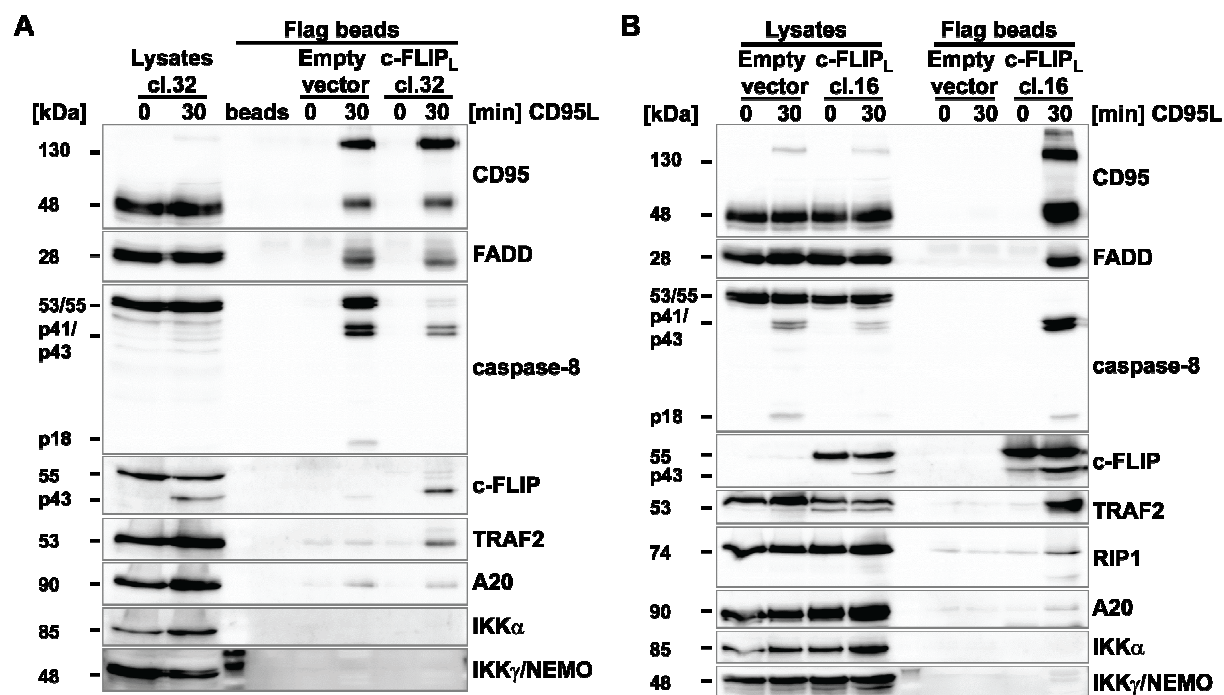


**Figure 30.** Immunoprecipitations of the DISC complex for analyses of novel interaction partners. Jurkat empty vector control cells and HA-c-FLIP<sub>L</sub> cl. 32 (**A**) or Flag-c-FLIP<sub>L</sub> cl. 16 (**B**) were either left untreated or stimulated with (**A**) CD95L ( $10^7$  cells per sample) or (**B**) 2  $\mu$ g/ml anti-CD95 (2R2) crosslinked with 10 ng/ml Protein A ( $3 \times 10^7$  cells per sample) for 30 min followed by immunoprecipitation on Flag-agarose beads. Interaction partners were identified by probing the Western blots with antibodies directed against CD95, FADD, caspase-8, c-FLIP, TRAF2, RIP1, A20, IKK $\alpha$  and IKK $\gamma$ /NEMO.

### 4.3. Constitutive expression of murine c-FLIP<sub>R</sub> causes autoimmunity in aged mice

#### 4.3.1. Endogenous expression of murine c-FLIP<sub>R</sub>

c-FLIP<sub>R</sub> has been described as the only short murine isoform of c-FLIP<sup>142</sup>. However, the endogenous protein expression has not been shown so far. Human c-FLIP<sub>S</sub> is induced upon T cell activation<sup>147, 175</sup>. To examine if murine c-FLIP<sub>R</sub> is induced in a similar way, lymph node cells were isolated from C57BL/6 WT mice followed by stimulation with either concanavalin A (Con A) or anti-CD3 and anti-CD28. Indeed, c-FLIP<sub>R</sub> expression was induced after 24 hours stimulation with Con A and remained expressed until 48 hours after stimulation started, whereas c-FLIP<sub>R</sub> was not detected in unstimulated lymph node cells (Figure 31A). Moreover, c-FLIP<sub>L</sub> was cleaved into the p43-fragment upon Con A stimulation, but caspase-8 and FADD expression remained constant during Con A stimulation (Figure 31A).

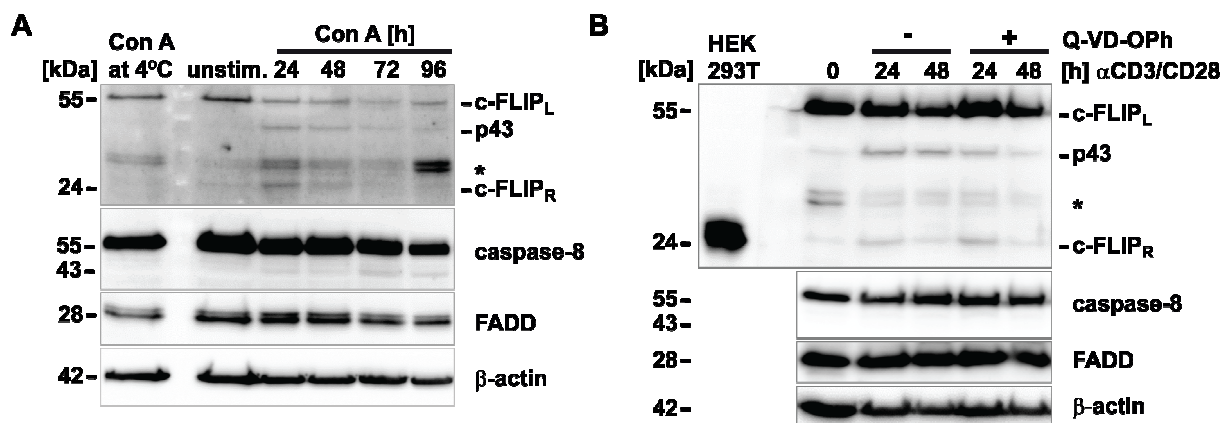


**Figure 31.** Endogenous c-FLIP<sub>R</sub> expression. **(A)** C57BL/6 WT lymph node cells were stimulated with 2 μg/ml concanavalin A for the indicated times. The expression of c-FLIP, FADD and caspase-8 was analysed by Western blotting. Expression of β-actin was controlled to ensure equal loading. **(B)** Peripheral lymph node cells from C57BL/6 WT mice were stimulated for the indicated times in wells coated with 2 μg/ml anti-CD3 and 2 μg/ml anti-CD28 in presence or absence of 20 μM Q-VD-OPh. Lysates were immunoblotted to analyse the expression of c-FLIP, caspase-8 and FADD. β-actin served as the loading control. Asterisks (\*) mark unspecific bands.

Additionally, C57BL/6 WT lymph node cells were stimulated with plate-bound anti-CD3 and anti-CD28 for up to two days in presence or absence of the pan-caspase-inhibitor Q-VD-OPh in order to exclude that the 24 kDa band is a proteolytical fragment and not c-FLIP<sub>R</sub>. Moreover, the size of c-FLIP<sub>R</sub> was controlled by HEK293T cells transiently transfected with a plasmid encoding murine c-FLIP<sub>R</sub>. Consistent with Con A stimulation, c-FLIP<sub>R</sub> was induced after 24 hours stimulation and its expression was unaltered by the addition of Q-VD-OPh (Figure 31B). Low expression of c-FLIP<sub>R</sub> could still be detected after 48 hours, again not affected by the pan-caspase inhibitor. Although Q-VD-OPh did not completely inhibit c-FLIP<sub>L</sub> cleavage, expression of the p43-fragments was clearly impaired indicating that p43, but not the 24 kDa c-FLIP<sub>R</sub> band, originated from caspase-mediated cleavage (Figure 31B). Taken together, c-FLIP<sub>R</sub> is indeed being induced upon T cell activation similar to human c-FLIP<sub>S</sub>.

#### 4.3.2. The c-FLIP<sub>R</sub> transgenic mouse model - vavFLIP<sub>R</sub>

The c-FLIP<sub>R</sub> transgenic mouse model vavFLIP<sub>R</sub>, generated by Prof. Dr. Ingo Schmitz (Helmholtz Centre for Infection Research, Brunswick, Germany and Institute for Molecular and Clinical Immunology, Otto-von-Guericke University, Magdeburg, Germany) was used to further examine the role of murine c-FLIP<sub>R</sub> in the immune system.

In this mouse model, murine c-FLIP<sub>R</sub> is under control of the *vav*-promoter (Figure 32A) and therefore expressed in all hematopoietic compartments. The plasmid used for generating the transgenic construct was described by Ogilvy and colleagues<sup>240</sup> and Bcl-2 under control of the *vav*-promoter was successfully expressed throughout the hematopoietic compartment<sup>251</sup>. Transgenic expression of c-FLIP<sub>R</sub> was controlled by PCR on tail biopsies, with  $\beta$ -actin as loading control (Figure 32B). Furthermore, c-FLIP<sub>R</sub> protein expression was controlled in the lymphoid organs thymus, spleen and peripheral lymph nodes (pLN). The expression of the DISC proteins caspase-8 and FADD remained unchanged (Figure 32C). The c-FLIP<sub>R</sub> expression in vavFLIP<sub>R</sub> mice was comparable to the endogenously expressed c-FLIP<sub>R</sub> in splenocytes induced by Con A (Figure 32D). c-FLIP<sub>L</sub> was cleaved into the cleavage product p43 and caspase-8 was processed into the p41/43 as well as p18 cleavage products upon Con A stimulation in splenocytes. This is consistent with previous studies where cleavage of caspases upon T cell receptor stimulation has been reported<sup>210, 211</sup>.

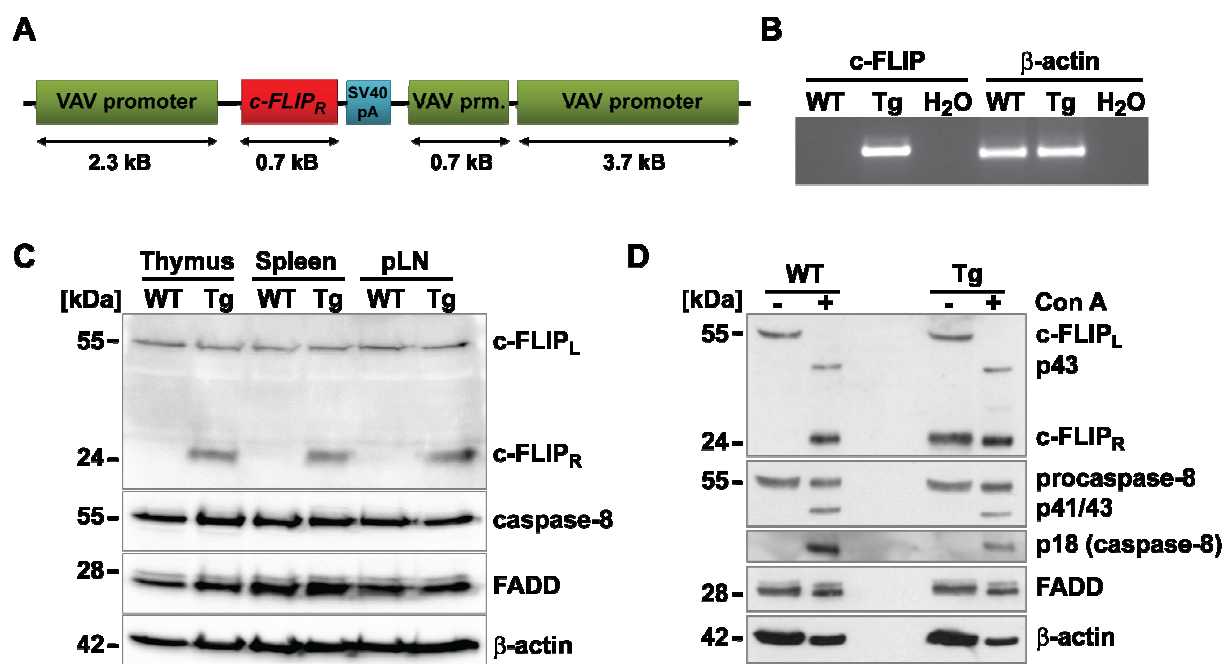


**Figure 32.** The c-FLIP<sub>R</sub> transgenic mouse model - vavFLIP<sub>R</sub>. **(A)** The c-FLIP<sub>R</sub> gene with a C-terminal simian virus 40 (SV40) polyadenylation signal sequence was placed under control of the vav-promoter. This construct was used for generating c-FLIP<sub>R</sub> transgenic mice. **(B)** Expression of the transgenic c-FLIP<sub>R</sub> construct was controlled by PCR of tail biopsies. PCR of β-actin was used as loading control and PCR of water (H<sub>2</sub>O) as negative control. **(C)** Protein expression of c-FLIP<sub>R</sub> was controlled in thymic, splenic and peripheral lymph node (pLN) lysates from WT and vavFLIP<sub>R</sub> (Tg) mice by Western blotting. Antibodies directed against c-FLIP, caspase-8 and FADD were used with β-actin as loading control. **(D)** Splenocytes from WT and vavFLIP<sub>R</sub> animals were either left untreated (-) or stimulated with 2 μg/ml concanavalin A (Con A) for 64 hours (+). Subsequently cells were lysed and analysed by Western blotting as described above.

#### 4.3.3. vavFLIP<sub>R</sub> mice are protected against CD95-induced apoptosis and AICD

c-FLIP proteins are well-known inhibitors of death-receptor mediated apoptosis<sup>118, 140, 141, 149</sup> and cell lines overexpressing c-FLIP<sub>R</sub> are protected against apoptosis<sup>140, 143</sup>. To analyse the functionality of the transgenic expression of murine c-FLIP<sub>R</sub>, thymocytes from WT and vavFLIP<sub>R</sub> mice were stimulated with CD95L or anti-CD95. Significantly more viable (AnnexinV<sup>+</sup> 7AAD<sup>-</sup>) cells were identified in stimulated samples from vavFLIP<sub>R</sub> mice compared with WT littermates (Figure 33B). Dexamethasone (Dex) is a synthetic glucocorticoid which induces apoptosis via binding to the glucocorticoid receptor<sup>252, 253</sup>. Thus, Dex-induced apoptosis is independent of the death-receptor mediated pathway and both WT and vavFLIP<sub>R</sub> thymocytes had comparable frequencies of viable cells after Dex-stimulation (Figure 33A, B). Furthermore, thymocytes from WT and vavFLIP<sub>R</sub> animals were stimulated with CD95L for up to eight hours to study the time-course of apoptosis. More early

apoptotic WT cells (AnnexinV<sup>+</sup> 7AAD<sup>-</sup>) were identified after four hours stimulation compared with vavFLIP<sub>R</sub> cells (Figure 33C, D). After eight hours CD95L-stimulation, higher frequencies of both late apoptotic (AnnexinV<sup>+</sup> 7AAD<sup>+</sup>) and early apoptotic WT cells were observed in comparison to vavFLIP<sub>R</sub> cells (Figure 33C, D). Thus, WT thymocytes were rapidly undergoing apoptosis, whereas vavFLIP<sub>R</sub> thymocytes were more resistant to CD95-induced apoptosis.

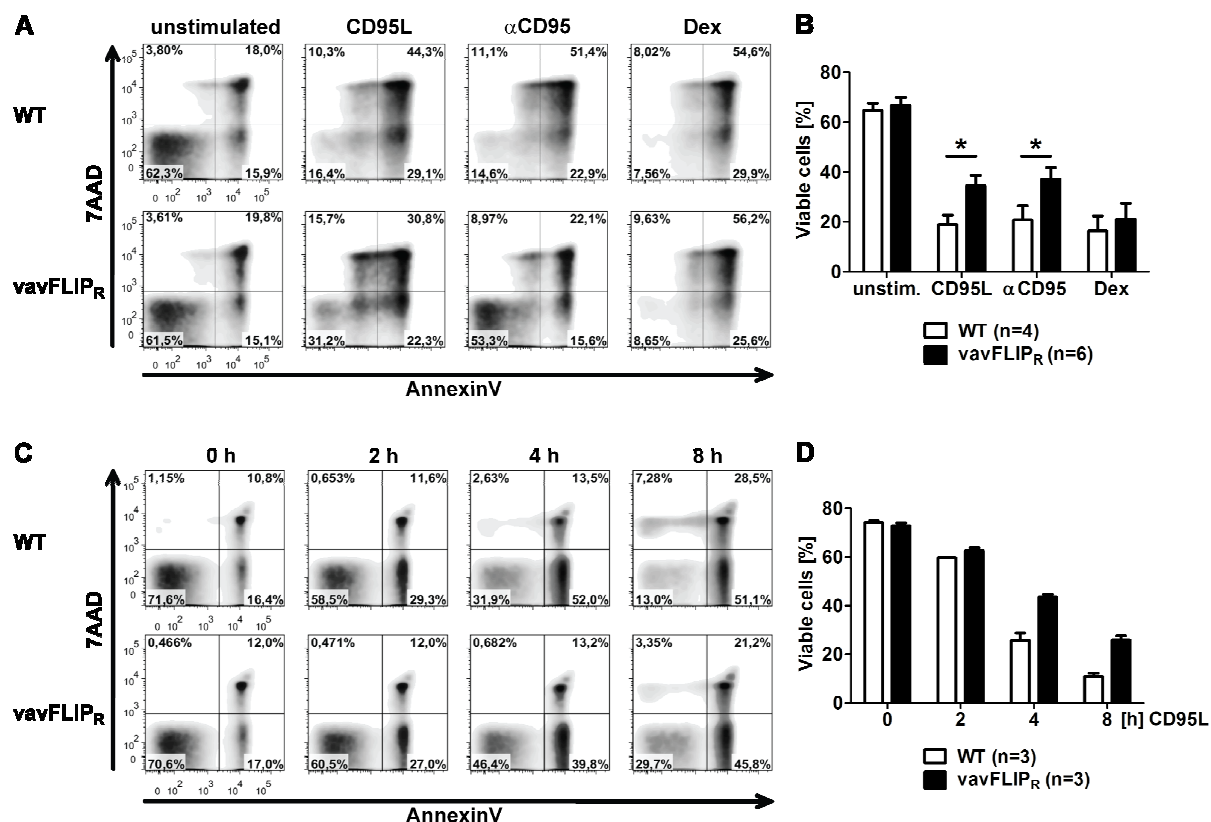


**Figure 33.** Analysis of CD95-mediated apoptosis in thymocytes from WT and vavFLIP<sub>R</sub> mice. **(A, B)** Thymocytes from WT and vavFLIP<sub>R</sub> animals were stimulated with 50 ng/ml CD95L, 1 μg/ml anti-CD95 (Jo2) crosslinked with 10 ng/ml Protein A or 1 μM dexamethasone (Dex) for 16 h (WT n=4, vavFLIP<sub>R</sub> n=6). Apoptosis was analysed by AnnexinV and 7AAD staining. Representative dot plots are shown in **(A)**. The percentages (mean ± s.e.m. of four independent experiments) of viable (AnnexinV<sup>-</sup> 7AAD<sup>-</sup>) cells for the different stimuli are shown in **(B)**. Statistical analyses were performed with one-tailed non-parametric Mann-Whitney *U* tests; asterisks (\*) indicate *p* < 0.05. **(C, D)** Thymocytes were stimulated with 50 ng/ml CD95L for 0, 2, 4 and 8 h (WT n=3, vavFLIP<sub>R</sub> n=3). Apoptosis was analysed by staining with AnnexinV and 7AAD measured by flow cytometry. Representative dot plots from one of two independent experiments are shown in **(C)**. The percentages (mean ± s.e.m.) of viable (AnnexinV<sup>-</sup> 7AAD<sup>-</sup>) cells for the different stimuli are represented in **(D)**.

Next, the apoptosis sensitivity in peripheral T and B cells was examined. Sorted CD4<sup>+</sup> and CD8<sup>+</sup> T cells as well as CD19<sup>+</sup> B cells were stimulated with CD95L and dexamethasone.

Significantly more viable (AnnexinV<sup>-</sup> 7AAD<sup>-</sup>) vavFLIP<sub>R</sub> CD4<sup>+</sup> and CD8<sup>+</sup> cells were identified compared with WT cells. The dexamethasone controls were comparable between WT and vavFLIP<sub>R</sub> cells (Figure 34A, B). Sorted CD19<sup>+</sup> B cells were activated with LPS for two days to induce expression of the CD95 receptor before CD95L- and dexamethasone stimulation. The B cells were fairly insensitive towards both CD95L- and dexamethasone-induced apoptosis. Nevertheless, the specific apoptosis of vavFLIP<sub>R</sub> B cells was significantly lower than the specific apoptosis of WT B cells (Figure 34C), whereas the specific apoptosis of dexamethasone-treated WT and vavFLIP<sub>R</sub> B cells was comparable (Figure 34D).

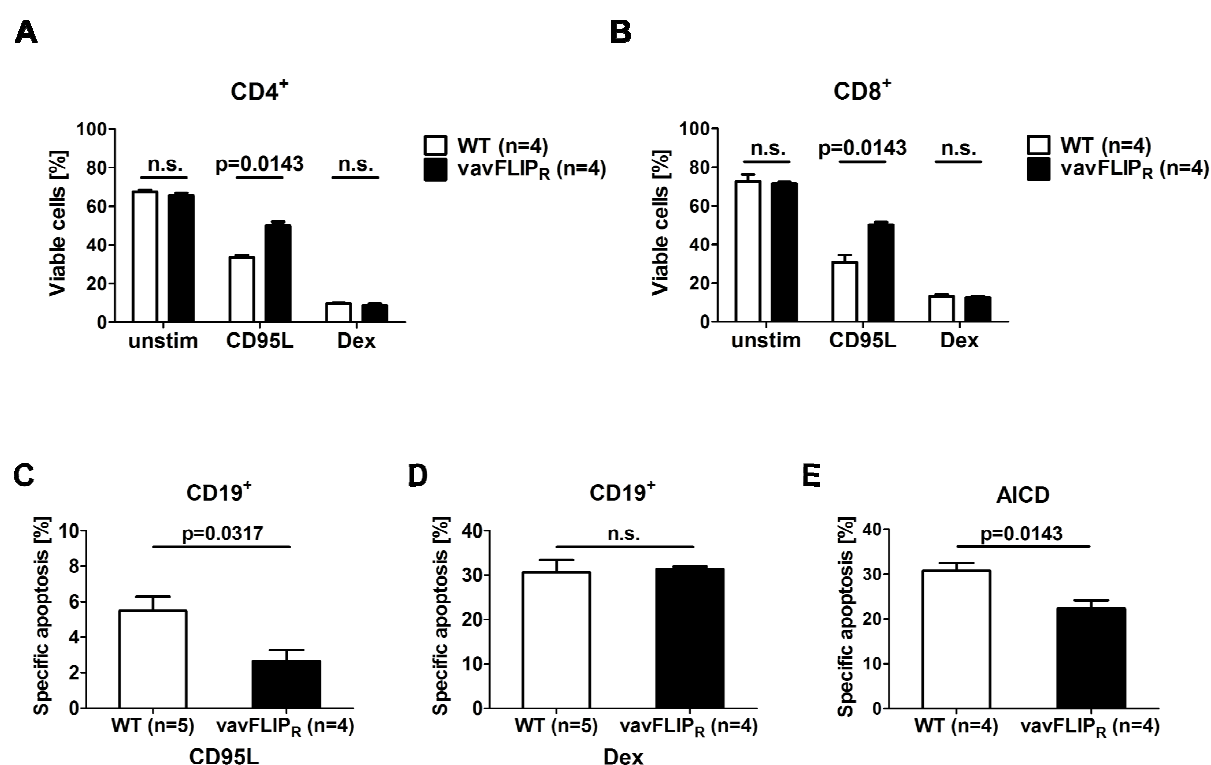


**Figure 34.** Apoptosis sensitivity of peripheral T and B cells and analysis of activation-induced cell death (AICD). **(A, B)** Sorted CD4<sup>+</sup> **(A)** and CD8<sup>+</sup> T cells **(B)** from peripheral lymphoid organs were stimulated with 50 ng/ml CD95L or 1  $\mu$ M dexamethasone (Dex) for 16 h (WT n=4, vavFLIP<sub>R</sub> n=4). Apoptosis was analysed by AnnexinV and 7AAD staining. The percentages of viable (AnnexinV<sup>-</sup> 7AAD<sup>-</sup>) cells are represented as the mean  $\pm$  s.e.m. from two independent experiments. **(C, D)** Sorted CD19<sup>+</sup> B cells from WT (n=5) and vavFLIP<sub>R</sub> (n=4) mice were activated with 10  $\mu$ g/ml LPS for 48 h. Apoptosis of activated B cells was assayed by stimulation with 100 ng/ml CD95L **(C)** or 1  $\mu$ M Dex **(D)** for 16 h, followed by AnnexinV and 7AAD staining. The specific apoptosis of CD95L- and Dex-stimulated cells is shown as the mean  $\pm$  s.e.m. from three independent experiments. **(E)** Peripheral lymph node cells from WT (n=4) and vavFLIP<sub>R</sub> (n=4) mice were activated with 10  $\mu$ g/ml plate-bound anti-CD3, 2  $\mu$ g/ml plate-bound anti-CD28 and 20 ng/ml IL-2 for two days and further expanded in IL-2 containing medium for three days. On day five, T cell blasts were cultured with 10  $\mu$ g/ml plate-bound anti-CD3 for 6 h to assess AICD. Apoptosis was analysed by AnnexinV and 7AAD staining. The specific apoptosis of anti-CD3 stimulated cells is displayed as the mean  $\pm$  s.e.m. from two independent experiments. Statistical analyses were performed with one-tailed non-parametric Mann Whitney *U* tests.

Reactivation of the T cell receptor leads to apoptosis by crosstalk with death receptors. The CD95 receptor has been shown to be involved in activation-induced cell death (AICD)<sup>166-169</sup>. To assay AICD, peripheral lymph node cells from WT and *vavFLIP<sub>R</sub>* mice were isolated and T cells were activated for two days with plate-bound anti-CD3 and anti-CD28 in presence of IL-2. Activated T cells were further expanded for three days in medium containing IL-2. AICD was assessed on day five by restimulating T cells with plate-bound anti-CD3 to induce cell death. Cells from *vavFLIP<sub>R</sub>* mice showed significantly less specific apoptosis compared to WT cells (Figure 34E).

The apoptosis assays confirm that *vavFLIP<sub>R</sub>* lymphocytes are protected against both CD95-induced apoptosis and AICD.

#### 4.3.4. Normal cell populations in young *vavFLIP<sub>R</sub>* mice

*Lpr* and *gld* mice with defective CD95 receptor and CD95 ligand respectively, show lymphoproliferative disease<sup>155, 160, 254</sup>. *c-FLIP* proteins inhibit the same pathway, however total cellularity of thymus, spleen and pLN were normal to slightly reduced in 7-week old *vavFLIP<sub>R</sub>* mice compared with WT littermates (Figure 35). The CD4/CD8 profiles in the thymuses of *vavFLIP<sub>R</sub>* and WT mice were comparable (Figure 36 and table 3).

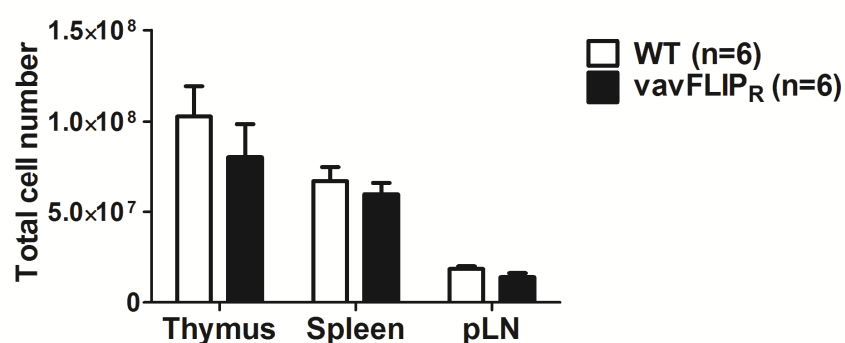


**Figure 35.** Total cell number of lymphoid organs thymus, spleen and peripheral lymph nodes from 7-week old *vavFLIP<sub>R</sub>* mice (n=6) and wild type littermates (n=6). The data is shown as the mean ± s.e.m. from two independent experiments.

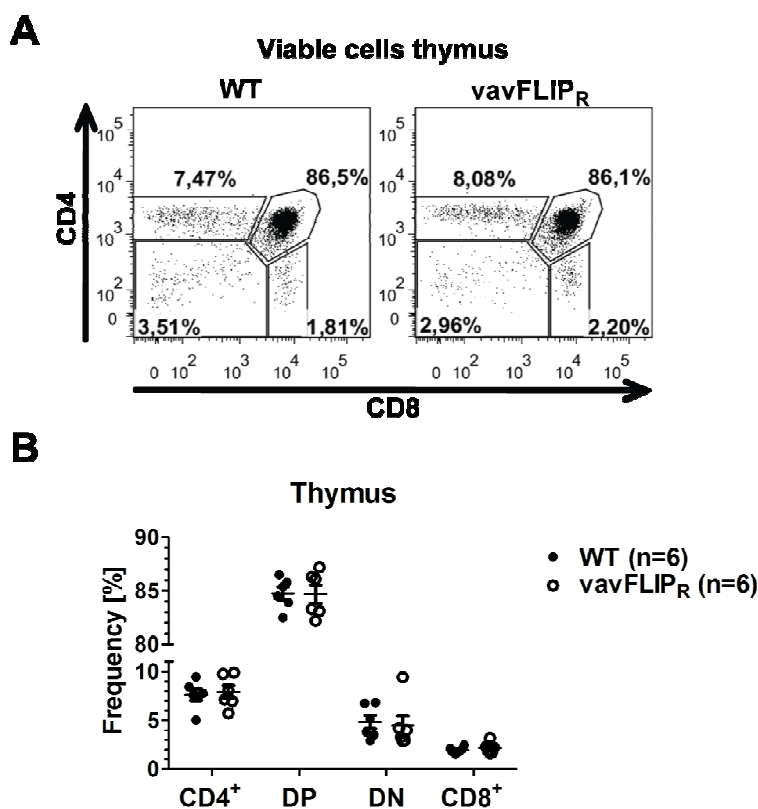


**Figure 36.** Cells from freshly isolated WT (n=6) and vavFLIP<sub>R</sub> (n=6) thymuses were stained for CD4 and CD8 followed by flow cytometry analysis. Representative dot plots are shown in (A). Frequencies of CD4<sup>+</sup> single positive, CD4<sup>+</sup>CD8<sup>+</sup> double positive (DP), CD4<sup>-</sup>CD8<sup>-</sup> double negative (DN) and CD8<sup>+</sup> single positive cells from two independent experiments are shown in (B). Individual mice are shown as separate symbols. Horizontal lines represent the mean; error bars display s.e.m.

The B cells and T cell subsets were analysed in spleen and peripheral lymph nodes from WT and vavFLIP<sub>R</sub> mice. Both frequencies and total cell numbers of CD19<sup>+</sup> B cells, CD3<sup>+</sup> T cells as well as the subsets CD4<sup>+</sup> helper T cells, CD8<sup>+</sup> cytotoxic T cells and CD4<sup>+</sup>CD25<sup>+</sup> regulatory T (T<sub>reg</sub>) cells were comparable between 7-week-old littermate WT and vavFLIP<sub>R</sub> mice (Figure 37, table 3).

**Table 3.** Total cell numbers of CD3<sup>+</sup>, CD4<sup>+</sup>, DP, DN, CD8<sup>+</sup>, CD19<sup>+</sup> and CD4<sup>+</sup>CD25<sup>+</sup> in 7-week old WT and vavFLIP<sub>R</sub> mice (s.d. = standard deviation, n.d. not determined).

Mouse strain (n=6)	Organ	Total cell number ×10 <sup>6</sup> (± s.d.)						
		CD3 <sup>+</sup>	CD4 <sup>+</sup>	DP	DN	CD8 <sup>+</sup>	CD19 <sup>+</sup>	CD4 <sup>+</sup> CD25 <sup>+</sup>
WT	thymus	n.d.	6.1 (2.0)	71.7 (30.8)	4.6 (3.2)	1.6 (0.6)	n.d.	n.d.
vavFLIP <sub>R</sub>	thymus	n.d.	4.7 (2.2)	55.5 (31.7)	3.2 (2.8)	1.3 (0.6)	n.d.	n.d.
WT	spleen	13.2 (4.7)	7.1 (2.6)	n.d.	n.d.	4.7 (1.5)	15.3 (3.7)	0.6 (0.2)
vavFLIP <sub>R</sub>	spleen	12.7 (4.5)	6.9 (2.8)	n.d.	n.d.	4.4 (1.5)	12.6 (4.6)	0.6 (0.3)
WT	pLN	9.0 (2.1)	5.0 (1.2)	n.d.	n.d.	3.7 (0.9)	2.6 (1.2)	0.5 (0.2)
vavFLIP <sub>R</sub>	pLN	6.8 (2.3)	4.0 (1.2)	n.d.	n.d.	2.5 (0.9)	2.0 (0.6)	0.4 (0.1)

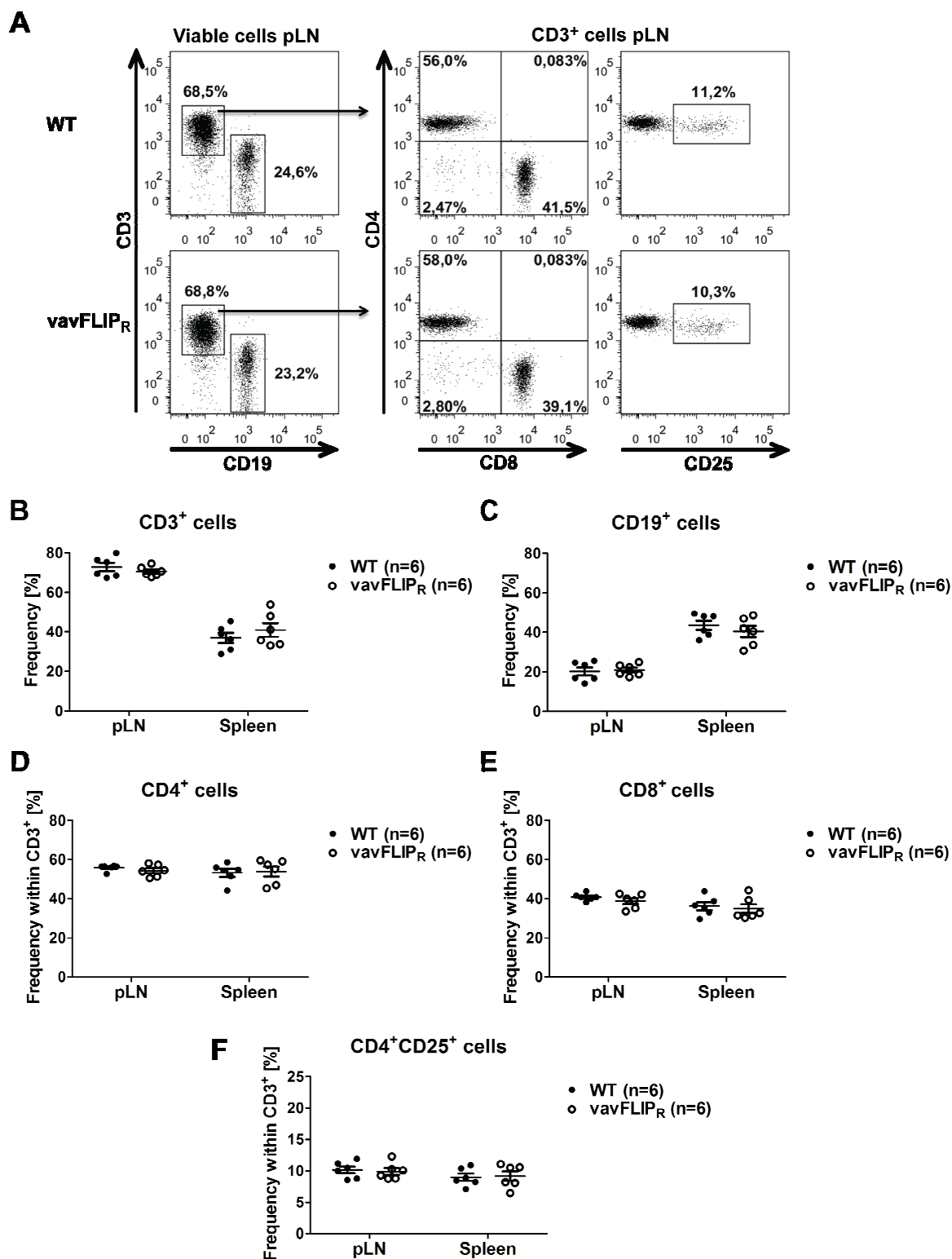


**Figure 37.** Freshly isolated splenocytes and peripheral lymph node cells (pLN) from WT (n=6) and vavFLIP<sub>R</sub> (n=6) mice were stained with antibodies directed against CD3, CD4, CD8, CD19 and CD25 followed by FACS analysis. Representative dot plots are shown in (A). (B - F) Individual mice are shown as separate symbols. Horizontal lines represent the mean of frequencies from two independent experiments; error bars display s.e.m. (B) CD3<sup>+</sup> T cells, (C) CD19<sup>+</sup> B cells, (D) CD4<sup>+</sup> T helper cells within the CD3<sup>+</sup> compartment, (E) CD8<sup>+</sup> cytotoxic T cells within the CD3<sup>+</sup> subset and (F) CD4<sup>+</sup>CD25<sup>+</sup> regulatory T cells within the CD3<sup>+</sup> compartment.

Furthermore, the activation status of T cells was analysed in spleen and peripheral lymph nodes from 7 weeks old WT and *vavFLIP<sub>R</sub>* mice by CD44 and CD62L staining. No difference in CD44<sup>+</sup> antigen-experienced T cells or CD62L<sup>+</sup> naïve T cells could be observed (Figure 38).

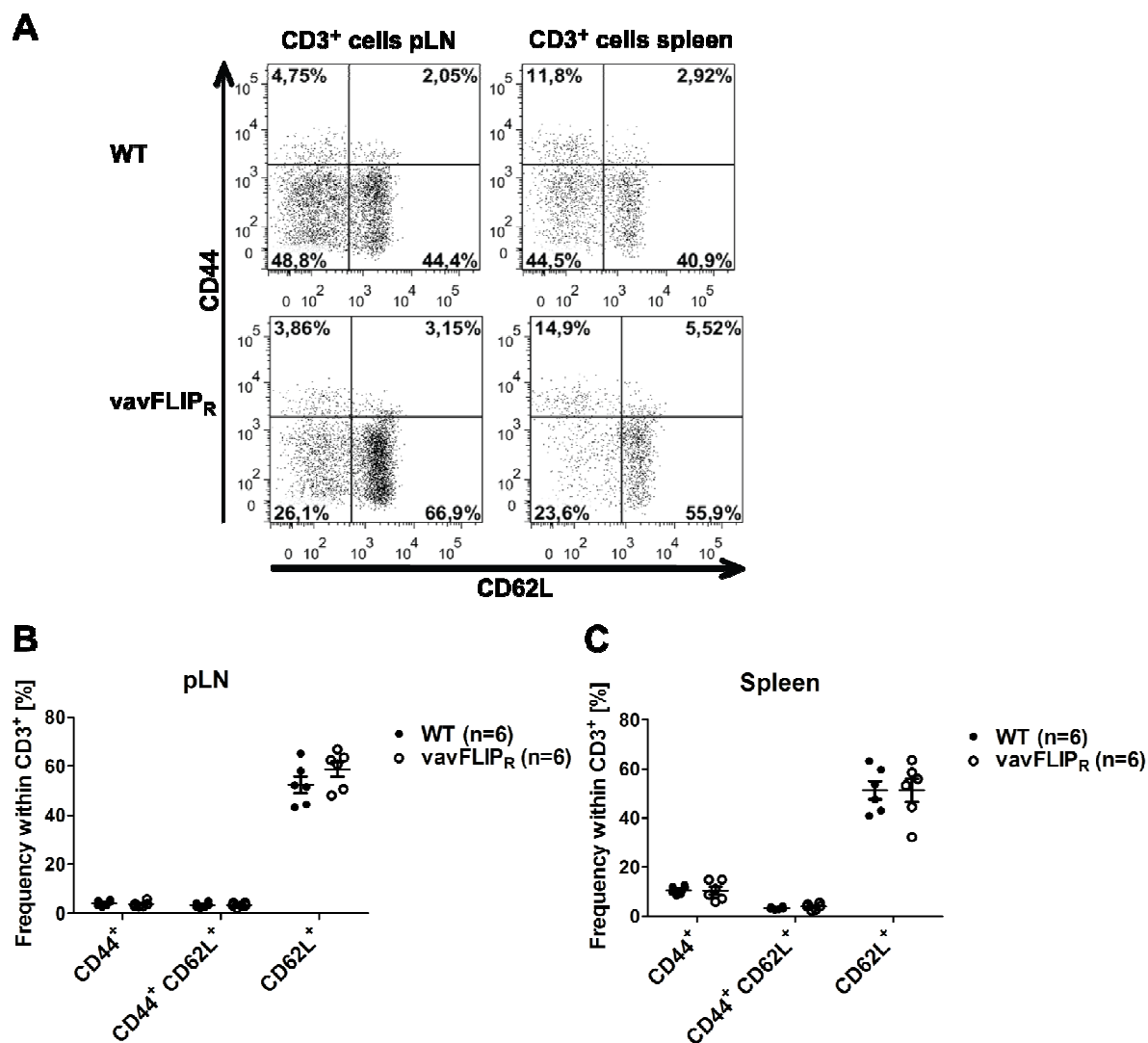


**Figure 38.** Flow cytometry analyses of activation status in 7-weeks old mice ( $n=6$ ). (A) Representative dot plots of CD44 and CD62L cells within the CD3<sup>+</sup> compartment from peripheral lymph nodes (left panel) and spleen (right panel). (B, C) Horizontal lines represent the mean of two independent experiments; error bars display s.e.m. Each symbol represents an individual mouse. The frequencies of CD44<sup>+</sup>, CD44<sup>+</sup>CD62L<sup>+</sup> and CD62L<sup>+</sup> in cells from peripheral lymph nodes (B) and spleenocytes (C) are shown.

#### 4.3.5. Experimental autoimmune encephalomyelitis

Experimental autoimmune encephalomyelitis (EAE) is an animal model for studying the human demyelinating inflammatory disorder multiple sclerosis (MS)<sup>255</sup>. The disease in the EAE model is caused by activated T cells with specific responses against myelin, which are migrating into the central nervous system (CNS)<sup>256</sup>. Experiments where EAE was induced in Lewis rats indicated that autoreactive T cells in the CNS are eliminated by activation-induced cell death via the CD95-receptor pathway<sup>257, 258</sup>. Therefore, the influence of constitutive murine c-FLIP<sub>R</sub> expression in T cells, macrophages and DCs in EAE disease progression was investigated. However, no differences between WT and vavFLIP<sub>R</sub> animals could be detected either in female (Figure 39A) or male mice (Figure 39B).

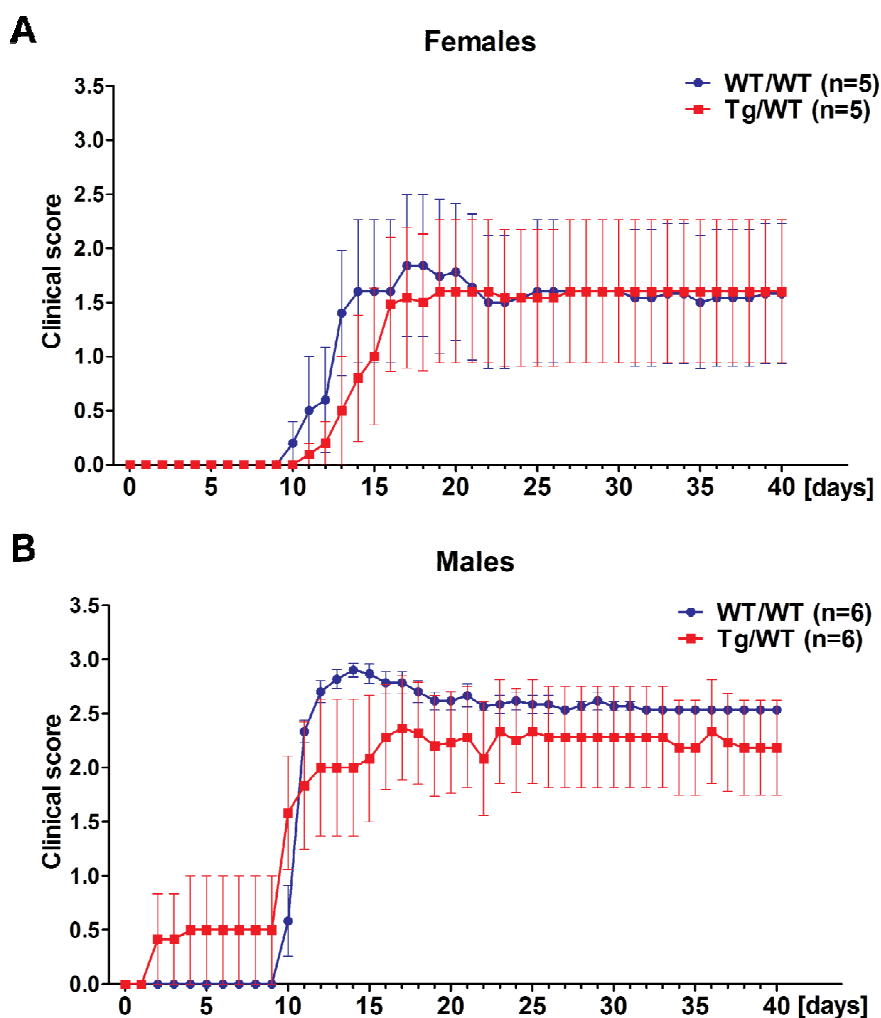


**Figure 39.** MOG(35-55)-peptide-induced experimental autoimmune encephalomyelitis (EAE). Female (A) and male (B) WT and vavFLIP<sub>R</sub> (Tg/WT) mice were injected with the MOG-peptide and two subsequent injections of pertussis toxin, followed by 40 days of scoring according to table 1 (see 3.3.5.). Data is represented as the mean ( $\pm$  s.e.m.).

#### 4.3.6. Altered cell populations in one year old vavFLIP<sub>R</sub> mice

Insufficient cell death can lead to autoimmunity and alterations in cell populations. *Lpr* and *gld* mice develop lymphoproliferation disease<sup>155, 160</sup>. Moreover, these mice accumulate CD4<sup>-</sup> CD8<sup>-</sup> double negative (DN) B220<sup>+</sup> T cells<sup>160, 161</sup>. WT and vavFLIP<sub>R</sub> littermates were aged to one year to examine the influence of constitutive expression of murine c-FLIP<sub>R</sub>. Peripheral lymph node cells of WT and vavFLIP<sub>R</sub> mice were analysed for DN B220<sup>+</sup> cells with three months old MRL/*lpr* mice as control. The characteristic DN B220<sup>+</sup> population was identified in MRL/*lpr* mice, but could not be detected in either WT or vavFLIP<sub>R</sub> animals (Figure 40), which is in agreement with c-FLIP<sub>L</sub> tg mice<sup>215</sup> and transgenic mice constitutively expressing human c-FLIP<sub>S</sub><sup>259</sup>. Furthermore, vavFLIP<sub>R</sub> animals did not show lymphoproliferation at one year of age. The cellularity of spleen and peripheral lymph nodes was normal in vavFLIP<sub>R</sub> mice (Figure 41).

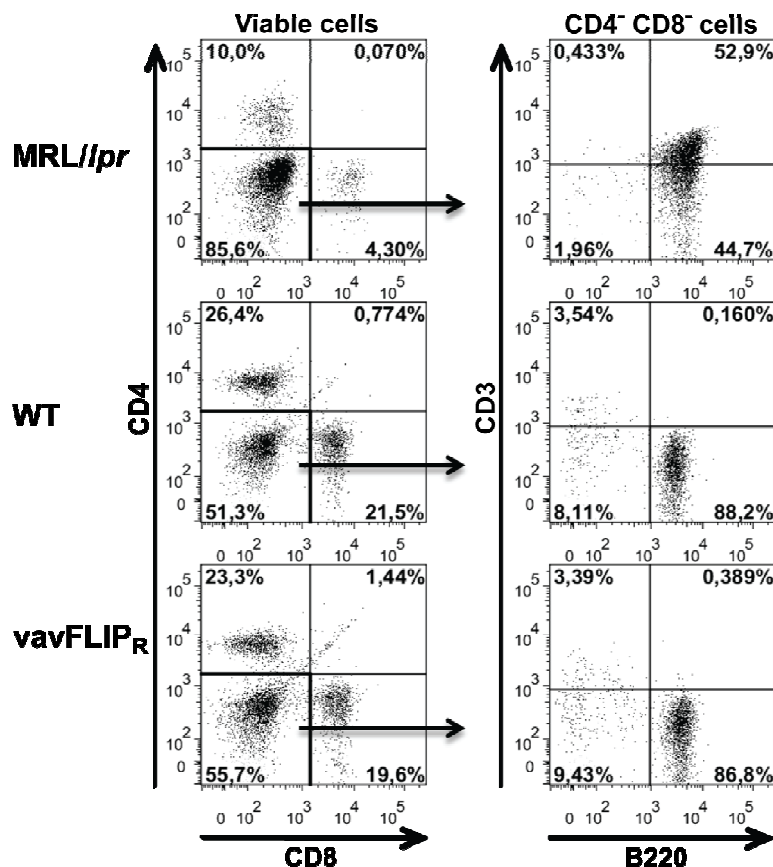


**Figure 40.** Analysis of DN B220<sup>+</sup> cells in peripheral lymph nodes from 1 year old WT and vavFLIP<sub>R</sub> animals. Representative dot plots are shown. Three months old MRL/*lpr* (CD95 mutated) mice develop the characteristic DN B220<sup>+</sup> cells (upper panel). This subset could not be found in either WT mice (mid panel) or vavFLIP<sub>R</sub> mice (lower panel). MRL/*lpr* n=2, WT n=6, vavFLIP<sub>R</sub> n=7.

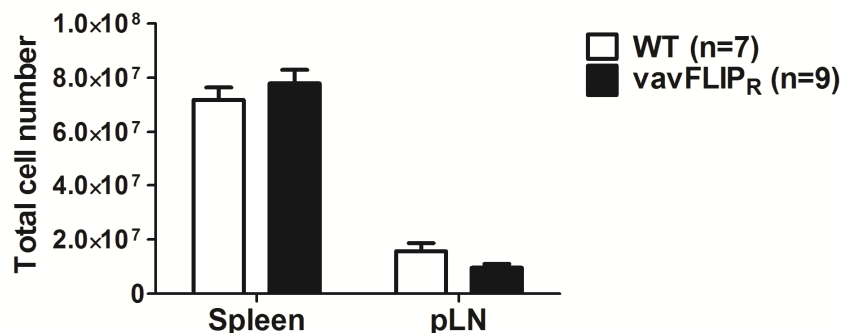


**Figure 41.** Total cell number of spleen and peripheral lymph nodes (pLN) from 1 year old vavFLIP<sub>R</sub> (n=9) and WT mice (n=7). The mean  $\pm$  s.e.m. is shown.

Flow cytometry analyses of lymphocyte subpopulations in spleens and pLN from one-year-old mice showed a slight reduction in both frequency and total cell number of vavFLIP<sub>R</sub> CD3<sup>+</sup> cells compared with WT CD3<sup>+</sup> cells. Nevertheless, CD4<sup>+</sup> and CD8<sup>+</sup> cell frequencies and total numbers were comparable between WT and vavFLIP<sub>R</sub> mice. Moreover, a minor increase in the frequency of vavFLIP<sub>R</sub> CD19<sup>+</sup> cells compared with WT was observed. However, the total cell numbers of CD19<sup>+</sup> cells were similar between WT and vavFLIP<sub>R</sub> mice. A slightly higher frequency of vavFLIP<sub>R</sub> CD4<sup>+</sup>CD25<sup>+</sup> cells in comparison to WT cells was identified, but WT and vavFLIP<sub>R</sub> total cell numbers were similar (Figure 42).

Next, the activation status in one year old WT and vavFLIP<sub>R</sub> mice was analysed. A slight increase in the frequencies of CD44<sup>+</sup> antigen-experienced cells as well as lower frequencies of CD62L<sup>+</sup> naïve cells could be identified in both peripheral lymph nodes and spleen of vavFLIP<sub>R</sub> mice compared with WT littermates. This was more pronounced in the spleen than peripheral lymph nodes, although the total cell numbers of CD44<sup>+</sup> and CD62L<sup>+</sup> cells were rather similar between WT and vavFLIP<sub>R</sub> mice (Figure 43). These data suggest that the higher frequency of CD4<sup>+</sup>CD25<sup>+</sup> cells in vavFLIP<sub>R</sub> mice are rather activated T helper cells than T<sub>reg</sub> cells (Figure 42).

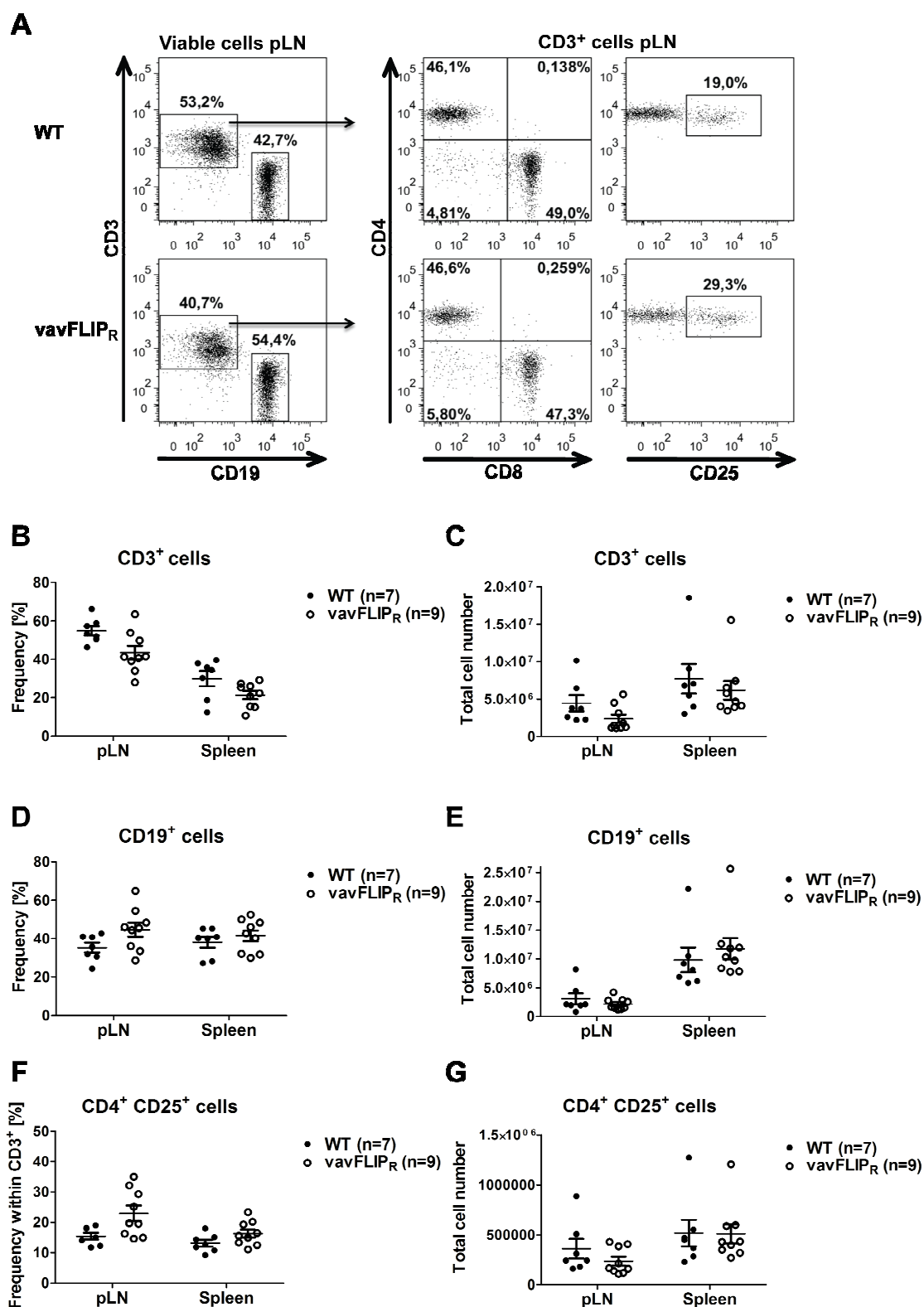


**Figure 42.** Analysis of B cells and T cell subsets by flow cytometry in 1 year old mice. **(A)** Representative dot plots of WT (n=7; upper panel) and vavFLIP<sub>R</sub> (n=9; lower panel) peripheral lymph node (pLN) cells. **(B, D, F)** Frequencies of CD3<sup>+</sup> cells **(B)**, CD19<sup>+</sup> cells **(D)** and CD4<sup>+</sup>CD25<sup>+</sup> cells **(F)** in freshly isolated peripheral lymph nodes and spleen. **(C, E, G)** Total cell numbers in peripheral lymph nodes and spleen of CD3<sup>+</sup> cells **(C)**, CD19<sup>+</sup> cells **(E)** and CD4<sup>+</sup>CD25<sup>+</sup> cells **(G)**. Individual mice are represented as separate symbols. Horizontal lines show the mean of four independent experiments; error bars display the s.e.m.

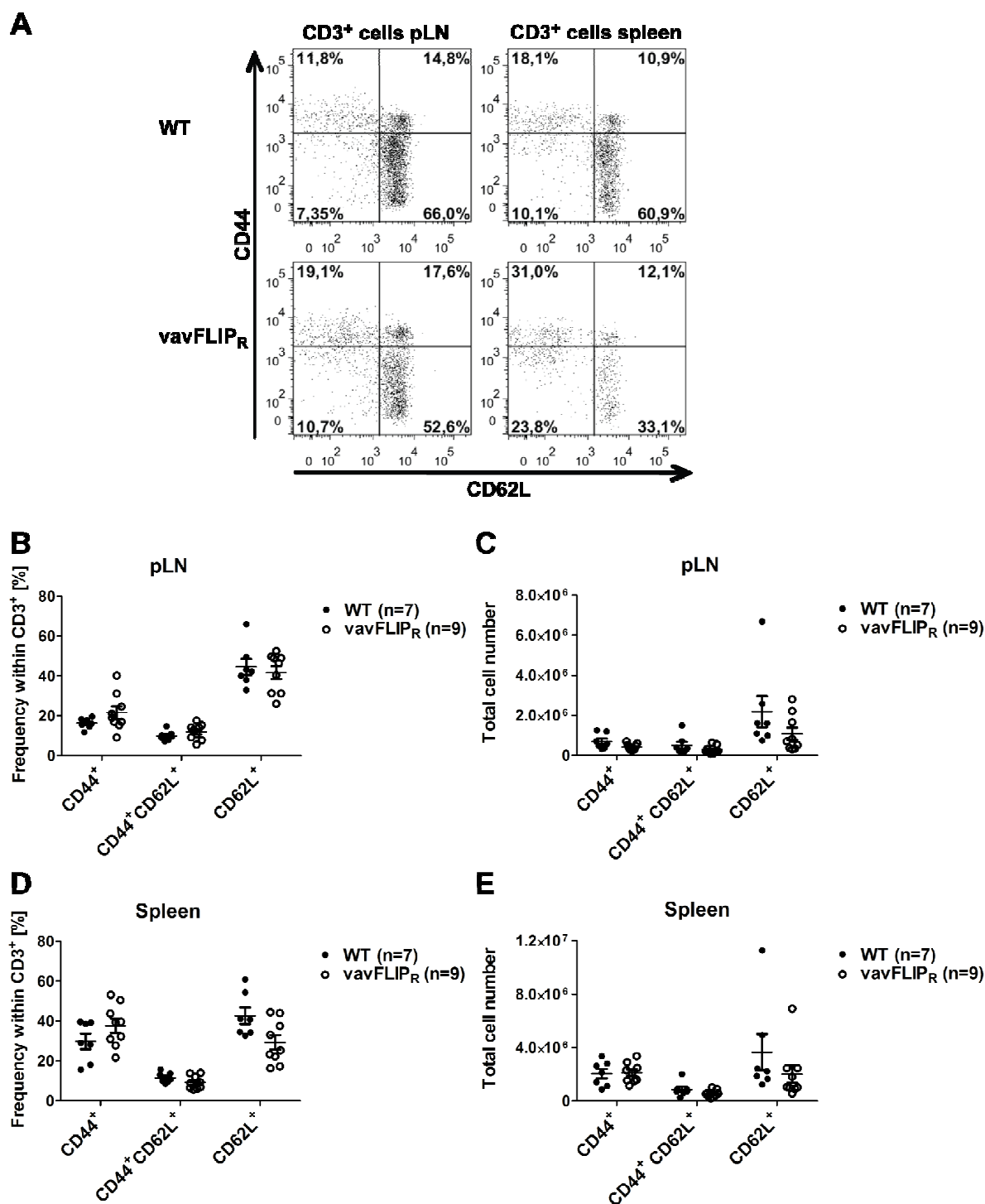


**Figure 43.** Freshly isolated peripheral lymph node (pLN) cells and splenocytes from 1 year old WT and vavFLIP<sub>R</sub> mice were stained for the activation markers CD44 and CD62L followed by flow cytometry analysis. **(A)** Representative dot plots of peripheral lymph node cells (left panel) and splenocytes (right panel) from WT ( $n=7$ ; upper panel) and vavFLIP<sub>R</sub> mice ( $n=9$ ; lower panel). **(B, D)** Frequencies of CD44<sup>+</sup>, CD44<sup>+</sup>CD62L<sup>+</sup> and CD62L<sup>+</sup> cells from peripheral lymph nodes **(B)** and spleen **(D)**. **(C and E)** Total cell numbers of CD44<sup>+</sup>, CD44<sup>+</sup>CD62L<sup>+</sup> and CD62L<sup>+</sup> cells from peripheral lymph nodes **(C)** and spleen **(E)**. **(B-E)** Symbols represent individual mice. Horizontal lines represent the mean of four independent experiments; error bars display s.e.m.

Dendritic cells, macrophages and granulocytes have been reported to be regulated through death receptors and c-FLIP proteins<sup>260, 261</sup>. Since vavFLIP<sub>R</sub> mice constitutively express murine c-FLIP<sub>R</sub> in all hematopoietic compartments, the frequencies of CD11c<sup>+</sup> dendritic cells, CD49b<sup>+</sup> natural killer (NK) cells, F4/80<sup>+</sup> macrophages and Gr1<sup>+</sup> granulocytes in one year old mice were analysed. The frequencies of CD11c<sup>+</sup>, CD49b<sup>+</sup>, F4/80<sup>+</sup> and Gr1<sup>+</sup> cells were comparable between WT and vavFLIP<sub>R</sub> mice (Table 4).

**Table 4.** Frequencies of CD11c<sup>+</sup>, F4/80<sup>+</sup>, Gr1<sup>+</sup> (WT n=4, vavFLIP<sub>R</sub> n=6) and CD49b<sup>+</sup> (WT n=2, vavFLIP<sub>R</sub> n=4) cells within the CD3<sup>-</sup>CD19<sup>-</sup> compartment in spleen and bone marrow (BM) from 1 year old mice. (s.d. = standard deviation)

Mouse strain	Organ	Frequency within CD3 <sup>-</sup> CD19 <sup>-</sup> subset ( $\pm$ s.d.) [%]			
		CD11c <sup>+</sup>	CD49b <sup>+</sup>	F4/80 <sup>+</sup>	Gr1 <sup>+</sup>
<b>WT</b>	<b>spleen</b>	3.2 (2.7)	12.9 (2.8)	8.5 (7.4)	2.7 (1.7)
<b>vavFLIP<sub>R</sub></b>	<b>spleen</b>	3.8 (3.4)	12.0 (3.9)	8.5 (7.3)	5.0 (3.1)
<b>WT</b>	<b>BM</b>	0.8 (0.2)	4.8 (1.6)	16.1 (7.5)	51.1 (8.5)
<b>vavFLIP<sub>R</sub></b>	<b>BM</b>	0.9 (0.5)	6.9 (2.5)	19.8 (14.8)	55.7 (21.2)

#### 4.3.7. Damage of kidneys and increased ANA-titers in one year old vavFLIP<sub>R</sub> mice

Livers and kidneys of one year old WT and vavFLIP<sub>R</sub> animals were analysed by histology. H&E stained livers were scored according to damage observed (see 3.3.6.). No differences could be identified between WT and vavFLIP<sub>R</sub> mice. Furthermore, kidneys were stained with PAS followed by histological scoring (see 3.3.6.). vavFLIP<sub>R</sub> kidneys had higher histological scores compared with WT kidneys, which implies more damage of vavFLIP<sub>R</sub> kidneys than WT kidneys in one year old mice (Figure 44).

Sera from one year old WT and vavFLIP<sub>R</sub> mice were analysed for anti-nuclear antibodies using an indirect immunofluorescence assay with HEp-2 cells as source of nuclear antigens. Significantly more autoantibodies could be identified in sera from vavFLIP<sub>R</sub> mice compared with WT mice. All WT animals, except one, had ANA-titers lower than serum dilution 1:320, whereas half of the vavFLIP<sub>R</sub> mice had ANA-titers at serum dilution 1:320 or higher (Figure 45).

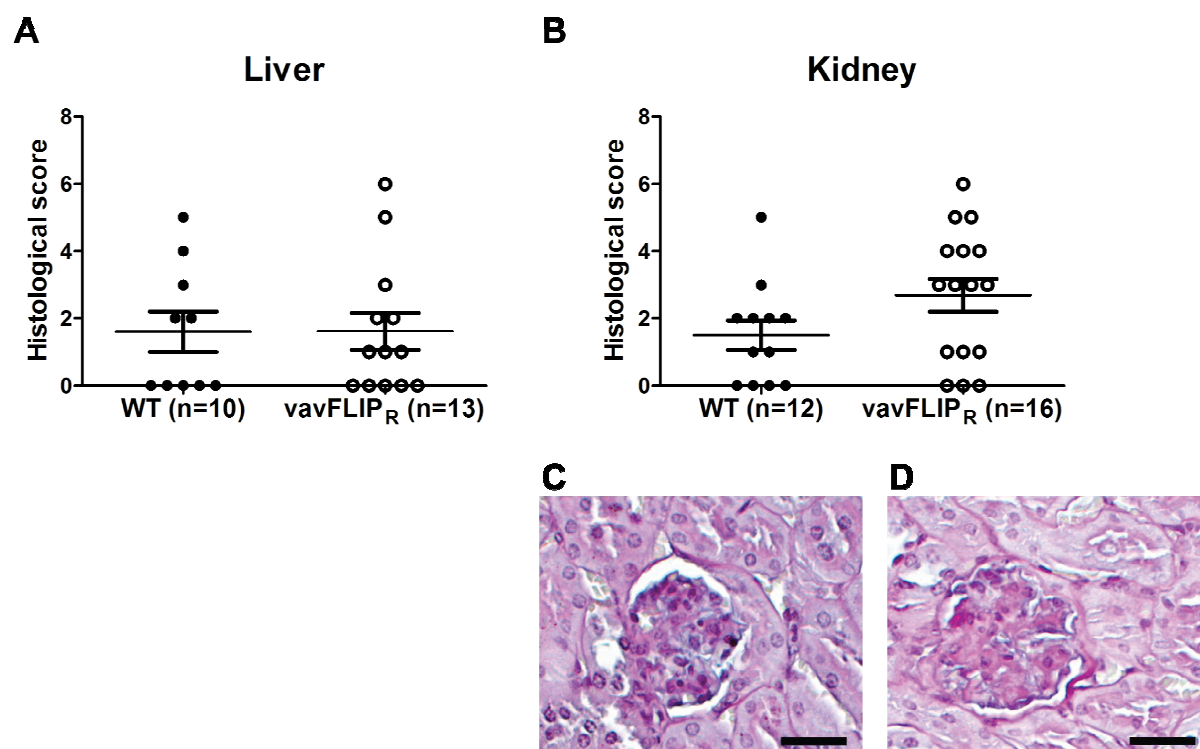


**Figure 44.** Histological scoring of H&E stained livers (A) and PAS stained kidneys (B) from 1 year old WT (liver n=10, kidney n=12) and vavFLIP<sub>R</sub> animals (liver n=13, kidney n=16). (A, B) Individual mice are displayed as separate symbols. Horizontal lines represent the mean; error bars show the s.e.m. (C, D) PAS staining of paraffin embedded kidneys; bar represents 25 $\mu$ m. (C) Normal glomerulum. (D) Glomerulum showing protein casts and thickening of the Bowman's capsule.

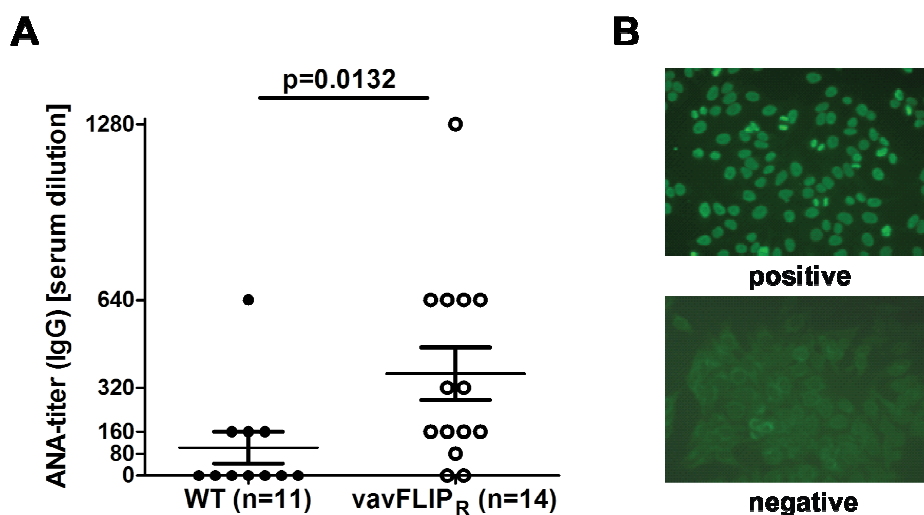


**Figure 45.** Anti-nuclear antibody (ANA) assay of sera from 1 year old WT (n=11) and vavFLIP<sub>R</sub> (n=14) mice. (A) Symbols represent individual mice. Horizontal lines represent the mean; error bars display s.e.m. (B) Examples of fluorescent homogenous pattern (positive) and negative fluorescent pattern.

## 5. Discussion

### 5.1. The role of c-FLIP splice variants in urothelial carcinoma

Apoptosis is crucial for maintaining tissue homeostasis and deregulation of apoptosis can lead to excessive cell growth and tumour formation<sup>60</sup>. Indeed, resistance to cell death is one hallmark of cancer cells. The resistance can be mediated by high expression levels of anti-apoptotic proteins<sup>262</sup>. Commonly upregulated anti-apoptotic proteins of the intrinsic pathway are Bcl-2, Bcl-x<sub>L</sub> and inhibitor of apoptosis proteins (IAPs)<sup>60, 262</sup>. The anti-apoptotic c-FLIP proteins inhibit apoptosis in the extrinsic pathway by preventing initiator caspase-activation at the signalling complex of death receptors<sup>118, 149</sup> and high expression levels of these proteins have been reported in various cancer types, i.e. melanoma<sup>141, 191</sup> and Hodgkin's lymphoma<sup>189, 190</sup>. Therefore, the lower expression of c-FLIP<sub>L</sub> in urothelial tumour tissue samples compared with normal tissue samples in this thesis was unexpected. The low c-FLIP<sub>L</sub> expression was confirmed in urothelial cell lines compared with normal urothelial cells. In contrast, c-FLIP<sub>S</sub> was not differentially expressed in either tissues or cell lines. Of note, a few tissue samples did not express c-FLIP<sub>S</sub> at all, most likely due to the presence of a functional SNP (rs10190751 A/G) in the *CFLAR* gene which determines whether c-FLIP<sub>R</sub> or c-FLIP<sub>S</sub> is produced<sup>142</sup>. In the context of a former study<sup>142</sup>, no significant changes in the distribution of this SNP between bladder cancer patients and controls were observed.

A previous study analysed the expression of c-FLIP, CD95 and CD95L in urothelial carcinomas by immunohistochemistry<sup>263</sup>. c-FLIP expression was observed in 81% of the 53 urothelial tumour samples, with increasing CD95L and c-FLIP expression with advancing stage of tumour. Normal urothelium was negative for c-FLIP and CD95L, whereas concurrent expression of CD95 and CD95L could be seen in half of the patient samples with 81.5% of these samples also being positive for c-FLIP. This suggests that c-FLIP is protecting the cells against CD95-mediated apoptosis. Indeed, down-regulation of c-FLIP by shRNA in this thesis sensitised the urothelial carcinoma cell lines towards both CD95L and TRAIL-mediated apoptosis. This is consistent with a previous report where a function of c-FLIP in the TRAIL resistance of urothelial tumour cells was observed<sup>264</sup>.

The differential expression of c-FLIP<sub>S</sub> and c-FLIP<sub>L</sub> isoforms in urothelial carcinoma found in this thesis raises the question of the splice variants' individual functions. The c-FLIP isoforms inhibit death-receptor mediated apoptosis by different mechanisms<sup>149</sup> and can even have

opposite outcomes on cell death<sup>152, 153</sup>. Overexpression of c-FLIP<sub>L</sub>, c-FLIP<sub>S</sub> and c-FLIP<sub>R</sub> by transient transfections in the VMcub1 and SD model systems demonstrated the protective effect towards CD95-induced apoptosis of all three c-FLIP isoforms in urothelial carcinoma. There are no antibodies available which recognise specific c-FLIP isoforms, therefore it is not possible to distinguish the different c-FLIP isoforms in tissue samples by immunohistochemistry. To address the question of individual functions of the long and short c-FLIP splice variants in urothelial tumours, RNA interference was used to specifically knock-down c-FLIP<sub>S</sub>, c-FLIP<sub>L</sub> or both isoforms (c-FLIP<sub>L/S</sub>) by lentiviral infection of shRNAs targeting these isoforms. In contrast to lymphocytes, where c-FLIP<sub>S</sub> has a dominant role in the protection against CD95-mediated apoptosis during the expansion phase of an immune reaction<sup>147</sup>, c-FLIP<sub>S</sub> only seems to have a supporting function in urothelial carcinoma. Instead, c-FLIP<sub>L</sub> was observed to play a more pronounced role in the apoptosis resistance of urothelial tumour cells. Single knock-down of c-FLIP<sub>L</sub> in SD cells was sufficient to sensitise the cells towards apoptosis induced by the death ligands CD95L and TRAIL. Importantly, complete knock-down of c-FLIP resulted in similar apoptosis levels as the co-treatment with CHX. This suggests that c-FLIP is the main short-lived anti-apoptotic protein in these cells. The VMcub1 cells responded somewhat different to death receptor stimulation; single knock-downs of c-FLIP<sub>L</sub> or c-FLIP<sub>S</sub> only slightly sensitised cells towards apoptosis. Minor cleavage of caspase-8 and -3 upon both CD95L- and TRAIL-stimulation was observed in VMcub1 cells with single knock-downs. This suggests that the c-FLIP isoforms are not complementary. Indeed, different functions of the long and short c-FLIP isoforms have been reported. c-FLIP<sub>S</sub> is particularly important in the activation phase of immune responses where it is upregulated to protect effector T cells from apoptosis, whereas c-FLIP<sub>L</sub> levels remain stable<sup>174, 175</sup>. Moreover, c-FLIP<sub>L</sub> can have both pro- and anti-apoptotic functions, whereas only anti-apoptotic functions have been reported for c-FLIP<sub>S</sub><sup>149, 151, 152</sup>. A pronounced effect on the apoptosis susceptibility in VMcub1 cells was only identified when both c-FLIP isoforms were knocked down. This indicates that both c-FLIP isoforms contribute to the apoptosis resistance in VMcub1 cells. Thus, cells can be sensitised by reducing the total c-FLIP levels below the protection threshold. The complete knock-down of c-FLIP in VMcub cells resulted in partial sensitisation compared with co-treatment with CHX. Consequently, additional factors apart from c-FLIP contribute to the apoptosis resistance in the VMcub1 cell line. Possibly, the VMcub1 cells are of type II in respect to the death receptor-mediated apoptosis. In contrast to type I cells, type II cells have less efficient DISC formation and

caspase-8 activation, therefore the death signals are amplified over the mitochondrial pathway in these cells<sup>114, 115</sup>. Of note, elevated expression of Bcl-2 and Bcl-x<sub>L</sub> was found in the previous characterisation of VMcub1 cells in the working group, which may contribute to the resistance against death receptor-mediated apoptosis<sup>237</sup>.

The downregulation of c-FLIP<sub>L</sub> observed in patient samples was surprising. High expression of an anti-apoptotic molecule would be thought to be beneficial for tumour survival and growth and this finding seems counterintuitive at first. However, CD95 signalling has been reported to have other functions in tumour cells. Tumour growth as well as the motility and invasiveness of tumour cells, especially in apoptosis-resistant tumours, can be promoted by CD95 signalling<sup>199, 200</sup>. The non-apoptotic functions of CD95 signalling require activation of the NF-κB and MAP kinase pathways. However, high c-FLIP expression was shown to reduce the activation of these pathways<sup>200, 265-267</sup>. This suggests that it is necessary for cancer cells to fine-tune the c-FLIP expression to optimise the effects of apoptosis inhibition and NF-κB/MAP kinase activation. Moreover, c-FLIP<sub>L</sub> has dual functions; the protein has an anti-apoptotic function at high expression levels, whereas it becomes pro-apoptotic at low expression levels<sup>153</sup>. Caspase-8 is more efficiently activated in heterodimers of c-FLIP<sub>L</sub>/caspase-8 than homodimers of caspase-8 itself at the DISC<sup>268, 269</sup>. The enzymatically inactive caspase-like domain of c-FLIP<sub>L</sub> induces the enzymatic activity of the caspase-8 protease domain, resulting in autoproteolytical cleavage and activation of the caspase-8 molecule<sup>151, 152, 268, 269</sup>. Furthermore, c-FLIP<sub>L</sub> acquires pro-apoptotic function in presence of high c-FLIP<sub>S</sub> expression<sup>153</sup>. Since c-FLIP<sub>S</sub> is also expressed in urothelial carcinoma cells, downregulation of c-FLIP<sub>L</sub> may be beneficial to prevent its proapoptotic activity.

At last, c-FLIP<sub>L</sub> and c-FLIP<sub>S</sub> are interplaying with the activation of the ripoptosome, a recently discovered multiprotein complex<sup>270, 271</sup>. Optimal c-FLIP<sub>L</sub> and c-FLIP<sub>S</sub> expression levels and ratio may be required to prevent activation of this cell death-inducing platform. The ripoptosome can initiate either apoptosis or necroptosis, depending on its molecular composition<sup>270, 271</sup>. RIP1 and RIP3 activation leads to necroptosis, whereas caspase-8 can cleave these kinases and thus, favours apoptosis. Interestingly, the c-FLIP<sub>S</sub> inhibition of caspase-8 cause increased levels of RIP1 in the ripoptosome and thereby activation of RIP3. This may promote necroptosis. In contrast, c-FLIP<sub>L</sub> and caspase-8 prevent ripoptosome formation, and thus inhibit necroptosis. Since necroptosis cause inflammation and thereby

attracts immune cells which can eliminate the tumour cells, it might be important for the development of urothelial carcinoma to inhibit ripoptosome assembly by c-FLIP<sub>L</sub>.

Taken together, c-FLIP proteins, especially c-FLIP<sub>L</sub>, are important resistance factors in urothelial carcinomas. Therefore, targeting c-FLIP in CD95L- and TRAIL-based therapies could be a promising approach to treat urothelial tumours.

## 5.2. Identification of novel CD95 DISC-interacting proteins

Even though the death-inducing signalling complex (DISC) has been studied for many years, the complexity of the platform and involved proteins in transducing both death and survival signals is not yet fully understood. Recently, the model of the DISC complex and its stoichiometry was reconsidered. It was assumed that there is a one to one ratio between the adaptor protein FADD and DED-containing proteins until two independent studies on the DISC complexes assembled at CD95 and TRAIL receptors were published<sup>228, 229</sup>. These reports gave evidence for chain formation of DED-proteins at CD95 and TRAIL receptor complexes. There are still open questions concerning the signalling pathways originating from the DISC. In this thesis the core components of the CD95 DISC under normal and c-FLIP<sub>L</sub> high circumstances were investigated by mass spectrometry. Moreover, the mass spectrometry data was used to identify novel DISC-interacting proteins.

The cell system chosen for mass spectrometry analysis was the Jurkat E6.1 cell line. This cell line was considered advantageous over the use of primary cells for different reasons. There are no constraints in protein amount compared with primary cells where it can be difficult to obtain the protein amount needed for mass spectrometry analyses. Moreover, it is a well-characterised model system and different knock-out cell lines are available<sup>243-245</sup>, which could be useful for the characterisation of a potential novel DISC-binding protein. Jurkat clones stably overexpressing c-FLIP<sub>L</sub> as well as empty vector control cells were generated. c-FLIP<sub>L</sub> is known to inhibit apoptosis<sup>118, 141</sup> and it was confirmed in this thesis that Jurkat clones overexpressing c-FLIP<sub>L</sub> were protected against CD95-mediated apoptosis. Death receptor expression of empty vector control cells and c-FLIP<sub>L</sub> overexpressing cells was comparable and thus, did not influence the level of apoptosis. Furthermore, c-FLIP has been described as an activator of NF-κB<sup>204, 206-208</sup>. Consistently, prolonged expression of phosphorylated IκBα

as well as increased expression of total I $\kappa$ B $\alpha$  was observed in c-FLIP<sub>L</sub> overexpressing clones. Thus, the Jurkat clones had functional expression of c-FLIP<sub>L</sub>.

The CD95 DISC was immunoprecipitated with somewhat different composition in empty vector control cells and cells overexpressing c-FLIP<sub>L</sub>. The high amount of c-FLIP and low amount of caspase-8 recruited to the DISC in c-FLIP<sub>L</sub> overexpressing clones is explained by the competition of DED-containing proteins for the same binding sites<sup>118</sup>. In addition, c-FLIP proteins have a higher affinity to these binding sites than caspase-8<sup>118</sup>. Minute amounts of RIP1 were immunoprecipitated with slightly more protein, possibly ubiquitinated, being detected in the DISC of c-FLIP<sub>L</sub> overexpressing cells. The DISC complex was also identified in c-FLIP<sub>L</sub>-immunoprecipitates upon anti-CD95 stimulation. Interestingly, RIP1 cleavage was observed, which could not be detected in the CD95L-immunoprecipitation. This could be caused by a different composition or localisation of the complex. Moreover, TRAF2 was recruited to the DISC in a c-FLIP<sub>L</sub>-dependent manner, which is consistent with the study of Kataoka and colleagues<sup>206</sup>. The low amount of RIP1 identified at the DISC might be explained by a study which identified more efficient recruitment of RIP1 to the CD95 DISC upon stimulation with membrane-bound CD95L than stimulation with soluble CD95L or agonistic antibodies<sup>272</sup>, the latter used in this thesis. The functions of RIP1 and TRAF2 in NF- $\kappa$ B activation have been studied for the TNF-R1 complex. Binding of TNF $\alpha$  to TNF-R1 leads to activation of the receptor and recruitment of the adaptor protein TRADD as well as RIP1 and TRAF2<sup>273</sup>. TRAF2 was reported to polyubiquitinate RIP1 at the TNF receptor complex<sup>250</sup>, which leads to activation of the NF- $\kappa$ B signalling cascade<sup>274, 275</sup>. Interestingly, a recent study by Gonzalvez and colleagues gave evidence for ubiquitination of caspase-8 by TRAF2 at the TRAIL-DISC<sup>276</sup>. The Lys48-linked ubiquitination of caspase-8 cleavage products p43 and p18 direct these fragments to proteosomal degradation, thereby ceasing the caspase-8 activity<sup>276</sup>. It is possible that the c-FLIP<sub>L</sub>-dependent association of TRAF2 to the CD95 DISC could be an additional mechanism by which c-FLIP proteins modulate caspase-8 activity. Still, the roles of RIP1 and TRAF2 need to be further characterised in the CD95 signalling pathway. It is not clear how c-FLIP<sub>L</sub> facilitates the binding of TRAF2 to the CD95 DISC. If there is a direct binding of c-FLIP<sub>L</sub> and TRAF2, the binding regions should be identified. Alternatively, c-FLIP<sub>L</sub> could have a stabilising effect on TRAF2- and/or RIP1-binding.

The core components of the CD95 DISC were confirmed to be the CD95 receptor itself as well as caspase-8 and caspase-10 for the empty vector control cells. Peculiarly, FADD was not detected in the empty vector DISC by mass spectrometry analysis even though it was clearly identified by Western blotting. Further, caspase-8 and -10 cannot be recruited to the DISC without FADD<sup>246, 247</sup>. Recent studies reported up to nine times more DED-containing proteins than FADD at the CD95 and TRAIL DISCs due to chain-formation of the DED-containing proteins<sup>228, 229</sup>. Consistent with these reports, it is likely that under the conditions used, the mass spectrometry was not sensitive enough to detect the low abundance of FADD at the DISC. Similarly, c-FLIP proteins have low expression levels in the empty vector control cells. This could explain why c-FLIP was not detected by mass spectrometry in the DISC of these cells. The CD95 DISC core components for the c-FLIP<sub>L</sub> overexpressing cells were the CD95 receptor, FADD, caspase-8, c-FLIP and TRAF2. Due to the low expression level of caspase-10, c-FLIP<sub>L</sub> outcompete caspase-10 at the DISC in c-FLIP<sub>L</sub> overexpressing cells. The slightly different composition of this DISC compared with the DISC of control cells possibly allows the detection of FADD. Mass spectrometry analyses could not identify RIP1 as a DISC-interacting protein in either empty vector control cells or c-FLIP<sub>L</sub> overexpressing cells. This may be due to the low amount of RIP1 binding to the CD95 DISC.

Interestingly, the mass spectrometry analyses revealed the proteins A20, hMMTAG2, Hcc-1 and Ssf-1 as potential novel CD95 DISC-associating proteins with c-FLIP<sub>L</sub>-dependent recruitment. The protein hMMTAG2 is linked to tumour transforming activities, Hcc-1 is a DNA-binding protein and Ssf-1 is a splicing factor<sup>277-279</sup>. Not much is known about these three proteins, but due to the nuclear localisation of Hcc-1 and involvement of Ssf-1 in mRNA splicing it seemed unlikely that these proteins would comprise functions in the DISC complex<sup>278, 279</sup>. There are no functional studies on hMMTAG2, the zinc finger protein A20 on the other hand has been implicated in NF- $\kappa$ B signalling at the TNF-R1 complex<sup>248, 249</sup>. Furthermore, reagents for A20 were available and therefore validation and further characterisation first concentrated on this protein. Western blot analyses could confirm the binding of A20 to the DISC. However, a c-FLIP<sub>L</sub>-dependent recruitment to the DISC could not be verified. A20 has been studied in the TNF-R1 receptor complex<sup>248</sup> where it can cease NF- $\kappa$ B activation by removing Lys63-linked polyubiquitin chains of RIP1. Thereafter, A20 can re-ubiquitinylate RIP1 with Lys48-linked polyubiquitin chains, which facilitates proteosomal degradation of the protein<sup>249</sup>. Hence, A20 is an ubiquitin editing enzyme and a

regulator of NF- $\kappa$ B activation. However, the association of A20 with the CD95 DISC has so far not been reported. A20 is known to interact with TRAF2<sup>280</sup> and could possibly thereby associate with the CD95 DISC. It remains to be clarified if the activation of NF- $\kappa$ B through c-FLIP<sub>L</sub> is regulated by A20. Further investigations are necessary to elucidate how A20 binds to the CD95 DISC and if the binding is c-FLIP-mediated or not. Moreover, the function of A20 at the CD95 DISC is not clear and remains to be examined.

### 5.3. Constitutive expression of murine c-FLIP<sub>R</sub> causes autoimmunity in aged mice

The murine *Cflar* gene structure only allows expression of c-FLIP<sub>R</sub> as short c-FLIP splice variant<sup>143</sup>. Nevertheless, up to this date c-FLIP<sub>R</sub> expression on the protein level has not been identified and it is not clear if this isoform has any functional relevance. Endogenous expression of c-FLIP<sub>R</sub> in lymph node cells was detected upon activation with Con A or anti-CD3/anti-CD28 in this thesis. A similar upregulation of human c-FLIP<sub>S</sub> was reported in short-term activated human T cells and was shown to be responsible for the protection against CD95-mediated apoptosis<sup>147, 175</sup>.

To further investigate the function of c-FLIP<sub>R</sub> in the immune system, transgenic mice were used with murine c-FLIP<sub>R</sub> under control of the *vav*-promoter to ensure expression in all hematopoietic compartments. Thymocytes as well as peripheral B and T cells from *vavFLIP<sub>R</sub>* mice were protected against CD95-induced apoptosis when induced by CD95L or agonistic antibodies, as expected. The death-receptor independent cell death induced by dexamethasone was not impaired in these lymphocytes. This implies that the transgenic c-FLIP<sub>R</sub> expression is functional. Furthermore, activated T cells from *vavFLIP<sub>R</sub>* mice were less sensitive towards cell death by restimulation of the T cell receptor. This finding is in contrast to the study of Lens and colleagues<sup>215</sup>, where overexpression of c-FLIP<sub>L</sub> did not protect murine T cells against AICD. However, particularly c-FLIP<sub>S</sub> is induced upon co-stimulatory signals, such as CD28, and was described to protect human T cells from AICD<sup>281</sup>. c-FLIP<sub>R</sub> might have a similar role in the mouse.

The T and B cell compartments were normal in young *vavFLIP<sub>R</sub>* mice. This is consistent with previous reports of T cell specific expression of human c-FLIP<sub>S</sub> in mice<sup>209, 259</sup>. Notably, a slight reduction in the thymus cellularity of *vavFLIP<sub>R</sub>* mice was observed. Reduced

thymocyte numbers were also reported for v-FLIP transgenic mice<sup>282, 283</sup>. Tai and colleagues described the same phenomenon for T cell specific c-FLIP<sub>L</sub> transgenic mice<sup>284</sup>. However, reduced thymus cellularity was not observed in further studies on c-FLIP<sub>S</sub><sup>209, 259</sup> and c-FLIP<sub>L</sub><sup>215</sup> transgenic mice. It is not clear why there are differences between the mouse models. Possible explanations are differences in the transgenic expression levels or the integration sites of the transgenic constructs.

The regulation of apoptosis is critical during embryonic development. c-FLIP knock-out mice die at day 10.5 of embryogenesis due to defects in vascularisation of the yolk sac and cardiac failure<sup>201</sup>. c-FLIP is also crucial for T cell development<sup>216, 217</sup>. CD4<sup>+</sup> and CD8<sup>+</sup> single positive T cells did not fully mature in the thymus of mice with T cell specific conditional knock-out of c-FLIP<sup>216</sup>. Moreover, transgenic mice expressing c-FLIP<sub>L</sub> in a T cell specific manner show disturbed T cell development and altered thymic selection<sup>284, 285</sup>. In contrast to c-FLIP<sub>L</sub> transgenic mice, alterations in T cell cellularity, frequencies of the main T cell subsets or activation status could not be identified in young vavFLIP<sub>R</sub> mice. Thus, it is not likely that c-FLIP<sub>R</sub> has a functional role in T cell development.

When EAE was induced in mice with mutated CD95<sup>155</sup>, prolonged and enhanced inflammation was observed in the CNS<sup>286</sup>. Hence, CD95/CD95L interactions are of importance to delete disease-initiating, autoreactive T cells in the CNS in the course of EAE. Both long and short c-FLIP isoforms have been reported to be upregulated in activated T cells from the cerebral spinal fluid in patients with active multiple sclerosis<sup>287, 288</sup>. Interestingly, transgenic mice overexpressing human c-FLIP<sub>L</sub> were resistant to EAE<sup>289</sup>. However, the progress of EAE in vavFLIP<sub>R</sub> and WT littermates was comparable. The autoimmune inflammation in EAE is mainly caused by Th1 and Th17 effector cells<sup>256</sup>. Since transgenic c-FLIP<sub>L</sub> expression enhances Th2 effector responses<sup>289-291</sup>, it is likely that c-FLIP<sub>L</sub>-expressing T cells can suppress the development of Th1-mediated autoimmune disease. Transgenic expression of c-FLIP<sub>R</sub> or c-FLIP<sub>S</sub> has so far not been reported to alter the cytokine production of T cells in this way, which may be one reason why the transgenic expression of c-FLIP<sub>R</sub> did not influence the progression of EAE. Furthermore, the opposing observations could be caused by the different transgenic constructs used; human c-FLIP<sub>L</sub> under control of the CD2 promoter versus vav-promoter-driven murine c-FLIP<sub>R</sub> transgenic expression, which most probably also influence the transgenic expression levels.

*Lpr* and *gld* mice with mutations in the CD95 receptor and ligand respectively, rapidly develop lymphoproliferative disease and autoimmunity<sup>155, 160</sup>. Furthermore, *lpr/gld* mice have altered lymphocyte populations and accumulate DN B220<sup>+</sup> cells<sup>161, 292</sup>. c-FLIP inhibits the same apoptosis pathway by preventing caspase-8 cleavage at the DISC<sup>118, 149</sup>. Indeed, T cell specific c-FLIP<sub>L</sub> transgenic mice were reported to develop autoimmunity when bred on Balb/c, but not C57BL/6, background<sup>285</sup>. It was therefore of interest to examine if constitutive expression of murine c-FLIP<sub>R</sub> in all hematopoietic compartments would lead to a similar phenotype. Up to one year old vavFLIP<sub>R</sub> mice had normal cellularity of spleen and lymph nodes. Moreover, no accumulation of DN B220<sup>+</sup> cells could be identified. Consistently, transgenic mice with T cell specific expression of murine c-FLIP<sub>L</sub> or human c-FLIP<sub>S</sub> did not develop a *lpr/gld* phenotype<sup>209, 215, 259</sup>. However, whether lymphoproliferative disease develops or not seems to be influenced by the expression level of FLIP as well as in which tissues the transgene is expressed. Notably, transgenic mice expressing the viral FLIP MC159 from the human Molluscum contagiosum virus under control of a CD2 enhancer cassette did not develop lymphoproliferation<sup>282</sup>. On the contrary, the *lpr/gld* phenotype was observed when MC159 was placed under control of the ubiquitous MHC class I H2K<sup>b</sup> promoter<sup>293</sup>. However, heterozygous MC159-expression was insufficient since lymphoproliferation and autoimmunity only was observed in mice with homozygous expression of MC159<sup>293</sup>. These studies imply that death-receptor-mediated apoptosis in non-T cells plays a central role in preventing autoimmunity. This was further emphasised in a study by Stranges and colleagues where lack of CD95 expression in dendritic cells resulted in systemic autoimmunity<sup>187</sup>. Even though vavFLIP<sub>R</sub> mice express c-FLIP<sub>R</sub> in all hematopoietic compartments, the animals are bred heterozygously, which might give a too low expression level of c-FLIP<sub>R</sub> to recapitulate the *lpr/gld* phenotype.

B and T cell numbers and distribution were normal in young vavFLIP<sub>R</sub> mice and no differences in dendritic cells, macrophages, granulocytes or NK cells could be identified even in mice at one year of age. However, one year old vavFLIP<sub>R</sub> mice had slightly lower frequencies of T cells and somewhat higher frequencies of B cells compared with WT littermates. Moreover, alterations in the ratio antigen-experienced/naïve T cells were observed. Human c-FLIP<sub>S</sub> is upregulated in the activation and expansion phase of an immune reaction, but is thereafter down-regulated to enable elimination of effector T cells<sup>281</sup>. Some effector cells survive and differentiate into memory T cells<sup>164</sup>. Evidence is provided in this

thesis that murine c-FLIP<sub>R</sub> is the functional orthologue of human c-FLIP<sub>S</sub>. Indeed, increased frequencies of activated T helper cells and antigen-experienced T cells as well as lower frequencies of naïve T cells were identified in vavFLIP<sub>R</sub> mice in comparison to WT mice. This is consistent with a previous report where an increased memory T cell pool was identified in c-FLIP<sub>S</sub> transgenic mice compared with WT animals after immunisation with the superantigen staphylococcal enterotoxin B <sup>259</sup>. Interestingly, histological analyses of kidneys from one year old mice revealed more tissue damage in kidneys from vavFLIP<sub>R</sub> mice in comparison to WT littermates. Moreover, elevated levels of antinuclear auto-antibodies were identified in sera from vavFLIP<sub>R</sub> animals at one year of age. These findings indicate that vavFLIP<sub>R</sub> mice develop a mild lupus-like phenotype. It is unclear which cell types are responsible for the autoimmunity in vavFLIP<sub>R</sub> mice. Persisting CD4<sup>+</sup> helper T cells could possibly prime B cells to produce auto-antibodies. Qiao and colleagues described lupus-like disease in c-FLIP<sub>L</sub> transgenic mice on the Balb/c background. The development of autoimmunity in this study required CD4<sup>+</sup> T cells and these cells were proposed to result from impaired thymic selection <sup>285</sup>. Nevertheless, the thymus profiles were normal in young vavFLIP<sub>R</sub> mice and no alteration of CD4<sup>+</sup> cell frequencies and total cell numbers could be identified in one year old vavFLIP<sub>R</sub> animals. The slightly increased frequency of B cells in vavFLIP<sub>R</sub> mice at one year of age could give another clue to the auto-antibody production. It remains to be investigated if B cells in aged vavFLIP<sub>R</sub> animals are hyperactivated.

Taken together, this thesis gives evidence for that c-FLIP<sub>R</sub> is a functional orthologue of human c-FLIP<sub>S</sub> and plays a role in the activation phase of the immune system. Young vavFLIP<sub>R</sub> mice have unaltered lymphocyte populations, though the activated and antigen-experienced T cell populations increase as the mice become older. Moreover, these animals develop mild lupus-like symptoms with age.

#### 5.4. Concluding remarks

The strict regulation of apoptosis is crucial for multicellular organisms. Insufficient apoptosis may result in diseases such as cancer or autoimmunity. The role of c-FLIP isoforms in urothelial carcinoma was investigated in this thesis. Interestingly, diminished c-FLIP<sub>L</sub> expression was observed in both urothelial carcinoma tissues and established carcinoma cell lines compared with normal tissue and cells. In contrast, c-FLIP<sub>S</sub> expression was comparable between tumour and normal tissues/cell lines. In spite of these observations, c-FLIP proteins,

especially c-FLIP<sub>L</sub>, were identified as important resistance factors in CD95- and TRAIL-mediated apoptosis in urothelial carcinoma. It is presumably necessary for tumours to fine-tune the c-FLIP expression to achieve an optimal balance between the anti-apoptotic and proliferative signalling of c-FLIP proteins.

Notably, mice with constitutive expression of c-FLIP<sub>R</sub> develop autoimmunity. One year old vav-FLIP<sub>R</sub> mice had increased levels of antigen-experienced T cells and reduced levels of naïve T cells compared with wild-type mice. Moreover, a higher degree of kidney damage and increased titers of autoantibodies were observed in one-year-old vavFLIP<sub>R</sub> mice in comparison to wild-type littermates. These mild lupus-like symptoms develop over time due to reduced apoptosis sensitivity.

Taken together, these findings underline the importance of careful control of apoptosis. Moreover, c-FLIP could be a relevant target in diseases where apoptosis is deregulated.

The DISC-interacting proteins c-FLIP, caspase-8 and FADD are reported to activate NF- $\kappa$ B signalling<sup>204-207</sup>. However, it is not fully understood how these proteins switch between apoptosis and proliferative signalling. The novel CD95 DISC interaction partner A20 was identified in this thesis. It remains to be investigated what role A20 plays in the life and death decisions of CD95.

## 6. Abbreviations

7AAD	7-amino-actinomycin D
A1	Bcl-2-related protein A1
ACN	acetonitrile
AICD	activation-induced cell death
AIF	apoptosis-inducing factor
ALPS	autoimmune lymphoproliferative syndrome
ANA	antinuclear antibody
Apaf-1	apoptotic protease-activating factor-1
APC	antigen presenting cell
APP	$\beta$ -amyloid precursor protein
Atg3	autophagy-related protein 3
Bad	Bcl-2 antagonist of cell death
Bak	Bcl-2 antagonist killer 1
Bax	Bcl-2-associated x protein
BCA	bicinchoninic acid
Bcl-2	B cell lymphoma-2
Bcl-w	Bcl-2-like protein 2
Bcl-x <sub>L</sub>	Bcl-lymphoma-extra large
BH domains	Bcl-2 homology domains
Bid	Bcl-2 interacting domain death agonist
BIC	ammonium hydrogencarbonate
Bik	Bcl-2-interacting killer
Bim	Bcl-2-interacting mediator of cell death
BM	bone marrow
Bmf	Bcl-2 modifying factor
Bok	Bcl-2-related ovarian killer
CAD	caspase activated DNase
CARD	caspase recruitment domain
CD	cluster of differentiation

---

CD95L	CD95 ligand
<i>C. Elegans</i>	<i>Caenorhabditis elegans</i>
c-FLIP	cellular FLICE-inhibitory protein
c-FLIP <sub>L</sub>	cellular FLICE-inhibitory protein long isoform
c-FLIP <sub>R</sub>	cellular FLICE-inhibitory protein Raji
c-FLIP <sub>S</sub>	cellular FLICE-inhibitory protein short isoform
Con A	concanavalin A
CHX	cycloheximide
CNS	central nervous system
DcR	decoy receptor
DD	death domain
DED	death effector domain
Dex	dexamethasone
Diablo	direct binding IAP protein with low pI
DISC	death-inducing signalling complex
DMEM	Dulbecco's modified Eagle's medium
DN	double negative (CD4 <sup>-</sup> CD8 <sup>-</sup> )
DNA	deoxyribonucleic acid
DP	double positive (CD4 <sup>+</sup> CD8 <sup>+</sup> )
DP5	death protein 5
DR	death receptor
EAE	experimental induced encephalomyelitis
<i>E. coli</i>	<i>Escherichia coli</i>
EndoG	endonuclease G
ER	endoplasmic reticulum
EtBr	ethidium bromide
FADD	Fas-associated death domain
FCS	fetal calf serum
FLIP	FLICE-inhibitory protein
FLICE	FADD-like IL-1 $\beta$ -converting enzyme
GAPDH	glyceraldehyde 3-phosphate dehydrogenase

---

GFP	green fluorescent protein
<i>gld</i>	generalized lymphoproliferative disease
H&E	hematoxylin and eosin
HA	hemagglutinin
HEK293T	human embryonic kidney 293T
HMGB1	high mobility group protein B1
Hrk	Harakiri
hu	human
ICAD	inhibitor of caspase activated DNase
ICAM3	intercellular adhesion molecule-3
IFN- $\gamma$	interferon- $\gamma$
Ig	immunoglobulin
I $\kappa$ B	inhibitor of NF- $\kappa$ B protein
IKK complex	I $\kappa$ B kinase complex
IL	interleukin
IMDM	Iscoe's modified Dulbecco's medium
iono	Ionomycin
IP	immunoprecipitation
IRES	internal ribosomal entry site
LC	liquid chromatography
LOX1	oxidized low-density lipoprotein-1
LV	lentivirus
<i>lpr</i>	lymphoproliferation
LPS	lipopolysaccharide
LT	lymphotoxin
MAP	mitogen-activated protein
Mcl-1	myeloid cell leukemia 1
MFG-E8	milk fat globule-EGF factor-8 protein
MHC	major histocompatibility complex
mk	monkey
mLN	mesenteric lymph nodes

---

MOMP	mitochondrial outer membrane permeabilisation
mRNA	messenger RNA
ms	mouse
MS	mass spectrometry
Mule	Mcl-1 ubiquitin ligase E3
n.d.	not determined
NFAT	calcineurin-nuclear factor of activated T cells
NF- $\kappa$ B	nuclear factor $\kappa$ B
NK cells	natural killer cells
NUC	normal urothelial cells
OPG	osteoprotegerin
OPGL	osteoprotegerin ligand
PAS	periodic acid schiff
PCR	polymerase chain reaction
PE	phosphatidylethanolamine
pLN	peripheral lymph nodes
PMA	phorbol-12-myristate-13-acetate
Puma	p53-upregulated modulator of apoptosis
QVD-Oph	quinoline-Val-Asp-difluorophenoxymethylketone
RIP	receptor-interacting protein
RNA	ribonucleic acid
ROCK I	Rho-associated coiled-coil-containing protein kinase I
ROS	reactive oxygen species
rt	rat
<i>S. aureus</i>	<i>Staphylococcus aureus</i>
s.d.	standard deviation
SDS-PAGE	SDS-polyacrylamide gel electrophoresis
s.e.m.	standard error of the mean
shRNA	short hairpin RNA
Smac	second mitochondria-derived activator of caspase
SNP	single nucleotide polymorphism

---

SP	single positive
SPF	specific pathogen free
SV40	simian virus 40
tBid	truncated Bid
TBP	TATA-binding protein
TCR	T cell receptor
TFA	trifluoroacetic acid
TGF- $\beta$	transforming growth factor $\beta$
TIM4	T cell immunoglobulin domain and mucin domain protein 4
Th1/2	T helper type 1/2
TM	transmembrane domain
TMRE	tetramethylrhodamine ethyl ester
TNF	tumour necrosis factor
TNF-R	tumour necrosis factor receptor
T <sub>reg</sub> cells	regulatory T cells
TRADD	TNF receptor-associated death domain protein
TRAF2	TNF receptor-associated factor 2
TRAIL	TNF-related apoptosis-inducing ligand
TRAIL-R	TNF-related apoptosis-inducing ligand receptor
TSP	thrombospondin
v-FLIP	viral FLICE-inhibitory protein
WAH-1	worm apoptosis-inducing factor homologue
WT	wild-type
XIAP	x-linked inhibitor of apoptosis protein

## 7. References

1. Degtarev, A. & Yuan, J. Expansion and evolution of cell death programmes. *Nat Rev Mol Cell Biol* **9**, 378-390 (2008).
2. Galluzzi, L. *et al.* Molecular definitions of cell death subroutines: recommendations of the Nomenclature Committee on Cell Death 2012. *Cell Death Differ* **19**, 107-120 (2012).
3. Clarke, P.G. Developmental cell death: morphological diversity and multiple mechanisms. *Anat Embryol (Berl)* **181**, 195-213 (1990).
4. Kerr, J.F., Wyllie, A.H. & Currie, A.R. Apoptosis: a basic biological phenomenon with wide-ranging implications in tissue kinetics. *Br J Cancer* **26**, 239-257 (1972).
5. Taylor, R.C., Cullen, S.P. & Martin, S.J. Apoptosis: controlled demolition at the cellular level. *Nat Rev Mol Cell Biol* **9**, 231-241 (2008).
6. Green, D.R., Ferguson, T., Zitvogel, L. & Kroemer, G. Immunogenic and tolerogenic cell death. *Nat Rev Immunol* **9**, 353-363 (2009).
7. Aravind, L., Dixit, V.M. & Koonin, E.V. Apoptotic molecular machinery: vastly increased complexity in vertebrates revealed by genome comparisons. *Science* **291**, 1279-1284 (2001).
8. Bouillet, P. & O'Reilly, L.A. CD95, BIM and T cell homeostasis. *Nat Rev Immunol* **9**, 514-519 (2009).
9. Lauber, K. *et al.* Apoptotic cells induce migration of phagocytes via caspase-3-mediated release of a lipid attraction signal. *Cell* **113**, 717-730 (2003).
10. Martin, S.J. *et al.* Early redistribution of plasma membrane phosphatidylserine is a general feature of apoptosis regardless of the initiating stimulus: inhibition by overexpression of Bcl-2 and Abl. *J Exp Med* **182**, 1545-1556 (1995).
11. Fadok, V.A. *et al.* Exposure of phosphatidylserine on the surface of apoptotic lymphocytes triggers specific recognition and removal by macrophages. *J Immunol* **148**, 2207-2216 (1992).
12. Hanayama, R. *et al.* Identification of a factor that links apoptotic cells to phagocytes. *Nature* **417**, 182-187 (2002).
13. Miyanishi, M. *et al.* Identification of Tim4 as a phosphatidylserine receptor. *Nature* **450**, 435-439 (2007).
14. Manodori, A.B., Barabino, G.A., Lubin, B.H. & Kuypers, F.A. Adherence of phosphatidylserine-exposing erythrocytes to endothelial matrix thrombospondin. *Blood* **95**, 1293-1300 (2000).
15. Greenberg, M.E. *et al.* Oxidized phosphatidylserine-CD36 interactions play an essential role in macrophage-dependent phagocytosis of apoptotic cells. *J Exp Med* **203**, 2613-2625 (2006).
16. Chang, M.K. *et al.* Monoclonal antibodies against oxidized low-density lipoprotein bind to apoptotic cells and inhibit their phagocytosis by elicited macrophages: evidence that oxidation-specific epitopes mediate macrophage recognition. *Proc Natl Acad Sci U S A* **96**, 6353-6358 (1999).
17. Oka, K. *et al.* Lectin-like oxidized low-density lipoprotein receptor 1 mediates phagocytosis of aged/apoptotic cells in endothelial cells. *Proc Natl Acad Sci U S A* **95**, 9535-9540 (1998).
18. Platt, N., Suzuki, H., Kurihara, Y., Kodama, T. & Gordon, S. Role for the class A macrophage scavenger receptor in the phagocytosis of apoptotic thymocytes in vitro. *Proc Natl Acad Sci U S A* **93**, 12456-12460 (1996).

19. Hall, S.E., Savill, J.S., Henson, P.M. & Haslett, C. Apoptotic neutrophils are phagocytosed by fibroblasts with participation of the fibroblast vitronectin receptor and involvement of a mannose/fucose-specific lectin. *J Immunol* **153**, 3218-3227 (1994).
20. Ogden, C.A. *et al.* C1q and mannose binding lectin engagement of cell surface calreticulin and CD91 initiates macropinocytosis and uptake of apoptotic cells. *J Exp Med* **194**, 781-795 (2001).
21. Savill, J., Hogg, N., Ren, Y. & Haslett, C. Thrombospondin cooperates with CD36 and the vitronectin receptor in macrophage recognition of neutrophils undergoing apoptosis. *J Clin Invest* **90**, 1513-1522 (1992).
22. Moffatt, O.D., Devitt, A., Bell, E.D., Simmons, D.L. & Gregory, C.D. Macrophage recognition of ICAM-3 on apoptotic leukocytes. *J Immunol* **162**, 6800-6810 (1999).
23. Arur, S. *et al.* Annexin I is an endogenous ligand that mediates apoptotic cell engulfment. *Dev Cell* **4**, 587-598 (2003).
24. Wu, Y., Tibrewal, N. & Birge, R.B. Phosphatidylserine recognition by phagocytes: a view to a kill. *Trends Cell Biol* **16**, 189-197 (2006).
25. Schwartzman, R.A. & Cidlowski, J.A. Apoptosis: the biochemistry and molecular biology of programmed cell death. *Endocr Rev* **14**, 133-151 (1993).
26. Zong, W.X. & Thompson, C.B. Necrotic death as a cell fate. *Genes Dev* **20**, 1-15 (2006).
27. Scaffidi, P., Misteli, T. & Bianchi, M.E. Release of chromatin protein HMGB1 by necrotic cells triggers inflammation. *Nature* **418**, 191-195 (2002).
28. Han, J., Zhong, C.Q. & Zhang, D.W. Programmed necrosis: backup to and competitor with apoptosis in the immune system. *Nat Immunol* **12**, 1143-1149 (2011).
29. Levine, B. & Deretic, V. Unveiling the roles of autophagy in innate and adaptive immunity. *Nat Rev Immunol* **7**, 767-777 (2007).
30. Baehrecke, E.H. Autophagy: dual roles in life and death? *Nat Rev Mol Cell Biol* **6**, 505-510 (2005).
31. Kroemer, G. & Levine, B. Autophagic cell death: the story of a misnomer. *Nat Rev Mol Cell Biol* **9**, 1004-1010 (2008).
32. Danial, N.N. & Korsmeyer, S.J. Cell death: critical control points. *Cell* **116**, 205-219 (2004).
33. Krammer, P.H., Arnold, R. & Lavrik, I.N. Life and death in peripheral T cells. *Nat Rev Immunol* **7**, 532-542 (2007).
34. Palmer, E. Negative selection--clearing out the bad apples from the T-cell repertoire. *Nat Rev Immunol* **3**, 383-391 (2003).
35. Strasser, A., Harris, A.W., Huang, D.C., Krammer, P.H. & Cory, S. Bcl-2 and Fas/APO-1 regulate distinct pathways to lymphocyte apoptosis. *EMBO J* **14**, 6136-6147 (1995).
36. Huang, D.C. *et al.* Activation of Fas by FasL induces apoptosis by a mechanism that cannot be blocked by Bcl-2 or Bcl-x(L). *Proc Natl Acad Sci U S A* **96**, 14871-14876 (1999).
37. Yuan, J., Shaham, S., Ledoux, S., Ellis, H.M. & Horvitz, H.R. The *C. elegans* cell death gene *ced-3* encodes a protein similar to mammalian interleukin-1 beta-converting enzyme. *Cell* **75**, 641-652 (1993).
38. Cerretti, D.P. *et al.* Molecular cloning of the interleukin-1 beta converting enzyme. *Science* **256**, 97-100 (1992).
39. Thornberry, N.A. *et al.* A novel heterodimeric cysteine protease is required for interleukin-1 beta processing in monocytes. *Nature* **356**, 768-774 (1992).

40. Eckhart, L. *et al.* Identification of novel mammalian caspases reveals an important role of gene loss in shaping the human caspase repertoire. *Mol Biol Evol* **25**, 831-841 (2008).
41. Li, J. & Yuan, J. Caspases in apoptosis and beyond. *Oncogene* **27**, 6194-6206 (2008).
42. Scaffidi, C., Medema, J.P., Krammer, P.H. & Peter, M.E. FLICE is predominantly expressed as two functionally active isoforms, caspase-8/a and caspase-8/b. *J Biol Chem* **272**, 26953-26958 (1997).
43. Saleh, M. *et al.* Differential modulation of endotoxin responsiveness by human caspase-12 polymorphisms. *Nature* **429**, 75-79 (2004).
44. Martinon, F. & Tschopp, J. Inflammatory caspases: linking an intracellular innate immune system to autoinflammatory diseases. *Cell* **117**, 561-574 (2004).
45. Fuentes-Prior, P. & Salvesen, G.S. The protein structures that shape caspase activity, specificity, activation and inhibition. *Biochem J* **384**, 201-232 (2004).
46. Wilson, K.P. *et al.* Structure and mechanism of interleukin-1 beta converting enzyme. *Nature* **370**, 270-275 (1994).
47. Cohen, G.M. Caspases: the executioners of apoptosis. *Biochem J* **326** ( Pt 1), 1-16 (1997).
48. Eckhart, L. *et al.* Terminal differentiation of human keratinocytes and stratum corneum formation is associated with caspase-14 activation. *J Invest Dermatol* **115**, 1148-1151 (2000).
49. Denecker, G. *et al.* Caspase-14 protects against epidermal UVB photodamage and water loss. *Nat Cell Biol* **9**, 666-674 (2007).
50. Boatright, K.M. & Salvesen, G.S. Mechanisms of caspase activation. *Curr Opin Cell Biol* **15**, 725-731 (2003).
51. Donepudi, M., Mac Sweeney, A., Briand, C. & Grutter, M.G. Insights into the regulatory mechanism for caspase-8 activation. *Mol Cell* **11**, 543-549 (2003).
52. Thornberry, N.A. *et al.* A combinatorial approach defines specificities of members of the caspase family and granzyme B. Functional relationships established for key mediators of apoptosis. *J Biol Chem* **272**, 17907-17911 (1997).
53. Fischer, U., Janicke, R.U. & Schulze-Osthoff, K. Many cuts to ruin: a comprehensive update of caspase substrates. *Cell Death Differ* **10**, 76-100 (2003).
54. Coleman, M.L. *et al.* Membrane blebbing during apoptosis results from caspase-mediated activation of ROCK I. *Nat Cell Biol* **3**, 339-345 (2001).
55. Sebbagh, M. *et al.* Caspase-3-mediated cleavage of ROCK I induces MLC phosphorylation and apoptotic membrane blebbing. *Nat Cell Biol* **3**, 346-352 (2001).
56. Liu, X., Zou, H., Slaughter, C. & Wang, X. DFF, a heterodimeric protein that functions downstream of caspase-3 to trigger DNA fragmentation during apoptosis. *Cell* **89**, 175-184 (1997).
57. Sakahira, H., Enari, M. & Nagata, S. Cleavage of CAD inhibitor in CAD activation and DNA degradation during apoptosis. *Nature* **391**, 96-99 (1998).
58. Enari, M. *et al.* A caspase-activated DNase that degrades DNA during apoptosis, and its inhibitor ICAD. *Nature* **391**, 43-50 (1998).
59. Schulze-Osthoff, K., Ferrari, D., Los, M., Wesselborg, S. & Peter, M.E. Apoptosis signaling by death receptors. *Eur J Biochem* **254**, 439-459 (1998).
60. Igney, F.H. & Krammer, P.H. Death and anti-death: tumour resistance to apoptosis. *Nat Rev Cancer* **2**, 277-288 (2002).
61. Wilson, N.S., Dixit, V. & Ashkenazi, A. Death receptor signal transducers: nodes of coordination in immune signaling networks. *Nat Immunol* **10**, 348-355 (2009).

62. Ashkenazi, A. Targeting death and decoy receptors of the tumour-necrosis factor superfamily. *Nat Rev Cancer* **2**, 420-430 (2002).
63. Itoh, N. & Nagata, S. A novel protein domain required for apoptosis. Mutational analysis of human Fas antigen. *J Biol Chem* **268**, 10932-10937 (1993).
64. Tartaglia, L.A., Ayres, T.M., Wong, G.H. & Goeddel, D.V. A novel domain within the 55 kd TNF receptor signals cell death. *Cell* **74**, 845-853 (1993).
65. Peter, M.E. & Krammer, P.H. The CD95(APO-1/Fas) DISC and beyond. *Cell Death Differ* **10**, 26-35 (2003).
66. Sprick, M.R. *et al.* FADD/MORT1 and caspase-8 are recruited to TRAIL receptors 1 and 2 and are essential for apoptosis mediated by TRAIL receptor 2. *Immunity* **12**, 599-609 (2000).
67. Kischkel, F.C. *et al.* Apo2L/TRAIL-dependent recruitment of endogenous FADD and caspase-8 to death receptors 4 and 5. *Immunity* **12**, 611-620 (2000).
68. Boldin, M.P. *et al.* A novel protein that interacts with the death domain of Fas/APO1 contains a sequence motif related to the death domain. *J Biol Chem* **270**, 7795-7798 (1995).
69. Chinnaiyan, A.M., O'Rourke, K., Tewari, M. & Dixit, V.M. FADD, a novel death domain-containing protein, interacts with the death domain of Fas and initiates apoptosis. *Cell* **81**, 505-512 (1995).
70. Kischkel, F.C. *et al.* Cytotoxicity-dependent APO-1 (Fas/CD95)-associated proteins form a death-inducing signaling complex (DISC) with the receptor. *EMBO J* **14**, 5579-5588 (1995).
71. Aggarwal, B.B. Signalling pathways of the TNF superfamily: a double-edged sword. *Nat Rev Immunol* **3**, 745-756 (2003).
72. Kischkel, F.C. *et al.* Death receptor recruitment of endogenous caspase-10 and apoptosis initiation in the absence of caspase-8. *J Biol Chem* **276**, 46639-46646 (2001).
73. Wang, J., Chun, H.J., Wong, W., Spencer, D.M. & Lenardo, M.J. Caspase-10 is an initiator caspase in death receptor signaling. *Proc Natl Acad Sci U S A* **98**, 13884-13888 (2001).
74. Nikolaev, A., McLaughlin, T., O'Leary, D.D. & Tessier-Lavigne, M. APP binds DR6 to trigger axon pruning and neuron death via distinct caspases. *Nature* **457**, 981-989 (2009).
75. Kroemer, G., Galluzzi, L. & Brenner, C. Mitochondrial membrane permeabilization in cell death. *Physiol Rev* **87**, 99-163 (2007).
76. Youle, R.J. & Strasser, A. The BCL-2 protein family: opposing activities that mediate cell death. *Nat Rev Mol Cell Biol* **9**, 47-59 (2008).
77. Tsujimoto, Y., Cossman, J., Jaffe, E. & Croce, C.M. Involvement of the bcl-2 gene in human follicular lymphoma. *Science* **228**, 1440-1443 (1985).
78. Bakhshi, A. *et al.* Cloning the chromosomal breakpoint of t(14;18) human lymphomas: clustering around JH on chromosome 14 and near a transcriptional unit on 18. *Cell* **41**, 899-906 (1985).
79. Cleary, M.L., Smith, S.D. & Sklar, J. Cloning and structural analysis of cDNAs for bcl-2 and a hybrid bcl-2/immunoglobulin transcript resulting from the t(14;18) translocation. *Cell* **47**, 19-28 (1986).
80. Vaux, D.L., Cory, S. & Adams, J.M. Bcl-2 gene promotes haemopoietic cell survival and cooperates with c-myc to immortalize pre-B cells. *Nature* **335**, 440-442 (1988).
81. Chipuk, J.E., Moldoveanu, T., Llambi, F., Parsons, M.J. & Green, D.R. The BCL-2 family reunion. *Mol Cell* **37**, 299-310 (2010).

82. Tait, S.W. & Green, D.R. Mitochondria and cell death: outer membrane permeabilization and beyond. *Nat Rev Mol Cell Biol* **11**, 621-632 (2010).
83. Zong, W.X., Lindsten, T., Ross, A.J., MacGregor, G.R. & Thompson, C.B. BH3-only proteins that bind pro-survival Bcl-2 family members fail to induce apoptosis in the absence of Bax and Bak. *Genes Dev* **15**, 1481-1486 (2001).
84. Lindsten, T. *et al.* The combined functions of proapoptotic Bcl-2 family members bak and bax are essential for normal development of multiple tissues. *Mol Cell* **6**, 1389-1399 (2000).
85. Ke, F. *et al.* BCL-2 family member BOK is widely expressed but its loss has only minimal impact in mice. *Cell Death Differ* **19**, 915-925 (2012).
86. Cory, S. & Adams, J.M. The Bcl2 family: regulators of the cellular life-or-death switch. *Nat Rev Cancer* **2**, 647-656 (2002).
87. Muchmore, S.W. *et al.* X-ray and NMR structure of human Bcl-xL, an inhibitor of programmed cell death. *Nature* **381**, 335-341 (1996).
88. Sattler, M. *et al.* Structure of Bcl-xL-Bak peptide complex: recognition between regulators of apoptosis. *Science* **275**, 983-986 (1997).
89. Willis, S.N. *et al.* Apoptosis initiated when BH3 ligands engage multiple Bcl-2 homologs, not Bax or Bak. *Science* **315**, 856-859 (2007).
90. Chen, L. *et al.* Differential targeting of prosurvival Bcl-2 proteins by their BH3-only ligands allows complementary apoptotic function. *Mol Cell* **17**, 393-403 (2005).
91. Ranger, A.M. *et al.* Bad-deficient mice develop diffuse large B cell lymphoma. *Proc Natl Acad Sci U S A* **100**, 9324-9329 (2003).
92. Shibue, T. *et al.* Integral role of Noxa in p53-mediated apoptotic response. *Genes Dev* **17**, 2233-2238 (2003).
93. Villunger, A. *et al.* p53- and drug-induced apoptotic responses mediated by BH3-only proteins puma and noxa. *Science* **302**, 1036-1038 (2003).
94. Bouillet, P. *et al.* Proapoptotic Bcl-2 relative Bim required for certain apoptotic responses, leukocyte homeostasis, and to preclude autoimmunity. *Science* **286**, 1735-1738 (1999).
95. Bouillet, P. *et al.* BH3-only Bcl-2 family member Bim is required for apoptosis of autoreactive thymocytes. *Nature* **415**, 922-926 (2002).
96. Nakano, K. & Vousden, K.H. PUMA, a novel proapoptotic gene, is induced by p53. *Mol Cell* **7**, 683-694 (2001).
97. Yu, J., Zhang, L., Hwang, P.M., Kinzler, K.W. & Vogelstein, B. PUMA induces the rapid apoptosis of colorectal cancer cells. *Mol Cell* **7**, 673-682 (2001).
98. Han, J. *et al.* Expression of bbc3, a pro-apoptotic BH3-only gene, is regulated by diverse cell death and survival signals. *Proc Natl Acad Sci U S A* **98**, 11318-11323 (2001).
99. Jeffers, J.R. *et al.* Puma is an essential mediator of p53-dependent and -independent apoptotic pathways. *Cancer Cell* **4**, 321-328 (2003).
100. Acehan, D. *et al.* Three-dimensional structure of the apoptosome: implications for assembly, procaspase-9 binding, and activation. *Mol Cell* **9**, 423-432 (2002).
101. Zou, H., Henzel, W.J., Liu, X., Lutschg, A. & Wang, X. Apaf-1, a human protein homologous to *C. elegans* CED-4, participates in cytochrome c-dependent activation of caspase-3. *Cell* **90**, 405-413 (1997).
102. Li, P. *et al.* Cytochrome c and dATP-dependent formation of Apaf-1/caspase-9 complex initiates an apoptotic protease cascade. *Cell* **91**, 479-489 (1997).
103. Pop, C., Timmer, J., Sperandio, S. & Salvesen, G.S. The apoptosome activates caspase-9 by dimerization. *Mol Cell* **22**, 269-275 (2006).

104. Renatus, M., Stennicke, H.R., Scott, F.L., Liddington, R.C. & Salvesen, G.S. Dimer formation drives the activation of the cell death protease caspase 9. *Proc Natl Acad Sci U S A* **98**, 14250-14255 (2001).
105. Boatright, K.M. *et al.* A unified model for apical caspase activation. *Mol Cell* **11**, 529-541 (2003).
106. Eckelman, B.P., Salvesen, G.S. & Scott, F.L. Human inhibitor of apoptosis proteins: why XIAP is the black sheep of the family. *EMBO Rep* **7**, 988-994 (2006).
107. Suzuki, Y. *et al.* A serine protease, HtrA2, is released from the mitochondria and interacts with XIAP, inducing cell death. *Mol Cell* **8**, 613-621 (2001).
108. Verhagen, A.M. *et al.* Identification of DIABLO, a mammalian protein that promotes apoptosis by binding to and antagonizing IAP proteins. *Cell* **102**, 43-53 (2000).
109. Du, C., Fang, M., Li, Y., Li, L. & Wang, X. Smac, a mitochondrial protein that promotes cytochrome c-dependent caspase activation by eliminating IAP inhibition. *Cell* **102**, 33-42 (2000).
110. Susin, S.A. *et al.* Molecular characterization of mitochondrial apoptosis-inducing factor. *Nature* **397**, 441-446 (1999).
111. Li, L.Y., Luo, X. & Wang, X. Endonuclease G is an apoptotic DNase when released from mitochondria. *Nature* **412**, 95-99 (2001).
112. Cregan, S.P., Dawson, V.L. & Slack, R.S. Role of AIF in caspase-dependent and caspase-independent cell death. *Oncogene* **23**, 2785-2796 (2004).
113. van Gurp, M., Festjens, N., van Loo, G., Saelens, X. & Vandenabeele, P. Mitochondrial intermembrane proteins in cell death. *Biochem Biophys Res Commun* **304**, 487-497 (2003).
114. Scaffidi, C. *et al.* Two CD95 (APO-1/Fas) signaling pathways. *EMBO J* **17**, 1675-1687 (1998).
115. Scaffidi, C. *et al.* Differential modulation of apoptosis sensitivity in CD95 type I and type II cells. *J Biol Chem* **274**, 22532-22538 (1999).
116. Li, H., Zhu, H., Xu, C.J. & Yuan, J. Cleavage of BID by caspase 8 mediates the mitochondrial damage in the Fas pathway of apoptosis. *Cell* **94**, 491-501 (1998).
117. Luo, X., Budihardjo, I., Zou, H., Slaughter, C. & Wang, X. Bid, a Bcl2 interacting protein, mediates cytochrome c release from mitochondria in response to activation of cell surface death receptors. *Cell* **94**, 481-490 (1998).
118. Scaffidi, C., Schmitz, I., Krammer, P.H. & Peter, M.E. The role of c-FLIP in modulation of CD95-induced apoptosis. *J Biol Chem* **274**, 1541-1548 (1999).
119. Chakrabandhu, K. *et al.* Palmitoylation is required for efficient Fas cell death signaling. *EMBO J* **26**, 209-220 (2007).
120. Feig, C., Tchikov, V., Schutze, S. & Peter, M.E. Palmitoylation of CD95 facilitates formation of SDS-stable receptor aggregates that initiate apoptosis signaling. *EMBO J* **26**, 221-231 (2007).
121. Muppidi, J.R. & Siegel, R.M. Ligand-independent redistribution of Fas (CD95) into lipid rafts mediates clonotypic T cell death. *Nat Immunol* **5**, 182-189 (2004).
122. Eramo, A. *et al.* CD95 death-inducing signaling complex formation and internalization occur in lipid rafts of type I and type II cells. *Eur J Immunol* **34**, 1930-1940 (2004).
123. Siegel, R.M. *et al.* SPOTS: signaling protein oligomeric transduction structures are early mediators of death receptor-induced apoptosis at the plasma membrane. *J Cell Biol* **167**, 735-744 (2004).
124. Algeciras-Schimmich, A. *et al.* Molecular ordering of the initial signaling events of CD95. *Mol Cell Biol* **22**, 207-220 (2002).

125. Schutze, S., Tchikov, V. & Schneider-Brachert, W. Regulation of TNFR1 and CD95 signalling by receptor compartmentalization. *Nat Rev Mol Cell Biol* **9**, 655-662 (2008).
126. Thome, M. *et al.* Viral FLICE-inhibitory proteins (FLIPs) prevent apoptosis induced by death receptors. *Nature* **386**, 517-521 (1997).
127. Hu, S., Vincenz, C., Buller, M. & Dixit, V.M. A novel family of viral death effector domain-containing molecules that inhibit both CD-95- and tumor necrosis factor receptor-1-induced apoptosis. *J Biol Chem* **272**, 9621-9624 (1997).
128. Bertin, J. *et al.* Death effector domain-containing herpesvirus and poxvirus proteins inhibit both Fas- and TNFR1-induced apoptosis. *Proc Natl Acad Sci U S A* **94**, 1172-1176 (1997).
129. Goltsev, Y.V. *et al.* CASH, a novel caspase homologue with death effector domains. *J Biol Chem* **272**, 19641-19644 (1997).
130. Shu, H.B., Halpin, D.R. & Goeddel, D.V. Casper is a FADD- and caspase-related inducer of apoptosis. *Immunity* **6**, 751-763 (1997).
131. Inohara, N., Koseki, T., Hu, Y., Chen, S. & Nunez, G. CLARP, a death effector domain-containing protein interacts with caspase-8 and regulates apoptosis. *Proc Natl Acad Sci U S A* **94**, 10717-10722 (1997).
132. Srinivasula, S.M. *et al.* FLAME-1, a novel FADD-like anti-apoptotic molecule that regulates Fas/TNFR1-induced apoptosis. *J Biol Chem* **272**, 18542-18545 (1997).
133. Hu, S., Vincenz, C., Ni, J., Gentz, R. & Dixit, V.M. I-FLICE, a novel inhibitor of tumor necrosis factor receptor-1- and CD-95-induced apoptosis. *J Biol Chem* **272**, 17255-17257 (1997).
134. Han, D.K. *et al.* MRIT, a novel death-effector domain-containing protein, interacts with caspases and BclXL and initiates cell death. *Proc Natl Acad Sci U S A* **94**, 11333-11338 (1997).
135. Rasper, D.M. *et al.* Cell death attenuation by 'Usurpin', a mammalian DED-caspase homologue that precludes caspase-8 recruitment and activation by the CD-95 (Fas, APO-1) receptor complex. *Cell Death Differ* **5**, 271-288 (1998).
136. Fernandes-Alnemri, T. *et al.* In vitro activation of CPP32 and Mch3 by Mch4, a novel human apoptotic cysteine protease containing two FADD-like domains. *Proc Natl Acad Sci U S A* **93**, 7464-7469 (1996).
137. Kischkel, F.C. *et al.* Assignment of CASP8 to human chromosome band 2q33-->q34 and Casp8 to the murine syntenic region on chromosome 1B-proximal C by in situ hybridization. *Cytogenet Cell Genet* **82**, 95-96 (1998).
138. Grenet, J., Teitz, T., Wei, T., Valentine, V. & Kidd, V.J. Structure and chromosome localization of the human CASP8 gene. *Gene* **226**, 225-232 (1999).
139. Djerbi, M., Darreh-Shori, T., Zhivotovsky, B. & Grandien, A. Characterization of the human FLICE-inhibitory protein locus and comparison of the anti-apoptotic activity of four different flip isoforms. *Scand J Immunol* **54**, 180-189 (2001).
140. Golks, A., Brenner, D., Fritsch, C., Krammer, P.H. & Lavrik, I.N. c-FLIPR, a new regulator of death receptor-induced apoptosis. *J Biol Chem* **280**, 14507-14513 (2005).
141. Irmeler, M. *et al.* Inhibition of death receptor signals by cellular FLIP. *Nature* **388**, 190-195 (1997).
142. Ueffing, N. *et al.* A single nucleotide polymorphism determines protein isoform production of the human c-FLIP protein. *Blood* **114**, 572-579 (2009).
143. Ueffing, N. *et al.* Mutational analyses of c-FLIPR, the only murine short FLIP isoform, reveal requirements for DISC recruitment. *Cell Death Differ* **15**, 773-782 (2008).

144. Budd, R.C., Yeh, W.C. & Tschopp, J. cFLIP regulation of lymphocyte activation and development. *Nat Rev Immunol* **6**, 196-204 (2006).
145. Micheau, O., Lens, S., Gaide, O., Alevizopoulos, K. & Tschopp, J. NF-kappaB signals induce the expression of c-FLIP. *Mol Cell Biol* **21**, 5299-5305 (2001).
146. Kreuz, S., Siegmund, D., Scheurich, P. & Wajant, H. NF-kappaB inducers upregulate cFLIP, a cycloheximide-sensitive inhibitor of death receptor signaling. *Mol Cell Biol* **21**, 3964-3973 (2001).
147. Ueffing, N., Schuster, M., Keil, E., Schulze-Osthoff, K. & Schmitz, I. Up-regulation of c-FLIP short by NFAT contributes to apoptosis resistance of short-term activated T cells. *Blood* **112**, 690-698 (2008).
148. Golks, A., Brenner, D., Krammer, P.H. & Lavrik, I.N. The c-FLIP-NH2 terminus (p22-FLIP) induces NF-kappaB activation. *J Exp Med* **203**, 1295-1305 (2006).
149. Krueger, A., Schmitz, I., Baumann, S., Krammer, P.H. & Kirchhoff, S. Cellular FLICE-inhibitory protein splice variants inhibit different steps of caspase-8 activation at the CD95 death-inducing signaling complex. *J Biol Chem* **276**, 20633-20640 (2001).
150. Medema, J.P. *et al.* FLICE is activated by association with the CD95 death-inducing signaling complex (DISC). *EMBO J* **16**, 2794-2804 (1997).
151. Chang, D.W. *et al.* c-FLIP(L) is a dual function regulator for caspase-8 activation and CD95-mediated apoptosis. *EMBO J* **21**, 3704-3714 (2002).
152. Micheau, O. *et al.* The long form of FLIP is an activator of caspase-8 at the Fas death-inducing signaling complex. *J Biol Chem* **277**, 45162-45171 (2002).
153. Fricker, N. *et al.* Model-based dissection of CD95 signaling dynamics reveals both a pro- and antiapoptotic role of c-FLIPL. *J Cell Biol* **190**, 377-389 (2010).
154. Takahashi, T. *et al.* Generalized lymphoproliferative disease in mice, caused by a point mutation in the Fas ligand. *Cell* **76**, 969-976 (1994).
155. Watanabe-Fukunaga, R., Brannan, C.I., Copeland, N.G., Jenkins, N.A. & Nagata, S. Lymphoproliferation disorder in mice explained by defects in Fas antigen that mediates apoptosis. *Nature* **356**, 314-317 (1992).
156. Sneller, M.C. *et al.* A novel lymphoproliferative/autoimmune syndrome resembling murine lpr/gld disease. *J Clin Invest* **90**, 334-341 (1992).
157. Bidere, N., Su, H.C. & Lenardo, M.J. Genetic disorders of programmed cell death in the immune system. *Annu Rev Immunol* **24**, 321-352 (2006).
158. Fisher, G.H. *et al.* Dominant interfering Fas gene mutations impair apoptosis in a human autoimmune lymphoproliferative syndrome. *Cell* **81**, 935-946 (1995).
159. Straus, S.E. *et al.* The development of lymphomas in families with autoimmune lymphoproliferative syndrome with germline Fas mutations and defective lymphocyte apoptosis. *Blood* **98**, 194-200 (2001).
160. Cohen, P.L. & Eisenberg, R.A. Lpr and gld: single gene models of systemic autoimmunity and lymphoproliferative disease. *Annu Rev Immunol* **9**, 243-269 (1991).
161. Yasutomo, K. *et al.* Defective T cells from gld mice play a pivotal role in development of Thy-1.2+B220+ cells and autoimmunity. *J Immunol* **153**, 5855-5864 (1994).
162. Coffman, R.L. & Weissman, I.L. B220: a B cell-specific member of the T200 glycoprotein family. *Nature* **289**, 681-683 (1981).
163. Fuss, I.J. *et al.* Characteristic T helper 2 T cell cytokine abnormalities in autoimmune lymphoproliferative syndrome, a syndrome marked by defective apoptosis and humoral autoimmunity. *J Immunol* **158**, 1912-1918 (1997).
164. Sprent, J. & Tough, D.F. T cell death and memory. *Science* **293**, 245-248 (2001).

165. Krueger, A., Fas, S.C., Baumann, S. & Krammer, P.H. The role of CD95 in the regulation of peripheral T-cell apoptosis. *Immunol Rev* **193**, 58-69 (2003).
166. Alderson, M.R. *et al.* Fas ligand mediates activation-induced cell death in human T lymphocytes. *J Exp Med* **181**, 71-77 (1995).
167. Brunner, T. *et al.* Cell-autonomous Fas (CD95)/Fas-ligand interaction mediates activation-induced apoptosis in T-cell hybridomas. *Nature* **373**, 441-444 (1995).
168. Dhein, J., Walczak, H., Baumler, C., Debatin, K.M. & Krammer, P.H. Autocrine T-cell suicide mediated by APO-1/(Fas/CD95). *Nature* **373**, 438-441 (1995).
169. Ju, S.T. *et al.* Fas(CD95)/FasL interactions required for programmed cell death after T-cell activation. *Nature* **373**, 444-448 (1995).
170. Ramaswamy, M. & Siegel, R.M. A FAScinating receptor in self-tolerance. *Immunity* **26**, 545-547 (2007).
171. Trauth, B.C. *et al.* Monoclonal antibody-mediated tumor regression by induction of apoptosis. *Science* **245**, 301-305 (1989).
172. Klas, C., Debatin, K.M., Jonker, R.R. & Krammer, P.H. Activation interferes with the APO-1 pathway in mature human T cells. *Int Immunol* **5**, 625-630 (1993).
173. Peter, M.E. *et al.* Resistance of cultured peripheral T cells towards activation-induced cell death involves a lack of recruitment of FLICE (MACH/caspase 8) to the CD95 death-inducing signaling complex. *Eur J Immunol* **27**, 1207-1212 (1997).
174. Kirchhoff, S., Muller, W.W., Krueger, A., Schmitz, I. & Krammer, P.H. TCR-mediated up-regulation of c-FLIPshort correlates with resistance toward CD95-mediated apoptosis by blocking death-inducing signaling complex activity. *J Immunol* **165**, 6293-6300 (2000).
175. Schmitz, I. *et al.* Resistance of short term activated T cells to CD95-mediated apoptosis correlates with de novo protein synthesis of c-FLIPshort. *J Immunol* **172**, 2194-2200 (2004).
176. Fas, S.C. *et al.* In vitro generated human memory-like T cells are CD95 type II cells and resistant towards CD95-mediated apoptosis. *Eur J Immunol* **36**, 2894-2903 (2006).
177. Schmitz, I. *et al.* An IL-2-dependent switch between CD95 signaling pathways sensitizes primary human T cells toward CD95-mediated activation-induced cell death. *J Immunol* **171**, 2930-2936 (2003).
178. Liao, W., Lin, J.X. & Leonard, W.J. Interleukin-2 at the crossroads of effector responses, tolerance, and immunotherapy. *Immunity* **38**, 13-25 (2013).
179. Sadlack, B. *et al.* Ulcerative colitis-like disease in mice with a disrupted interleukin-2 gene. *Cell* **75**, 253-261 (1993).
180. Suzuki, H. *et al.* Deregulated T cell activation and autoimmunity in mice lacking interleukin-2 receptor beta. *Science* **268**, 1472-1476 (1995).
181. Willerford, D.M. *et al.* Interleukin-2 receptor alpha chain regulates the size and content of the peripheral lymphoid compartment. *Immunity* **3**, 521-530 (1995).
182. Hughes, P.D. *et al.* Apoptosis regulators Fas and Bim cooperate in shutdown of chronic immune responses and prevention of autoimmunity. *Immunity* **28**, 197-205 (2008).
183. Hutcheson, J. *et al.* Combined deficiency of proapoptotic regulators Bim and Fas results in the early onset of systemic autoimmunity. *Immunity* **28**, 206-217 (2008).
184. Weant, A.E. *et al.* Apoptosis regulators Bim and Fas function concurrently to control autoimmunity and CD8+ T cell contraction. *Immunity* **28**, 218-230 (2008).
185. Mizuno, T., Zhong, X. & Rothstein, T.L. Fas-induced apoptosis in B cells. *Apoptosis* **8**, 451-460 (2003).

186. Hennino, A., Berard, M., Casamayor-Palleja, M., Krammer, P.H. & Defrance, T. Regulation of the Fas death pathway by FLICE-inhibitory protein in primary human B cells. *J Immunol* **165**, 3023-3030 (2000).
187. Stranges, P.B. *et al.* Elimination of antigen-presenting cells and autoreactive T cells by Fas contributes to prevention of autoimmunity. *Immunity* **26**, 629-641 (2007).
188. Shirley, S. & Micheau, O. Targeting c-FLIP in cancer. *Cancer Lett* (2010).
189. Dutton, A. *et al.* Expression of the cellular FLICE-inhibitory protein (c-FLIP) protects Hodgkin's lymphoma cells from autonomous Fas-mediated death. *Proc Natl Acad Sci U S A* **101**, 6611-6616 (2004).
190. Mathas, S. *et al.* c-FLIP mediates resistance of Hodgkin/Reed-Sternberg cells to death receptor-induced apoptosis. *J Exp Med* **199**, 1041-1052 (2004).
191. Griffith, T.S., Chin, W.A., Jackson, G.C., Lynch, D.H. & Kubin, M.Z. Intracellular regulation of TRAIL-induced apoptosis in human melanoma cells. *J Immunol* **161**, 2833-2840 (1998).
192. Medema, J.P., de Jong, J., van Hall, T., Melief, C.J. & Offringa, R. Immune escape of tumors in vivo by expression of cellular FLICE-inhibitory protein. *J Exp Med* **190**, 1033-1038 (1999).
193. Djerbi, M. *et al.* The inhibitor of death receptor signaling, FLICE-inhibitory protein defines a new class of tumor progression factors. *J Exp Med* **190**, 1025-1032 (1999).
194. Wajant, H., Gerspach, J. & Pfizenmaier, K. Engineering death receptor ligands for cancer therapy. *Cancer Lett* (2011).
195. Walczak, H. *et al.* Tumoricidal activity of tumor necrosis factor-related apoptosis-inducing ligand in vivo. *Nat Med* **5**, 157-163 (1999).
196. Wiley, S.R. *et al.* Identification and characterization of a new member of the TNF family that induces apoptosis. *Immunity* **3**, 673-682 (1995).
197. Voelkel-Johnson, C. TRAIL-mediated signaling in prostate, bladder and renal cancer. *Nat Rev Urol* **8**, 417-427 (2011).
198. Newsom-Davis, T., Prieske, S. & Walczak, H. Is TRAIL the holy grail of cancer therapy? *Apoptosis* **14**, 607-623 (2009).
199. Chen, L. *et al.* CD95 promotes tumour growth. *Nature* **465**, 492-496 (2010).
200. Barnhart, B.C. *et al.* CD95 ligand induces motility and invasiveness of apoptosis-resistant tumor cells. *EMBO J* **23**, 3175-3185 (2004).
201. Yeh, W.C. *et al.* Requirement for Casper (c-FLIP) in regulation of death receptor-induced apoptosis and embryonic development. *Immunity* **12**, 633-642 (2000).
202. Varfolomeev, E.E. *et al.* Targeted disruption of the mouse Caspase 8 gene ablates cell death induction by the TNF receptors, Fas/Apo1, and DR3 and is lethal prenatally. *Immunity* **9**, 267-276 (1998).
203. Zhang, J., Cado, D., Chen, A., Kabra, N.H. & Winoto, A. Fas-mediated apoptosis and activation-induced T-cell proliferation are defective in mice lacking FADD/Mort1. *Nature* **392**, 296-300 (1998).
204. Hu, W.H., Johnson, H. & Shu, H.B. Activation of NF-kappaB by FADD, Casper, and caspase-8. *J Biol Chem* **275**, 10838-10844 (2000).
205. Chaudhary, P.M. *et al.* Activation of the NF-kappaB pathway by caspase 8 and its homologs. *Oncogene* **19**, 4451-4460 (2000).
206. Kataoka, T. *et al.* The caspase-8 inhibitor FLIP promotes activation of NF-kappaB and Erk signaling pathways. *Curr Biol* **10**, 640-648 (2000).
207. Kataoka, T. & Tschoop, J. N-terminal fragment of c-FLIP(L) processed by caspase 8 specifically interacts with TRAF2 and induces activation of the NF-kappaB signaling pathway. *Mol Cell Biol* **24**, 2627-2636 (2004).

208. Dohrman, A. *et al.* Cellular FLIP (long form) regulates CD8+ T cell activation through caspase-8-dependent NF-kappa B activation. *J Immunol* **174**, 5270-5278 (2005).
209. Hinshaw-Makepeace, J. *et al.* c-FLIP(S) reduces activation of caspase and NF-kappaB pathways and decreases T cell survival. *Eur J Immunol* **38**, 54-63 (2008).
210. Kennedy, N.J., Kataoka, T., Tschopp, J. & Budd, R.C. Caspase activation is required for T cell proliferation. *J Exp Med* **190**, 1891-1896 (1999).
211. Alam, A., Cohen, L.Y., Aouad, S. & Sekaly, R.P. Early activation of caspases during T lymphocyte stimulation results in selective substrate cleavage in nonapoptotic cells. *J Exp Med* **190**, 1879-1890 (1999).
212. Salmena, L. *et al.* Essential role for caspase 8 in T-cell homeostasis and T-cell-mediated immunity. *Genes Dev* **17**, 883-895 (2003).
213. Chun, H.J. *et al.* Pleiotropic defects in lymphocyte activation caused by caspase-8 mutations lead to human immunodeficiency. *Nature* **419**, 395-399 (2002).
214. Reed, J.C. *et al.* Comparative analysis of apoptosis and inflammation genes of mice and humans. *Genome Res* **13**, 1376-1388 (2003).
215. Lens, S.M. *et al.* The caspase 8 inhibitor c-FLIP(L) modulates T-cell receptor-induced proliferation but not activation-induced cell death of lymphocytes. *Mol Cell Biol* **22**, 5419-5433 (2002).
216. Zhang, N. & He, Y.W. An essential role for c-FLIP in the efficient development of mature T lymphocytes. *J Exp Med* **202**, 395-404 (2005).
217. Chau, H. *et al.* Cellular FLICE-inhibitory protein is required for T cell survival and cycling. *J Exp Med* **202**, 405-413 (2005).
218. Newton, K., Harris, A.W., Bath, M.L., Smith, K.G. & Strasser, A. A dominant interfering mutant of FADD/MORT1 enhances deletion of autoreactive thymocytes and inhibits proliferation of mature T lymphocytes. *EMBO J* **17**, 706-718 (1998).
219. Walsh, C.M. *et al.* A role for FADD in T cell activation and development. *Immunity* **8**, 439-449 (1998).
220. Zhang, N., Hopkins, K. & He, Y.W. The long isoform of cellular FLIP is essential for T lymphocyte proliferation through an NF-kappaB-independent pathway. *J Immunol* **180**, 5506-5511 (2008).
221. He, M.X. & He, Y.W. A role for c-FLIP(L) in the regulation of apoptosis, autophagy, and necroptosis in T lymphocytes. *Cell Death Differ* **20**, 188-197 (2013).
222. Lee, J.S. *et al.* FLIP-mediated autophagy regulation in cell death control. *Nat Cell Biol* **11**, 1355-1362 (2009).
223. Zhang, H. *et al.* Functional complementation between FADD and RIP1 in embryos and lymphocytes. *Nature* **471**, 373-376 (2011).
224. Dillon, C.P. *et al.* Survival function of the FADD-CASPASE-8-cFLIP(L) complex. *Cell Rep* **1**, 401-407 (2012).
225. Kaiser, W.J. *et al.* RIP3 mediates the embryonic lethality of caspase-8-deficient mice. *Nature* **471**, 368-372 (2011).
226. Vandenabeele, P., Galluzzi, L., Vanden Berghe, T. & Kroemer, G. Molecular mechanisms of necroptosis: an ordered cellular explosion. *Nat Rev Mol Cell Biol* **11**, 700-714 (2010).
227. Oberst, A. *et al.* Catalytic activity of the caspase-8-FLIP(L) complex inhibits RIPK3-dependent necrosis. *Nature* **471**, 363-367 (2011).
228. Dickens, L.S. *et al.* A death effector domain chain DISC model reveals a crucial role for caspase-8 chain assembly in mediating apoptotic cell death. *Mol Cell* **47**, 291-305 (2012).

229. Schleich, K. *et al.* Stoichiometry of the CD95 death-inducing signaling complex: experimental and modeling evidence for a death effector domain chain model. *Mol Cell* **47**, 306-319 (2012).
230. Shein, H.M. & Enders, J.F. Transformation induced by simian virus 40 in human renal cell cultures. I. Morphology and growth characteristics. *Proc Natl Acad Sci U S A* **48**, 1164-1172 (1962).
231. Shein, H.M., Enders, J.F. & Levinthal, J.D. Transformation induced by simian virus 40 in human renal cell cultures. II. Cell-virus relationships. *Proc Natl Acad Sci U S A* **48**, 1350-1357 (1962).
232. Zur Hausen, H. Induction of specific chromosomal aberrations by adenovirus type 12 in human embryonic kidney cells. *J Virol* **1**, 1174-1185 (1967).
233. DuBridge, R.B. *et al.* Analysis of mutation in human cells by using an Epstein-Barr virus shuttle system. *Mol Cell Biol* **7**, 379-387 (1987).
234. Pear, W.S., Nolan, G.P., Scott, M.L. & Baltimore, D. Production of high-titer helper-free retroviruses by transient transfection. *Proc Natl Acad Sci U S A* **90**, 8392-8396 (1993).
235. Williams, R.D. Human urologic cancer cell lines. *Invest Urol* **17**, 359-363 (1980).
236. Paulie, S., Hansson, Y., Lundblad, M.L. & Perlmann, P. Lectins as probes for identification of tumor-associated antigens on urothelial and colonic carcinoma cell lines. *Int J Cancer* **31**, 297-303 (1983).
237. Ewald, F. *et al.* The role of c-FLIP splice variants in urothelial tumours. *Cell Death Dis* **2**, e245 (2011).
238. Schneider, U., Schwenk, H.U. & Bornkamm, G. Characterization of EBV-genome negative "null" and "T" cell lines derived from children with acute lymphoblastic leukemia and leukemic transformed non-Hodgkin lymphoma. *Int J Cancer* **19**, 621-626 (1977).
239. Weiss, A., Wiskocil, R.L. & Stobo, J.D. The role of T3 surface molecules in the activation of human T cells: a two-stimulus requirement for IL 2 production reflects events occurring at a pre-translational level. *J Immunol* **133**, 123-128 (1984).
240. Ogilvy, S. *et al.* Promoter elements of vav drive transgene expression in vivo throughout the hematopoietic compartment. *Blood* **94**, 1855-1863 (1999).
241. Fulda, S., Meyer, E. & Debatin, K.M. Metabolic inhibitors sensitize for CD95 (APO-1/Fas)-induced apoptosis by down-regulating Fas-associated death domain-like interleukin 1-converting enzyme inhibitory protein expression. *Cancer Res* **60**, 3947-3956 (2000).
242. Krueger, A., Baumann, S., Krammer, P.H. & Kirchhoff, S. FLICE-inhibitory proteins: regulators of death receptor-mediated apoptosis. *Mol Cell Biol* **21**, 8247-8254 (2001).
243. Abraham, R.T. & Weiss, A. Jurkat T cells and development of the T-cell receptor signalling paradigm. *Nat Rev Immunol* **4**, 301-308 (2004).
244. Juo, P., Kuo, C.J., Yuan, J. & Blenis, J. Essential requirement for caspase-8/FLICE in the initiation of the Fas-induced apoptotic cascade. *Curr Biol* **8**, 1001-1008 (1998).
245. Juo, P. *et al.* FADD is required for multiple signaling events downstream of the receptor Fas. *Cell Growth Differ* **10**, 797-804 (1999).
246. Carrington, P.E. *et al.* The structure of FADD and its mode of interaction with procaspase-8. *Mol Cell* **22**, 599-610 (2006).
247. Muzio, M. *et al.* FLICE, a novel FADD-homologous ICE/CED-3-like protease, is recruited to the CD95 (Fas/APO-1) death-inducing signaling complex. *Cell* **85**, 817-827 (1996).

248. Zhang, S.Q., Kovalenko, A., Cantarella, G. & Wallach, D. Recruitment of the IKK signalosome to the p55 TNF receptor: RIP and A20 bind to NEMO (IKK $\gamma$ ) upon receptor stimulation. *Immunity* **12**, 301-311 (2000).
249. Wertz, I.E. *et al.* De-ubiquitination and ubiquitin ligase domains of A20 downregulate NF- $\kappa$ B signalling. *Nature* **430**, 694-699 (2004).
250. Lee, T.H., Shank, J., Cusson, N. & Kelliher, M.A. The kinase activity of Rip1 is not required for tumor necrosis factor- $\alpha$ -induced IkappaB kinase or p38 MAP kinase activation or for the ubiquitination of Rip1 by Traf2. *J Biol Chem* **279**, 33185-33191 (2004).
251. Ogilvy, S. *et al.* Constitutive Bcl-2 expression throughout the hematopoietic compartment affects multiple lineages and enhances progenitor cell survival. *Proc Natl Acad Sci U S A* **96**, 14943-14948 (1999).
252. Wyllie, A.H. Glucocorticoid-induced thymocyte apoptosis is associated with endogenous endonuclease activation. *Nature* **284**, 555-556 (1980).
253. Ashwell, J.D., King, L.B. & Vacchio, M.S. Cross-talk between the T cell antigen receptor and the glucocorticoid receptor regulates thymocyte development. *Stem Cells* **14**, 490-500 (1996).
254. Roths, J.B., Murphy, E.D. & Eicher, E.M. A new mutation, gld, that produces lymphoproliferation and autoimmunity in C3H/HeJ mice. *J Exp Med* **159**, 1-20 (1984).
255. Iglesias, A., Bauer, J., Litzenburger, T., Schubart, A. & Linington, C. T- and B-cell responses to myelin oligodendrocyte glycoprotein in experimental autoimmune encephalomyelitis and multiple sclerosis. *Glia* **36**, 220-234 (2001).
256. Fletcher, J.M., Lalor, S.J., Sweeney, C.M., Tubridy, N. & Mills, K.H. T cells in multiple sclerosis and experimental autoimmune encephalomyelitis. *Clin Exp Immunol* **162**, 1-11 (2010).
257. Tabi, Z., McCombe, P.A. & Pender, M.P. Apoptotic elimination of V beta 8.2+ cells from the central nervous system during recovery from experimental autoimmune encephalomyelitis induced by the passive transfer of V beta 8.2+ encephalitogenic T cells. *Eur J Immunol* **24**, 2609-2617 (1994).
258. White, C.A., McCombe, P.A. & Pender, M.P. The roles of Fas, Fas ligand and Bcl-2 in T cell apoptosis in the central nervous system in experimental autoimmune encephalomyelitis. *J Neuroimmunol* **82**, 47-55 (1998).
259. Oehme, I., Neumann, F., Bosser, S. & Zornig, M. Transgenic overexpression of the Caspase-8 inhibitor FLIP(short) leads to impaired T cell proliferation and an increased memory T cell pool after staphylococcal enterotoxin B injection. *Eur J Immunol* **35**, 1240-1249 (2005).
260. Leverkus, M. *et al.* Maturation of dendritic cells leads to up-regulation of cellular FLICE-inhibitory protein and concomitant down-regulation of death ligand-mediated apoptosis. *Blood* **96**, 2628-2631 (2000).
261. Huang, Q.Q. *et al.* FLIP: a novel regulator of macrophage differentiation and granulocyte homeostasis. *Blood* **116**, 4968-4977 (2010).
262. Hanahan, D. & Weinberg, R.A. Hallmarks of cancer: the next generation. *Cell* **144**, 646-674 (2011).
263. Korkolopoulou, P. *et al.* c-FLIP expression in bladder urothelial carcinomas: its role in resistance to Fas-mediated apoptosis and clinicopathologic correlations. *Urology* **63**, 1198-1204 (2004).

264. Steele, L.P., Georgopoulos, N.T., Southgate, J., Selby, P.J. & Trejdosiewicz, L.K. Differential susceptibility to TRAIL of normal versus malignant human urothelial cells. *Cell Death Differ* **13**, 1564-1576 (2006).
265. Legembre, P., Barnhart, B.C. & Peter, M.E. The relevance of NF-kappaB for CD95 signaling in tumor cells. *Cell Cycle* **3**, 1235-1239 (2004).
266. Kreuz, S. *et al.* NFkappaB activation by Fas is mediated through FADD, caspase-8, and RIP and is inhibited by FLIP. *J Cell Biol* **166**, 369-380 (2004).
267. Nakajima, A. *et al.* An antiapoptotic protein, c-FLIPL, directly binds to MKK7 and inhibits the JNK pathway. *EMBO J* **25**, 5549-5559 (2006).
268. Yu, J.W., Jeffrey, P.D. & Shi, Y. Mechanism of procaspase-8 activation by c-FLIPL. *Proc Natl Acad Sci U S A* **106**, 8169-8174 (2009).
269. Boatright, K.M., Deis, C., Denault, J.B., Sutherlin, D.P. & Salvesen, G.S. Activation of caspases-8 and -10 by FLIP(L). *Biochem J* **382**, 651-657 (2004).
270. Feoktistova, M. *et al.* cIAPs block Ripoptosome formation, a RIP1/caspase-8 containing intracellular cell death complex differentially regulated by cFLIP isoforms. *Mol Cell* **43**, 449-463 (2011).
271. Tenev, T. *et al.* The Ripoptosome, a signaling platform that assembles in response to genotoxic stress and loss of IAPs. *Mol Cell* **43**, 432-448 (2011).
272. Morgan, M.J., Kim, Y.S. & Liu, Z.G. Membrane-bound Fas ligand requires RIP1 for efficient activation of caspase-8 within the death-inducing signaling complex. *J Immunol* **183**, 3278-3284 (2009).
273. Hsu, H., Huang, J., Shu, H.B., Baichwal, V. & Goeddel, D.V. TNF-dependent recruitment of the protein kinase RIP to the TNF receptor-1 signaling complex. *Immunity* **4**, 387-396 (1996).
274. Ea, C.K., Deng, L., Xia, Z.P., Pineda, G. & Chen, Z.J. Activation of IKK by TNFalpha requires site-specific ubiquitination of RIP1 and polyubiquitin binding by NEMO. *Mol Cell* **22**, 245-257 (2006).
275. Micheau, O. & Tschopp, J. Induction of TNF receptor I-mediated apoptosis via two sequential signaling complexes. *Cell* **114**, 181-190 (2003).
276. Gonzalez, F. *et al.* TRAF2 Sets a Threshold for Extrinsic Apoptosis by Tagging Caspase-8 with a Ubiquitin Shutoff Timer. *Mol Cell* **48**, 888-899 (2012).
277. Tian, J.Y. *et al.* Cloning and sequence analysis of tumor-associated gene hMMTAG2 from human multiple myeloma cell line ARH-77. *Sheng Wu Hua Xue Yu Sheng Wu Wu Li Xue Bao (Shanghai)* **35**, 143-148 (2003).
278. Leaw, C.L., Ren, E.C. & Choong, M.L. Hcc-1 is a novel component of the nuclear matrix with growth inhibitory function. *Cell Mol Life Sci* **61**, 2264-2273 (2004).
279. Suarez-Huerta, N., Boeynaems, J.M. & Communi, D. Cloning, genomic organization, and tissue distribution of human Ssf-1. *Biochem Biophys Res Commun* **275**, 37-42 (2000).
280. Song, H.Y., Rothe, M. & Goeddel, D.V. The tumor necrosis factor-inducible zinc finger protein A20 interacts with TRAF1/TRAF2 and inhibits NF-kappaB activation. *Proc Natl Acad Sci U S A* **93**, 6721-6725 (1996).
281. Kirchhoff, S., Muller, W.W., Li-Weber, M. & Krammer, P.H. Up-regulation of c-FLIPshort and reduction of activation-induced cell death in CD28-costimulated human T cells. *Eur J Immunol* **30**, 2765-2774 (2000).
282. Wu, Z. *et al.* Viral FLIP impairs survival of activated T cells and generation of CD8+ T cell memory. *J Immunol* **172**, 6313-6323 (2004).

283. OhYama, T., Tsukumo, S., Yajima, N., Sakamaki, K. & Yonehara, S. Reduction of thymocyte numbers in transgenic mice expressing viral FLICE-inhibitory protein in a Fas-independent manner. *Microbiol Immunol* **44**, 289-297 (2000).
284. Tai, T.S., Fang, L.W. & Lai, M.Z. c-FLICE inhibitory protein expression inhibits T-cell activation. *Cell Death Differ* **11**, 69-79 (2004).
285. Qiao, G. *et al.* Altered thymic selection by overexpressing cellular FLICE inhibitory protein in T cells causes lupus-like syndrome in a BALB/c but not C57BL/6 strain. *Cell Death Differ* **17**, 522-533 (2010).
286. Suvannavejh, G.C., Dal Canto, M.C., Matis, L.A. & Miller, S.D. Fas-mediated apoptosis in clinical remissions of relapsing experimental autoimmune encephalomyelitis. *J Clin Invest* **105**, 223-231 (2000).
287. Sharief, M.K. Increased cellular expression of the caspase inhibitor FLIP in intrathecal lymphocytes from patients with multiple sclerosis. *J Neuroimmunol* **111**, 203-209 (2000).
288. Semra, Y.K., Seidi, O.A. & Sharief, M.K. Overexpression of the apoptosis inhibitor FLIP in T cells correlates with disease activity in multiple sclerosis. *J Neuroimmunol* **113**, 268-274 (2001).
289. Tseveleki, V. *et al.* Cellular FLIP (long isoform) overexpression in T cells drives Th2 effector responses and promotes immunoregulation in experimental autoimmune encephalomyelitis. *J Immunol* **173**, 6619-6626 (2004).
290. Wu, W. *et al.* Cellular FLIP long form-transgenic mice manifest a Th2 cytokine bias and enhanced allergic airway inflammation. *J Immunol* **172**, 4724-4732 (2004).
291. Fang, Y., Sharp, G.C. & Braley-Mullen, H. Effect of transgenic overexpression of FLIP on lymphocytes on development and resolution of experimental autoimmune thyroiditis. *Am J Pathol* **179**, 1211-1220 (2011).
292. Budd, R.C., Van Houten, N., Clements, J. & Mixter, P.F. Parallels in T lymphocyte development between *lpr* and normal mice. *Semin Immunol* **6**, 43-48 (1994).
293. Woelfel, M., Bixby, J., Brehm, M.A. & Chan, F.K. Transgenic expression of the viral FLIP MC159 causes *lpr/gld*-like lymphoproliferation and autoimmunity. *J Immunol* **177**, 3814-3820 (2006).

## 8. Acknowledgements

I especially want to thank my supervisor Prof. Dr. Ingo Schmitz for giving me the opportunity to complete my thesis in his working group and for the interesting and challenging projects. I appreciate the helpful discussions, the willingness to share his excellent scientific knowledge and the support throughout my whole time in his lab.

I also want to thank my colleagues Michaela, Yvonne, Sabrina, Carlos, Tobi, Svenja, Alisha, Ralf, Marc, Dominique, Stephanie and Tanja for the enjoyable and helpful atmosphere in the lab.

Thanks to Lothar Groebe for helping me with cell sorting, Dirk Reinhold for the ANA assays and Josef Wissing for performing the mass spectrometry analyses.

I am deeply grateful to my parents Ingrid and Jürgen as well as my siblings Benjamin, Jonatan, Jonas, Fia and Johanna for all the support and interest in my work.

Finally, I want to thank Michael for always being there for me with love, support and understanding for my work.

## 9. Declaration of originality

Frida Kerstin Elisabeth Ewald

Hohes Feld 4

38124 Braunschweig

Hiermit erkläre ich, dass ich die von mir eingereichte Dissertation mit dem Thema

### **The apoptosis regulator c-FLIP**

Functional role in urothelial carcinoma and autoimmunity

and

Identification of novel CD95 DISC-interacting proteins

selbständig verfasst, nicht schon als Dissertation verwendet habe und die benutzten Hilfsmittel und Quellen vollständig angegeben wurden.

Weiterhin erkläre ich, dass ich weder diese noch eine andere Arbeit zur Erlangung des akademischen Grades doctor rerum naturalium (Dr. rer. nat.) an anderen Einrichtungen eingereicht habe.

Magdeburg, 25. Februar 2013

Frida Ewald

## 10. Curriculum Vitae

### Personal Details

*Name* Frida Kerstin Elisabeth Ewald  
*Date of birth* July 17, 1982 in Sillerud, Sweden  
*Nationality* Swedish  
*Address* Hohes Feld 4  
 38124 Braunschweig

### Education

*1989-1990* Primary school, Svensbyn's school, Sillerud, Sweden  
*1990-1996* Primary school, Tveta school, Säffle, Sweden  
*1996-1998* Lower secondary school, Tegnér's school, Säffle Sweden  
*1998-2001* Upper secondary school (International Baccalaureate), Tingvalla upper secondary school, Karlstad, Sweden  
*2003-2004* Chemistry studies at Carl von Ossietzky University, Oldenburg, Germany  
*2004-2009* Bioengineering studies at Chalmers University of Technology, Gothenburg, Sweden  
*2007-2008* Exchange studies at Griffith University, Brisbane, Australia  
*Jan-June 2009* Master Thesis at Astra Zeneca Transgenics & Comparative Genomics, Mölndal, Sweden  
*Nov 2009* Beginning of Ph.D. studies in Prof. Dr. Ingo Schmitz working group at Otto-von-Guericke University, Magdeburg, Germany and Helmholtz Centre for Infection Research, Braunschweig, Germany

### Work Experience

*2005 - 2007* Swedbank Telemarketing, Gothenburg, Sweden  
*Aug-Dec 2008* Swedbank Telemarketing, Gothenburg, Sweden  
*July-Aug 2009* Laboratory assistant at Astra Zeneca Transgenics & Comparative Genomics, Mölndal, Sweden

### Training

*Nov 2011* Introduction to Laboratory Animal Science, FELASA – category B

### Publications

- 1) **The role of c-FLIP splice variants in urothelial tumours**  
 F. Ewald, N. Ueffing, L. Brockmann, C. Hader, T. Telieps, M. Schuster, W. A. Schulz and I. Schmitz, *Cell Death and Disease* 2011
- 2) **c-FLIP<sub>R</sub> modulates cell death induction upon T cell activation and infection**  
 T. Telieps\*, F. Ewald\*, M. Gereke, M. Annemann, Y. Rauter, M. Schuster, N. Ueffing, D. von Smolinski, A. D. Gruber, D. Bruder and I. Schmitz, *European Journal of Immunology*, accepted. \* Equal contribution